

Activity of Ni / γ Al₂O₃ Catalyst For a Methanation Reaction

by

Syed Sameen Ali Zaidi

A Thesis Presented to the

FACULTY OF THE COLLEGE OF GRADUATE STUDIES

KING FAHD UNIVERSITY OF PETROLEUM & MINERALS

DHAHRAN, SAUDI ARABIA

In Partial Fulfillment of the
Requirements for the Degree of

MASTER OF SCIENCE

In

CHEMICAL ENGINEERING

May, 1992

INFORMATION TO USERS

This manuscript has been reproduced from the microfilm master. UMI films the text directly from the original or copy submitted. Thus, some thesis and dissertation copies are in typewriter face, while others may be from any type of computer printer.

The quality of this reproduction is dependent upon the quality of the copy submitted. Broken or indistinct print, colored or poor quality illustrations and photographs, print bleedthrough, substandard margins, and improper alignment can adversely affect reproduction.

In the unlikely event that the author did not send UMI a complete manuscript and there are missing pages, these will be noted. Also, if unauthorized copyright material had to be removed, a note will indicate the deletion.

Oversize materials (e.g., maps, drawings, charts) are reproduced by sectioning the original, beginning at the upper left-hand corner and continuing from left to right in equal sections with small overlaps. Each original is also photographed in one exposure and is included in reduced form at the back of the book.

Photographs included in the original manuscript have been reproduced xerographically in this copy. Higher quality 6" x 9" black and white photographic prints are available for any photographs or illustrations appearing in this copy for an additional charge. Contact UMI directly to order.

U·M·I

University Microfilms International
A Bell & Howell Information Company
300 North Zeeb Road, Ann Arbor, MI 48106-1346 USA
313/761-4700 800/521-0600

Order Number 1355322

Activity of Ni/ γ Al₂O₃ catalyst for a methanation reaction

Zaidi, Syed Sameen Ali, M.S.

King Fahd University of Petroleum and Minerals (Saudi Arabia), 1992

U·M·I
300 N. Zeeb Rd.
Ann Arbor, MI 48106

**ACTIVITY OF $\text{Ni} / \gamma\text{Al}_2\text{O}_3$ CATALYST
FOR A METHANATION REACTION**

BY

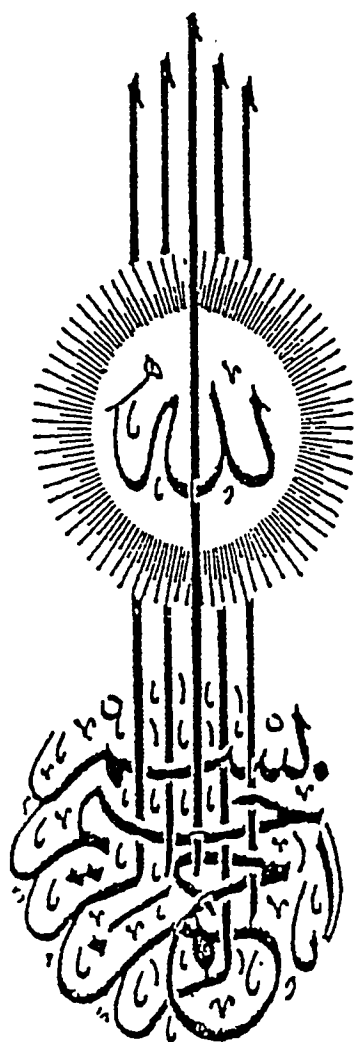
SYED SAMEEN ALI ZAIDI

**A Thesis Presented to the
FACULTY OF THE COLLEGE OF GRADUATE STUDIES
KING FAHD UNIVERSITY OF PETROLEUM & MINERALS
DHAHRAN, SAUDI ARABIA**

**In Partial Fulfillment of the
Requirements for the Degree of**

**MASTER OF SCIENCE
In
CHEMICAL ENGINEERING**

MAY, 1992



**KING FAHD UNIVERSITY OF PETROLEUM AND MINERALS
DHAHRAN 31261, SAUDI ARABIA**

COLLEGE OF GRADUATE STUDIES

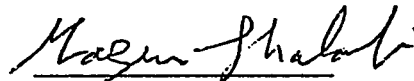
This thesis, written by

SYED SAMEEN ALI ZAIDI

under the direction of his Thesis Advisor and approved by his Thesis Committee, has been presented to and accepted by the Dean of the College of Graduate Studies, in partial fulfillment of the requirements for the degree of

MASTER OF SCIENCE IN CHEMICAL ENGINEERING.

Thesis Committee



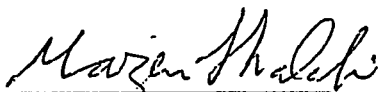
Dr. Mazen A. Shalabi
(Chairman)



Dr. Muhammad A. Al-Saleh
(Member)



Dr. Dulaihan K. Al-Rarbi
(Member)



Dr. Mazen A. Shalabi
(Department Chairman)



Dr. Ala H. Al-Rabeh
(Dean, College of Graduate Studies)

Date : 3-6-92



This thesis is dedicated

To

My beloved parents, brothers, sisters

and

Moosh

ACKNOWLEDGEMENTS

Praise and gratitude be to Allah Almighty, with whose gracious help it was possible to accomplish this work. Acknowledgement is due to King Fahd University of Petroleum and Minerals for providing access to all facilities and financial support for this research.

I wish to express my gratitude to Dr. Mazen A. Shalabi who served as my major advisor during the course of this investigation. Also, I am grateful for his continuous encouragement, advice, and valuable guidance throughout my graduate studies. I also wish to express sincere thanks to Dr. Mohammed A. Al-Saleh and Dr. Dulaihan K. Al-Harbi for their helpful suggestions and for serving as members of my thesis committee.

I am grateful to Mr. Mohammed Saeed Al-Buraiky of SAMAD Fertilizer Co. Ltd. (Al-Jubail), who provided us the methanation Ni-catalyst for this study.

My special thanks are due to workshop technicians Mr. John Chapman, Mr. Romeo Carpeso, and Mr. Mehdi; and laboratory technician Mr. Kamal Ahmed for their assistance in the trouble-shooting of our experimental setup.

I owe my family an expression of gratitude for their patience, understanding, and encouragement.

Finally, I am thankful to all faculty, peers, and friends who made my stay at the university a memorable and valuable experience.

TABLE OF CONTENTS

	<i>Page</i>
ACKNOWLEDGEMENTS	iv
LIST OF TABLES.....	ix
LIST OF FIGURES.....	xi
ABSTRACT (English)	xiii
ABSTRACT (Arabic).....	xiv
 CHAPTER 1. INTRODUCTION	
 1.1 Importance of Methanation Catalyst	1
1.2 Outline of Present Study.....	3
 CHAPTER 2. LITERATURE REVIEW	
 2.1 Adsorption Study	5
2.1.1 Adsorption of CO	5
2.1.2 Adsorption of H ₂	9
2.1.3 Coadsorption of CO and H ₂	10
2.2 Methanation Chemistry and Thermodynamics	11
2.3 Kinetics of Methanation Reaction.....	15
2.4 Methanation Mechanisms	24
2.5 Chemistry and Thermodynamics of Reduction of Nickel Catalyst	29

2.6 Kinetics of Reduction of Nickel Catalyst	29
2.7 Mechanism of Reduction of Nickel Catalyst.....	33
2.8 Methanation Catalyst	34
2.8.1 Ruthenium.....	34
2.8.2 Nickel.....	35
2.8.3 Cobalt and Iron.....	35
2.8.4 Molybdenum and Tungsten.....	36
2.9 Commercial and Laboratory Processes for Methanation	36
2.9.1 Laboratory Reactor for Methanation	40
2.10 Studies on the Activity of Nickel Catalyst.....	43

CHAPTER 3. EXPERIMENTAL INVESTIGATION

3.1 Introduction	52
3.2 Experimental Equipments.....	52
3.2.1 Feed metering System.....	54
3.2.2 High Pressure Reactor System	54
3.2.3 Control Box.....	56
3.2.4 Power Supply.....	58
3.2.5 Analytical Section	58
3.3 Materials.....	61
3.4 Experimental Procedure.....	61
3.5 Reduction Procedure for Ni-Catalyst.....	65
3.6 Gas Sample Analysis.....	66

CHAPTER 4 RESULTS

4.1 Overall View	67
4.2 Calibration of Gas Chromatograph.....	69
4.3 Reaction Rate Vs Speed of Impeller.....	74
4.4 Deactivation	74
4.5 Reproducibility of Data.....	77
4.6 Temperature Difference Across the Catalytic Bed	77
4.7 Activity of Ni-Catalyst at Different Reduction Conditions.....	77
4.8 Reaction Rate Vs Space-Velocity.....	80
4.9 Reaction Rate Vs Pressure	80
4.10 Reaction Rate Vs H_2/CO Ratio.....	80
4.11 Selectivity for Methane.....	80

CHAPTER 5 DISCUSSION

5.1 The Effect of Speed of Impeller	82
5.2 Deactivation	83
5.3 The Effects of Reduction Conditions on the Activity of $Ni/\gamma Al_2O_3$ Catalyst.....	84
5.3.1 Reduction Temperature	84
5.3.2 Duration of Reduction.....	92
5.3.3 Effects of Heating rate and Space-Velocity	98
5.4 The Effects of Space-Time on the Activity of $Ni/\gamma Al_2O_3$ Catalyst	100
5.5 The Effects of $H_2:CO$ Ratio on the Activity of $Ni/\gamma Al_2O_3$ Catalyst..	102

5.6 The Effects of Pressure on the Activity of Ni/ γ -Al ₂ O ₃ Catalyst.....	105
5.7 The Effects of Different Operating Conditions on the Selectivity for CH ₄ over Ni/ γ -Al ₂ O ₃ Catalyst.....	105
5.7.1 The Effects of Temperature of Reduction	105
5.7.2 The Effects of Duration of Reduction	108
5.7.3 The Effects of Space-Time.....	108
5.7.4 The Effects of H ₂ :CO Ratio.....	111
5.7.5 The Effects of Pressure of Reactor System.....	113
5.8 A Comparison of Specific Activities from Different Studies.....	113
 CHAPTER 6 CONCLUSIONS AND RECOMMENDATIONS	
6.1 Conclusions	117
6.2 Recommendations	118
 NOMENCLATURE	119
 REFERENCES	122
 APPENDICES	128
Appendix A: Reactor Performance	128
Appendix B: Sample Calculations	132
Appendix C: Calculations of Transport Effects.....	138
Appendix D: Data of Runs	142

LIST OF TABLES

<i>Table</i>	<i>Page</i>
2.1 Assignment of Infrared Bands to Surface Species for CO Chemisorbed on Supported Ni Samples at Room Temperature.....	7
2.2 Thermodynamic Data on Five Reactions Relevant to the Methanation Process Catalyzed by Nickel Based Catalyst	14
2.3 Thermodynamic Properties of NiO Reduction.....	30
3.1 Calibration of rpm Controller Vs Measured rpm.....	57
3.2 Catalyst Analysis.....	62
3.3 Fresh Catalyst Analysis	63
4.1 Operating Conditions of GC	71
4.2 Retention Times of Compounds.....	72
4.3 Response Factors Obtained by GC Calibration.....	73
4.4 Reproducibility of Data.....	78
5.1 Reduction Conditions of Ni/ γ -Al ₂ O ₃ (C13-4-04;20%Ni) Catalyst at Different Temperatures.....	85
5.2 Percentage of Reduced Ni obtained by Reducing Ni/ γ -Al ₂ O ₃ (C13-4-04;20%Ni) Catalyst at Different Temperatures	88
5.3 Analysis of Spent Ni/ γ -Al ₂ O ₃ (C13-4-04;20%Ni) Catalyst.....	89
5.4 Reduction Conditions of Ni/ γ -Al ₂ O ₃ (C13-4-04;20%Ni) Catalyst for Different Durations.....	94
5.5 Percentage of Reduced Ni Obtained by Reducing Ni/ γ -Al ₂ O ₃ (C13-4-04;20%Ni) Catalyst for Various Durations.....	96
5.6 Analysis of Spent Ni/ γ -Al ₂ O ₃ (C13-4-04;20%Ni) Catalyst.....	97

5.7	Comparison of Specific Activity from Different Studies.....	115
-----	---	-----

LIST OF FIGURES

<i>Figure</i>	<i>Page</i>
2.1 Carbon Deposition Boundaries in the Methanation Process.....	16
3.1 The Methanation Reaction Unit Flow-Sheet	53
3.2 A Descriptive View of Berty Reactor.....	55
4.1 Effect of Speed of Impeller on the Methanation Reaction Rates of Ni-Catalyst.....	75
4.2 Activity and Reproducibility of Ni-Catalyst.....	76
4.3 Reproducibility of Two Runs Over Ni-Catalyst.....	79
5.1 Effects of Reduction Temperature on the Activity of Ni-Catalyst.....	87
5.2 Comparison of Activity Between Two Samples of Ni-Catalysts Reduced in H_2 and H_2/He Mix.	93
5.3 Effects of Reduction Time on the Activity of Ni-Catalyst	95
5.4 Effects of Reduction Time on Nickel Metal Area	99
5.5 Effects of Space-Time on the Activity of Ni-Catalyst.....	101
5.6 Effects of H_2/CO Ratio on the Activity of Ni-Catalyst.....	103
5.7 Effects of Pressure on the Activity of Ni-Catalyst	106
5.8 Selectivity for CH_4 Formation as a Function of Reduction Temperature	107
5.9 Effects of Time of Reduction on the Selectivity of CH_4 Formation....	109
5.10 Effects of Space-Time on the Selectivity of Ni-Catalyst	110
5.11 Effects of H_2/CO Ratio on the Selectivity of Ni-Catalyst.....	112

5.12	Effects of Pressure on the Selectivity of Ni-Catalyst at 350 °C	114
------	---	-----

THESIS ABSTRACT

NAME OF STUDENT : SYED SAMEEN ALI ZAIDI
TITLE OF STUDY : Activity of $\text{Ni}/\gamma\text{Al}_2\text{O}_3$ Catalyst For a Methanation Reaction
MAJOR FIELD : Chemical Engineering
DATE OF DEGREE : May, 1992

The reduction of a commercial $\text{Ni}/\gamma\text{Al}_2\text{O}_3$ catalyst was carried out at temperature ranged from 250 to 500 °C and for duration from 2 to 16 hours. The effects of reduction conditions on the activity and selectivity of $\text{Ni}/\gamma\text{Al}_2\text{O}_3$ were studied for a methanation reaction in a gradientless Berty reactor. These effects were used to determine optimal reduction conditions of the catalyst. The optimal reduction conditions are: temperature 300° C, duration 8 hrs, space velocity 3000 hr⁻¹, and heating rate of bed 5° C/min.

The reaction rates were measured by injecting a feed containing H_2 (26 mol%), CO (6.7 mol%), and the balance being nitrogen. The product stream contained H_2 , N_2 , CO, CH_4 , and small amounts of CO_2 gas. The operating temperature and pressure of the reaction were kept constant at 350 °C, and 30 psig, respectively. The flow rate of the feed was kept constant at 600 ml/min and 10 gm. of catalyst was charged for each run.

The catalyst used was a commercial $\text{Ni}/\gamma\text{Al}_2\text{O}_3$ (C13-4-04) containing 20% Ni supported on $\gamma\text{Al}_2\text{O}_3$; manufactured by UCI (United Catalyst Inc.) and supplied by SAMAD Fertilizer Co. Al-Jubail, Saudi Arabia.

The effects of speed of impeller on the rate of methanation were studied and it was found that mass transfer limitations disappeared at a speed of 786 rpm.

The effects of space-time, H_2 :CO ratio, and pressure on the activity and selectivity of the catalyst were studied. It is found that by increasing the space-time, the activity decreases while selectivity to CH_4 formation increases from 90 to 96%. Use of higher H_2 /CO ratio (3.0-6.5) improves selectivity up to 98%, but decreases the rate of methanation. Lower H_2 /CO ratio (3.0-1.0) increases rate of CO conversion but decreases both the selectivity and the rate of CH_4 production. Reaction pressure apparently has an insignificant effect on the activity of catalyst. However, improvement in the selectivity is observed.

MASTER OF SCIENCE DEGREE

KING FAHD UNIVERSITY OF PETROLEUM AND MINERALS

Dhahran , Saudi Arabia

May 1992

« الخلاصة »

إسم الطالب : سيد ثمين علي زبيدي

عنوان الرسالة : فاعلية الحفاز $Ni/\gamma Al_2O_3$ لتفاعل الميثان

التخصص : هندسة كيميائية

تاريخ الرسالة : مايو ، ١٩٩٢م

تم إختزال الحفاز التجاري $Ni/\gamma Al_2O_3$ في درجات حرارة من ٢٥٠ - ٥٠٠ م ولمدة تتراوح من ٢ - ١٦ ساعة تمت دراسة تأثير ظروف الاختزال على فاعلية وانتقائية الحفاز لتفاعل الميثان في مفاعل بيرتي وإستعملت هذه التأثيرات لإيجاد الظروف المثلى لاختزال الحفاز كما يلي : الحرارة ٣٠٠ م ، المدة ٨ ساعات ، السرعة ٢٠٠٠ دورة / الساعة ، معدل التسخين ٥ م / الدقيقة .

تم قياس معدل التفاعلات بحقن خليط من الهيدروجين (٢٦٪) وأول أكسيد الكربون (٦,٧٪) والنييتروجين وقد احتوى الناتج على الهيدروجين ، النيتروجين ، أول أكسيد الكربون ، والميثان وكمية قليلة من ثاني أكسيد الكربون . تم تثبيت درجة الحرارة والضغط في ٢٥٠ م و ٣٠ رطل / بوصة على التوالي كما تم تثبيت معدل الانسياب في ٦٠٠ مل/الدقيقة وتزويد المفاعل بعشرة جرامات من الحفاز لكل تجربة .

تم إستعمال الحفاز التجاري $Ni/\gamma Al_2O_3$ (سي. ١٣ - ٤ - ٠٤) والذي يحتوي على ٣٠٪ نخل محمل على γAl_2O_3 والذي تم تصنيعه بواسطة UCC (الشركة المتخصصة للحفازات) وتم إمدادنا به بواسطة شركة سعاد للمخصبات بالجبيل بالمملكة العربية السعودية .

تمت دراسة تأثير سرعة الدوار على معدل التفاعل ووجد أن قصور انتقال المادة يختفي عند السرعة ٧٨٦ دورة / الدقيقة .

تمت دراسة تأثير الزمن ، نسبة الهيدروجين الى أول أكسيد الكربون والضغط على فاعلية وانتقائية الحفاز ووجد أن الفاعلية تتناقص بزيادة الزمن بينما تزداد الانتقائية من ٩٠ - ٩٦٪ . إستعمال نسب أعلى من الهيدروجين الى أول أكسيد الكربون (٣ - ٦,٥) أدى الى تحسين الانتقائية الى ٩٨٪ مع تقليل معدل التفاعل . إستعمال نسب أقل من الهيدروجين الى أول أكسيد الكربون (١ - ٣) أدى لزيادة تحويل أول أكسيد الكربون مع إنقاص الانتقائية ومعدل إنتاج الميثان ولم يكن هنالك تأثير مهم للضغط على فاعلية الحفاز ولكن لوحظ تحسن في الانتقائية .

درجة ماجستير العلوم

جامعة الملك فهد للبترول والمعادن

الظهران . السعودية

CHAPTER 1

INTRODUCTION

1.1 IMPORTANCE OF METHANATION CATALYST

Carbon monoxide and carbon dioxide are catalyst poisons in many hydrogenation reactions, including ammonia synthesis. It is necessary in ammonia plants and in hydrogen plants to reduce the final amount of carbon oxides, remaining in the process gas after carbon dioxide removal stage, to extremely low levels. In about all ammonia and hydrogen plants constructed since 1960s the simple and relatively inexpensive catalytic conversion of traces of carbon oxides to methane and water has been used. This process is called methanation.

The catalytic methanation reaction has been studied during the past 89 years. Sabatier and Senderens (in their pioneering work) [1], found that nickel was a very efficient catalyst for methanation. Prior to the availability of copious supplies of natural gas, methane was made commercially by reacting carbon monoxide and hydrogen, derived from the pyrolysis of coal with subsequent gas processing. Although the production of methane on a large scale virtually ceased following the discovery of natural gas, the methanation reaction was employed in ammonia processing plants for the removal of small quantities of carbon monoxide from the ammonia synthesis gas. For this purpose, it is adequate to use a 20-25 wt% nickel catalyst (expressed as NiO)

supported on alumina (Al_2O_3) at 300-350°C and at any pressure (depending on downstream plant requirements) ranging from 1 to 300 bar [2].

Methanation catalyst, designed for ammonia and hydrogen plants, can also be used for purification of hydrogen in refineries and ethylene plants where recycle streams free from carbon oxides are required. Methanation reactions are also used in the production of various substitute natural gas (SNG) that contain large amounts of methane. These processes may be of well importance in future.

The methanation reaction, which is the reverse of methane steam reforming reaction, is highly exothermic and could cause thermal deactivation to catalyst. Therefore, the process gas is recycled in order to acquire better temperature control. The catalyst deactivation could also occur by the formation of carbidic precursors which can rapidly lead to undesirable carbon deposition, therefore, the conditions during start-up and during operation must be carefully controlled [3]. For this reason knowledge of deactivation process is of considerable importance.

Commercial nickel catalysts, available in market, are generally supported on SiO_2 or Al_2O_3 . The activity and the selectivity of supported nickel catalysts are dependent on their chemical and physical properties. These properties include the chemical composition (bulk & surface), thermal behavior, crushing strength, pore size distribution, the total and active surface area, dispersion, crystallite size of nickel, and process conditions.

Nickel based catalysts, because of their pyrophoric nature, are loaded in

reactor in oxidized form. The active catalyst, however, is in the reduced form. The activation of catalyst requires a suitable gaseous reducing agent (i.e. H_2). Now-a-days, prereduced catalysts requiring less time for reduction are also available.

In this investigation a commercial $Ni/\gamma Al_2O_3$ (C13-4-04;20%Ni) catalyst was reduced at several reduction conditions of temperature and duration. Methanation reaction was carried out, after the reduction, to establish the optimal reduction condition of $Ni/\gamma Al_2O_3$ catalyst in order to acquire highest activity of the catalyst. Different process conditions were also employed for methanation reaction to observe their effects on the activity and selectivity of the $Ni/\gamma Al_2O_3$ catalyst. Reduction of the catalyst was carried out at different operating conditions as specified in a recent report of King Abdulaziz City for Science and Technology (KACST), Saudi Arabia [4]. The catalyst, 1/4" spheres of $Ni/\gamma Al_2O_3$, was supplied by SAMAD Fertilizer Co. (Al-Jubail, Saudi Arabia) for this research work.

1.2 OUTLINE OF PRESENT STUDY

In this investigation, the reduction of a commercial $Ni/\gamma Al_2O_3$ (C13-4-04;20%Ni) catalyst is carried out at different operating conditions of temperature and duration, as specified in a technical report of KACST project [4]. A study is conducted, by carrying out methanation reaction using CO and H_2 , to investigate the effects of reduction conditions on the activity and selectivity of the $Ni/\gamma Al_2O_3$ catalyst in order to obtain the optimal reduction

conditions. The obtained optimal reduction conditions and their effects on the activity are compared with the reduction conditions recommended in the KACST report [4]. An investigation on a change in activity of $\text{Ni}/\gamma\text{Al}_2\text{O}_3$ catalyst with time is carried out in order to investigate the stability of the catalyst. The degree of mixing of reactants are investigated by changing the speed of impeller, which is further used to establish the absence of mass transfer resistances in the reactor after a certain speed of impeller.

An investigation is carried, at optimal reduction conditions, in which several higher and lower stoichiometric ratios (7:1 to 1:1) of H_2/CO are used for methanation reaction in order to observe their effects on the activity and selectivity of the $\text{Ni}/\gamma\text{Al}_2\text{O}_3$ catalyst. The process conditions (e.g. flow rate of feed and pressure of reactor) are varied during the course of methanation reaction study and their effects on the activity and selectivity of the catalyst are also studied.

CHAPTER 2

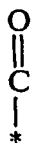
LITERATURE REVIEW

2.1 ADSORPTION STUDIES

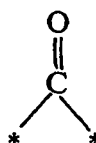
The study of adsorption of CO and H₂ on the surface of Ni-catalyst for a methanation reaction provides important information regarding the bond strength (heat of adsorption) between metal and reactant, and the composition of reactive surface complexes. This knowledge clarifies the reaction path for methanation. For years, arguments have existed regarding the adsorption of H₂ and CO for methanation, and the arguments for and against have been mentioned elsewhere [5-8].

2.1.1 *Adsorption of CO*

The several pathways of CO adsorption on the surface of Ni-catalyst can be divided into two general groups: one which involves hydrogenation of adsorbed CO prior to the rupture of CO bond, and the other in which CO first dissociates into surface carbon and atomic oxygen which is then hydrogenated. The CO can be adsorbed on nickel in two forms: it can be adsorbed on only one site of the nickel or can be adsorbed on two neighbouring metal sites by making a bridge.



Linear adsorption



Bridged adsorption

Both of these forms may exist on Ni-surface, but bridged adsorption is only observed for a very well reduced surface [5,73]. It is observed that linear species are less stable than the bridged, and can be removed rapidly. Vannice [9] found a relationship between heat of adsorption of CO and the rate of methanation i.e. the rate of methanation decreases as the heat of adsorption increases. The chemisorption of CO on Ni-surface was further studied by Yates et al. [10] through IR spectroscopy. An assignment of the IR bands to surface species was made for CO chemisorbed on Ni-samples at room temperature and is shown in Table 2.1.

Vlasenko [11] found that by increasing the pressure to 3mm of Hg, there was a rapid increase in the amount of CO (7.5 cu.cm./g) adsorbed on the Ni-surface. After initial CO adsorption, the amount of the adsorbed CO increased more slowly by increasing the pressure. However, no desorption of CO was observed by decreasing the pressure. This type of isotherm suggested that at low pressure, CO was adsorbed in form of bridged species. The change in bond character from bridged to linear species occurred by increasing the pressure.

The presence of oxygen atoms, in comparison to a pure metal, alters the energy of adsorption on the adjacent nickel atoms. This happens because of incomplete reduction of NiO [5]. CO does not adsorb on NiO. Therefore, addition of oxygen at room temperature to the adsorbed CO on nickel causes

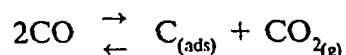
*Table 2.1 Assignment of Infrared Bands to Surface Species for CO
Chemisorbed on Supported Ni Samples at Room Temperature [23]*

Band	Frequency cm ⁻¹	Species	Site	Strength of adsorption
A	1915	$\begin{array}{c} \text{O} \\ \\ \text{C} \\ / \quad \backslash \\ \text{Ni} \quad \text{Ni} \end{array}$	Crystalline Ni	Very strong
C	2035	$\begin{array}{c} \text{O} \\ \\ \text{C} \\ \\ \text{---Ni---} \end{array}$	Crystalline Ni	Very strong
B	1963	$\begin{array}{c} \text{O} \text{ O} \text{ O} \\ \quad \quad \\ \text{C} \text{ C} \text{ C} \\ / \quad \backslash \quad / \\ \text{---Ni---Ni---} \end{array}$	Crystalline Ni	Moderately strong
D	2057	$\begin{array}{c} \text{O} \\ \\ \text{C} \\ \\ \text{---Ni---} \end{array}$	Semi- crystalline Ni	Moderately strong
E	2082	$\begin{array}{c} \text{O} \\ \\ \text{C} \\ \\ \text{---Ni---} \end{array}$	Dispersed Ni	Weak

rapid removal of CO from the surface [5].

The support in a homogeneous metal catalyst plays an important role; because, the addition of support not only increases the surface area and metal exposure to adsorbing gas but also dispersed metal may interact with support in such a way that the catalytic properties of the metal can be modified. Alumina and titania, as support, induce variations in the relative proportions of both species (linear & bridged) on the surface and their strengths of adsorption. Silica, on the other hand, does not affect adsorption [5].

Fischer and Tropsch [12] discovered that the adsorbed carbon species on nickel surface may not be a metal carbide. This modification of the "carbon intermediate" mechanism removed the difficulties of their model that they were encountering. [13]. Concurrent studies by Wentreck et al. [14] and by Araki et al. [15] have conclusively shown that surface carbon produced from dissociated CO can be readily hydrogenated to form methane. In the former study, the surface carbon was deposited on a commercial Ni/Al₂O₃ catalyst via Boudard reaction at 553°K in a pulse microreactor at 446kPa:



The quantity of carbon deposited was measured by the amount of CO₂ produced. When amount of H₂ was pulsed through the catalyst bed, the amount of CH₄ formed was in agreement with the amount of carbon deposited. It was also found that this reactive (carbide) form can also be converted to a less active (graphite) form. Araki et al. [15] used labeled CO isotopes over Ni and Ni-Cu films at low pressure (80Pa) in a non-circulating

batch reactor. When CO/H_2 were introduced to a clean reduced Ni-film, CO_2 was immediately produced. On the other hand CH_4 was formed after an induction period. When a $^{12}\text{CO}/\text{H}_2$ mixture introduced to a $^{13}\text{C}_s$ covered surface, the formation of $^{13}\text{CH}_4$ and $^{12}\text{CH}_4$ took place rapidly and $^{12}\text{CO}_2$ formed after an induction period. It was proposed that C_s forms as an intermediate in methanation reaction and easily reacts with H_2 to form methane.

McCarty et al. [16] in their TPR (Temperature Programme Reaction) studies proved that different types of surface carbons are formed. Some are active and some are less active. Only the most active carbon reacts readily at low temperatures with H_2 to produce CH_4 . They also found that at high temperature, non-dissociatively adsorbed CO directly reacts with H_2 thus reduces the rate of reaction.

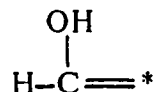
2.1.2 Adsorption of H_2

The adsorption of H_2 is such that one atom of hydrogen occupies one site of Ni-surface. Vlasenko [11] found that hydrogen adsorption was very sensitive to a pressure up to 20 mmHg. It was found that hydrogen adsorption decreases with rise in temperature (100-700 °K) [17]. Beeck [18] measured the heat of adsorption (14-30 kcal/mol) of H_2 at 23°C. The heat of adsorption decreases with fraction surface coverage. The rate of H_2 adsorption is instantaneous indicating a very low activation energy for adsorption; hence, the heat of adsorption at lower temperature would be the

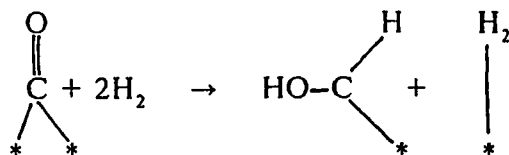
same as it is at room temperature.

2.1.3 *Coadsorption of CO and H₂*

An increase in the heat of adsorption is measured during a simultaneous adsorption of CO and H₂ on the surface of catalyst as compare to either of the gases in pure state [19,20]. It is observed that in the presence of hydrogen, linear type chemisorption takes place [11]. Some studies suggest [9,11,38] that the following complex forms on the surface:



Vlasenko [11] also showed that in presence of adsorbed CO, the amount of hydrogen adsorbed was about twice the amount adsorbed on a surface free from CO. This is explained as follows:



Farrauto [21] performed an adsorption study on Ni/Al₂O₃ at 1 atm. and the temperature ranging from 100-400 °C for the methanation reaction. He observed that at 200°C, the surface reaction leading to products was slow and most of the surface was covered with active methanation complex; as the temperature increased, the surface reaction became competitive with the adsorption rate and the steady-state coverage started to decrease; at 300°C

the rate of reaction was so rapid that the life-time of adsorbed active surface species was quite low.

Zagli et al. [22] have employed both TPD (Temperature Programme Desorption) and TPR (Temperature Programme Reaction) techniques in a study of three supported Ni catalysts. The desorption states of CO and the formation patterns during TPD were quite different for each catalyst. They found as others had previously [20], that CO and H₂ coadsorb at 300°K in approximately a 1:1 mole ratio and in addition, hydrogen remains on the surface during TPR to react and finally desorbs as CH₄ and H₂O. During runs of TPR, CH₄ and H₂O desorbed simultaneously which indicated that C-O bond-breaking step is rate determining.

2.2 METHANATION CHEMISTRY AND THERMODYNAMICS

The methanation chemistry can be described by four independent reactions in which a mixture of carbon oxides and hydrogen are reacted on a nickel catalyst. These reactions are: the methanation reaction, the water-gas shift reaction, the Boudard reaction and the decomposition of methane to carbon and hydrogen.

When hydrogen to carbon monoxide ratio in synthesis gas is equal to or greater than 3, then the methanation reaction can be described by the following reaction:



Methane can also be formed by the hydrogenation of carbon oxides in two other reactions:



However, reaction (3) does not occur in presence of carbon monoxide.

The water-gas shift reaction, in which one mole of carbon monoxide combines with one mole of water to give carbon dioxide and hydrogen, is shown as follows:



The formation of carbon is a possible side reaction and can be represented by two reactions. The first reaction is a Boudard reaction in which two moles of carbon monoxide react with each other to form one mole of carbon and one mole of carbon dioxide. This reaction proceeds at a fast rate at temperatures close to 315°C. It is represented as follows:



The second carbon formation reaction is the decomposition of methane to carbon and hydrogen. It proceeds at a fast rate at high temperatures of about 700°C. The reaction is shown as follows:



Methanation (eq.1) is the desirable reaction. The equilibrium product distribution can be obtained by three reactions which are: the methanation reaction, the water-gas shift reaction and the Boudard reaction.

Thermodynamic values for above mentioned reactions are taken from the reviews of Mills [23] and are tabulated in Table 2.2. It is observed that all reactions are exothermic, and except reaction (4) others are highly exothermic. The high release of heat either thermally deactivates the catalyst or limits the rate of methanation reaction by thermodynamic equilibrium. It is noted that heat of reactions is not greatly influenced by temperature, but the free energies and equilibrium constants of these reactions are highly dependent on temperature.

Equilibrium methane yields are affected by temperature and by H_2/CO ratios. Theoretically, methane yields are highest at lower temperatures and at higher ratios. Pressure does not appreciably affect methane yield until a temperature of about $425^\circ C$ is exceeded.

The effect of temperature, pressure and synthesis gas ratios on the degree of carbon deposition from reaction (5) was studied by the bureau of mines and White et al. [24,25]. The possibility of formation of metal carbide increase with the existence of carbon on the surface of catalyst, which can alter the catalytic behavior of metal. The Bureau of mines [24] has reported limiting ratios of hydrogen to carbon monoxide for various temperatures and pressures below which carbon deposition occurs on the catalyst. These temperatures range from 500 to $1400^\circ K$ and pressures from 1 to 26 Kg/cm^2 . A similar behavior was also reported by Madhava [26] for the same range of

Table 2.2 *Thermodynamic Data on Five Reactions Relevant to the Methanation Process Catalyzed by Nickel Based Catalyst [23]*

1. $\text{CO} + 3\text{H}_2 \rightleftharpoons \text{CH}_4 + \text{H}_2\text{O}$
2. $2\text{CO} + 2\text{H}_2 \rightleftharpoons \text{CH}_4 + \text{CO}_2$
3. $4\text{H}_2 + \text{CO}_2 \rightleftharpoons \text{CH}_4 + 2\text{H}_2\text{O}$
4. $\text{CO} + \text{H}_2\text{O} \rightleftharpoons \text{CO}_2 + \text{H}_2$
5. $2\text{CO} \rightleftharpoons \text{C} + \text{CO}_2$

Temperature		Reaction				
°K	°C	1	2	3	4	5
Heat of Reaction ΔH (kcal)						
300	27	-49.298	-59.136	-39.460	-9.838	-41.227
400	127	-50.360	-60.070	-40.650	-9.710	-41.434
500	227	-51.297	-60.815	-40.779	-9.518	-41.499
600	317	-52.084	-61.376	-42.792	-9.292	-41.460
700	427	-52.730	-61.780	-43.680	-9.050	-41.350
800	527	-53.248	-62.047	-44.449	-9.799	-41.190
900	627	-53.654	-62.203	-45.105	-8.549	-40.996
1000	727	-53.957	-62.261	-45.653	-8.304	-40.729
Free Energy of Reaction ΔG° (kcal)						
300	27	-33.904	-40.731	-27.077	-6.827	-23.621
400	127	-28.610	-34.451	-22.769	-5.841	-24.385
500	227	-23.062	-27.956	-18.168	-4.894	-20.111
600	327	-17.338	-21.329	-13.347	-3.991	-15.836
700	427	-11.493	-14.620	-8.366	-3.127	-11.574
800	527	-5.567	-7.865	-3.269	-2.298	-7.332
900	627	+0.594	-1.079	+1.921	-1.500	-3.108
1000	727	+6.444	+5.715	+7.173	-0.729	+1.090
Equilibrium Constant (Log K_p)						
300	27	-24.698	-29.670	19.724	4.973	20.849
400	127	15.630	18.822	12.440	3.191	13.322
500	227	10.080	12.219	7.940	2.139	8.790
600	327	6.314	7.768	4.861	1.453	5.768
700	427	3.588	4.540	2.611	0.976	3.613
800	527	1.521	2.148	0.893	0.825	2.003
900	627	-0.144	0.261	-0.466	0.364	0.755
1000	727	-1.408	-1.248	-1.568	0.159	-0.238

temperature and pressure. Figure 2.1 shows the deposition of carbon that may occur in the area beneath curve but above the curve no carbon will be deposited. It was observed that operation at high pressure tends to permit the use of lower H_2/CO ratios without the deposition of carbon on the catalyst. However, operation at higher pressures produces a large quantity of heat per unit volume. If adequate means of heat removal are not available then there will be an increase in catalyst bed temperatures and decrease in the methane yield.

Nickel-molybdenum catalysts do not appear to deposit significant carbon at 1.5 hydrogen to carbon monoxide ratio [27]. This suggests that a major improvement in the catalyst may be achieved by adding molybdenum as a promoter to nickel catalysts.

2.3 KINETICS OF METHANATION REACTION

Extensive literature is available on kinetics of methanation reaction over Ni catalyst. Different systems e.g. packed bed reactor, differential reactor and different operating parameters have been used to carry out kinetic studies.

Several rate expressions have been published for the methanation of CO, but very few of these are related to actual ammonia/hydrogen plants conditions. Power-law rate equation, as shown below, is frequently used to describe the formation of methane.

$$\text{rate} = k P_{CO}^n P_{H_2}^m$$

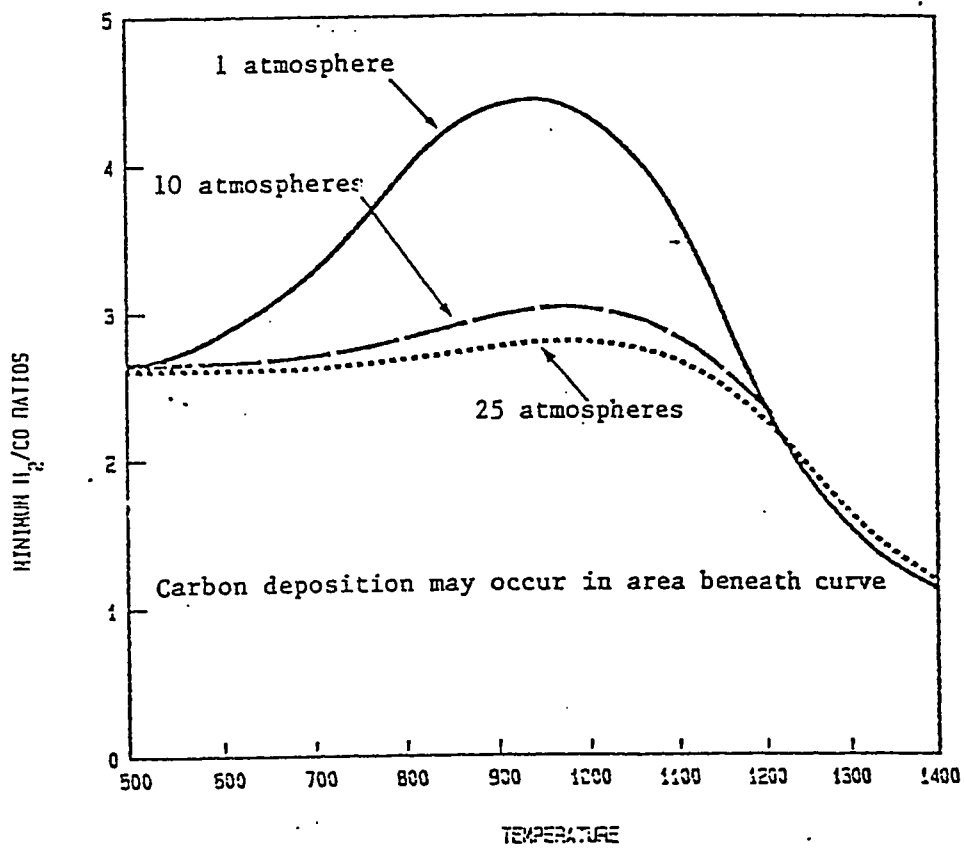


Figure 2.1 Carbon Deposition Boundaries in the Methanation Process [23]

The value of m for most conditions is positive and close or equal to unity. However, negative as well as positive values of n ranging from -1 to +1 have been mentioned in the literature. Only, at low CO partial pressures combined with high hydrogen pressure, hydrogen can compete sufficiently with carbon monoxide for adsorption studies; n then becomes greater than zero. Under process conditions the methanation of CO is first order, but the reaction may not show first-order dependence on total pressure because of diffusion and retardation effects. Some selected rate expressions for CO methanation are discussed as follows:

The first kinetic equation was presented by Nicolai [28] for a nickel catalyst at low pressures ranging from 0.1 to 1 atm. and temperature from 180 to 300 °C. The carbon monoxide was strongly adsorbed and reacted first. Carbon dioxide began to react rapidly after the carbon monoxide was used up. A kinetic expression was derived based upon Langmuir's theory as follows:

$$r = K(P_{H_2})^{0.9}(P_{CO})^{-0.2}$$

where,

P_{H_2} and P_{CO} are partial pressures of hydrogen and carbon monoxide, respectively.

In 1969, Schoubye [29] investigated the kinetics of methanation of carbon monoxide and hydrogen over a number of nickel catalysts in a once-through differential reactor. He used catalyst pellets of varying sizes (0.3mm to 0.5mm). The study was carried out with mixtures containing 10-20% carbon monoxide at temperatures ranging from 200-300 °C and pressures from 2-15

atmosphere. These operating conditions resembled the dilute concentrations as found in tail-end cleanup in ammonia synthesis plants. He developed the following rate expression from his study:

$$r = \frac{Z_1 e^{\frac{-E}{RT}} P_{H_2}^m P_{CO}}{1 + [Z_2 e^{\frac{-16,500}{RT}} \frac{P_{CO}}{P_{H_2}}]^{0.5}}$$

where

Z_1 is the specific reaction rate constant, Z_2 is the adsorption equilibrium constant, and $m=0.15$ is obtained experimentally. He also observed diffusion limitations for particles larger than 0.3mm.

In 1973, Van Herwijnen et al. [30] studied the kinetics of carbon monoxide methanation on supported nickel catalyst in the temperature range of 170-210 °C and at a pressure of 1atm. The CO percentage varied from 0.1 to 2.5% on crushed G-65 Girdler catalyst containing 33.6% Ni on γAl_2O_3 having a particle size of 0.35-0.45mm. These conditions also resemble the concentration in commercial methanators. The rate expression was given as:

$$r = \frac{K_1 P_{CO}}{1 + K_2 P_{CO}^2}$$

They found that H_2O and CH_4 in small concentrations had no effect on the reaction rate. They also concluded that diffusion limitations were not significant.

In 1970, Lee et al. [31] investigated the methanation reaction using feed mixtures containing variable quantities of carbon monoxide, hydrogen,

helium, methane, benzene, mercaptans (0.3mm), thiophene (0.8ppm), steam (up to 5%), and nitrogen less than 50%). These mixtures contained carbon monoxide percentages varying from 2.4 to 10%, the ratio of H_2 to CO being kept constant at 3. The nickel pellets which were used as the catalyst for this study varied from 1/8" to 1/4", and temperature and pressure ranged from 550 to 900 °F (260 to 482 °C) and 1 to 72 atm., respectively. The effect of high concentration of methane in the feed, ranging from 53 to 82%, was studied. They found that methane affected the rate only near equilibrium. The following rate expression was developed:

$$r = \frac{kP_{CO}P_{H_2}^{0.5}}{(1 + K_2P_{H_2} + K_3P_{CH_4})}$$

Steam, benzene and sulfur compounds were found to have no appreciable effects on the methanation rates. It was concluded that the operating conditions were more representative of those for making synthetic methane, but diffusion effects were quite significant.

It is difficult to have an intrinsic (without diffusion resistance) kinetic data for methanation reaction by using conventional packed studies at industrial temperatures and pressures. For such difficulties the Berty reactor is found to be applicable. Hausberger et al. [32] developed an approximate empirical procedure for preliminary design using commercial nickel catalyst and compared it to a number of other equations in the literature. Mills et al. [23] in 1973 and Vannice [19] in 1976 have reviewed some of the published rate expressions.

Madhava [26] in 1977 in his Ph.D dissertation studied the methanation reaction on cylindrical pellets (3mmx3mm) of 58%Ni catalyst supported on kieselguhr support in a Berty reactor. The reaction conditions being the pressure ranged from 14.50-71.30Kg/ cm² and temperature ranged from 315 to 593 °C. The rate expression obtained is given as:

$$\text{rate} = 1.21 \times 10^7 e^{\frac{-13,000}{RT}} P_{\text{CO}} P_{\text{H}_2} - 2.9 \times 10^8 e^{\frac{-28688}{RT}} P_{\text{CH}_4} P_{\text{H}_2\text{O}}$$

At 315 °C the rate expression simplified to only forward rate. His measurements indicated the existence of interphase mass transfer resistance. Measurements of the reaction rate made on a sample of powdered catalyst indicated minimal intraphase resistance.

Al-Saleh [27] studied methanation reaction in a spinning basket reactor using three different catalysts supported on alumina: nickel, nickel-molybdenum, and molybdenum. Different rate expressions, free from any physical resistance, were obtained for these catalyst. All kinetic data was taken at 22 psia with feed gases containing 4/1 and 2.3/1 ratios of H₂ and CO. The turnover rate expressions were as follows:

Ni-catalyst

$$N_{\text{CH}_4} = 1.361 \times 10^6 \text{Exp}\left(\frac{-21134}{RT}\right) P_{\text{CO}}^{0.7} P_{\text{H}_2}^{0.3} \quad (400-500^\circ\text{F})$$

selectivity to CH₄ was 90%

where, N_{CH₄} is turnover number defined as number of molecules reacted per site per second.

Ni-Mo catalyst

$$N_{CH_4} = 8.12 \times 10^7 \text{Exp}\left(\frac{-26334}{RT}\right) P_{CO} \quad (450-600^\circ\text{F})$$

selectivity to CH_4 was 80%

Mo-catalyst

$$N_{CH_4} = 3.14 \times 10^7 \text{Exp}\left(\frac{+10494}{RT}\right) P_{CO} \quad (680-800^\circ\text{F})$$

selectivity to CH_4 was 60%

It was observed that Ni-Mo catalyst was less active than Ni catalyst. It was also observed that Ni-Mo was found to be a potential candidate for both methanation and shift reaction since it did not promote carbon deposition when a hydrogen deficient gas is used.

Becker et al. [33] studied the methanation kinetics on nickel catalyst at high pressures (30 & 90 bar) and at isothermal conditions, which are close to an industrial process conditions, in a fixed bed reactor. The measurements of kinetic data were performed at p_{H_2} between 22.5 and 67.5 bar and p_{CO} between 7.5 and 22.5 bar, and temperature varied between 360 °C and 540 °C. Following rate expression was observed:

$$-r_{CO} = 3 \times 10^{10} e^{\frac{108000}{RT}} P_{H_2}^{0.56}$$

Saha et al. [34] performed kinetic studies for methanation on Pd supported on ZMS5 and Y-zeolite catalyst. Studies were carried out at

atmospheric pressure and temperature ranging from 300-550 °C in a quartz flow reactor. They developed the following rate expression from the kinetic data:

$$R_{CH_4} = 3 \times 10^7 e^{\frac{-238000}{RT}} P_{H_2}^{0.73} P_{CO}^{-0.27}$$

They found that activation energy of 23.8kcal/mol was in agreement with the values of 21.2kcal/mol reported by Vannice [9]. However, Vannice [9] reported a positive order of 0.84 and 0.3 for H₂ and CO pressures, respectively. Saha et al. [34] have also tabulated rate expression in terms of turnover numbers for Pd catalyst with different support.

Hays et al. [35] studied 9%Ni-catalyst (containing 1.5%Pt) for methanation reaction at temperatures ranging from 260-300 °C and pressures from 0.1-0.5MPa. They used a packed microreactor, capable of operating at elevated pressures, in order to study reaction rates and catalyst deactivation. They fitted the kinetic data to an empirical power law model and developed the following rate expression:

$$r = 8.79 \exp\left(\frac{-9270}{T}\right) P_{H_2}^{1.27} P_{CO}^{-0.87} P_{H_2O}^{-0.13}$$

where, reaction rate is expressed in mol/g.s, the partial pressures in bar and temperature in degree Kelvin. The activation energy was found to be 78kJ/mol which was slightly lower than normally reported for methanation over nickel. It is seen that in rate expression, partial pressure of water is included which is inhibiting the rate. On the other hand, methane is excluded, as it did not influence the rate.

Lowe et al. [36] studied methanation reaction over Ni/Al₂O₃ (commercial Girdler G65) in a concentration controlled recycle reactor to obtain separate single reaction kinetics. Kinetic data was obtained at 30bar and at 310-330 °C. The following power-law rate equation was fitted to kinetic data:

$$r = x_{CO}^n x_{H_2}^m x_{H_2O}^u$$

The reaction orders were found as: $n = -0.173$, $m = -0.81$, $u = -0.098$. The activation energy was found as 107kJ/mol. It was found that CH₄ and CO₂ has no effect on rate of reaction.

Levi et al. [37] studied kinetics of sulfided bimetallic Mo-Fe and Mo-Co supported on γ -Al₂O₃ catalyst. They found besides methanation reaction, dimethyl ether was also significantly formed. They used the following equation for rate which is generally used to describe the activity of most of methanation catalysts:

$$N_{CH_4} = A \exp\left(\frac{-\Delta E_a}{RT}\right) p_{H_2}^n p_{CO}^m$$

where, N_{CH_4} is turnover frequency defined as number of molecules reacted per site per unit time.

The values of constants in above expression for different catalysts are given as follows:

for pMoFeS/ Al₂O₃, $A = 2.1 \times 10^3$ 1/S, $\Delta E_a = 85.2$ kJ/mol, $n = 0.7$, $m = 0.37$

for bMoFeS/ Al₂O₃, $A = 3.8 \times 10^4$ 1/S, $\Delta E_a = 97.9$ kJ/mol, $n = 0.7$, $m = 0.34$

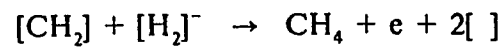
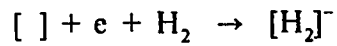
for MoCoS/ Al_2O_3 , $A = 2.7 \times 10^2 \text{ l/S}$, $\Delta E_a = 79.7 \text{ kJ/mol}$, $n = 1.21$, $m = 0.14$

They found that the effect of CO on the rate for MoCo-catalyst was nearly insignificant.

2.4 METHANATION MECHANISMS

The earliest proposal for hydrocarbon synthesis was the carbide theory by Fischer Tropsch [12]. According to this theory, adsorbed carbon monoxide is reduced to carbide at the surface of the catalyst. The surface carbide is hydrogenated and the adsorbed methylene radicals polymerize to form paraffinic hydrocarbons (methane in our case). Carbide theory was originally based on metal catalysts i.e. iron, cobalt, and nickel. This theory was found inadequate when applied to metal catalysts of iron group. Other theories of methanation stated the formation of oxygenated complexes like methanol or formaldehyde intermediates. However, experimentally these theories were not verified.

Several workers have concluded that synthesis based on CO and H_2 involves the production of an unstable intermediate complex, containing C, H, and O atoms; which is the precursor of both hydrocarbon and alcohols. Generally, two relative mechanisms deserve special considerations. Both involve the concept of initial formation of a HCOH surface complex, but differ in subsequent steps. The first one assumes methylene radical formation from HCHO and emphasizes on the electronic charge or the polarization factors. Vlasenko [38] suggested a scheme applicable to transition metals (Ni, Co etc.) shown as follows:

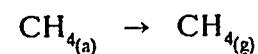
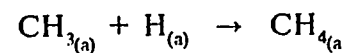
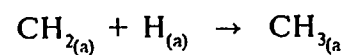
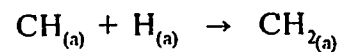
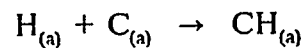
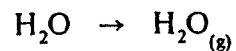
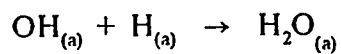
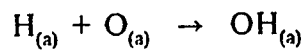


where

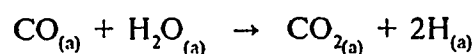
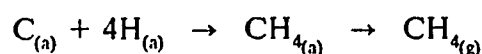
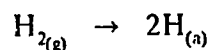
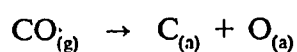
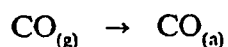
$[]$ is a vacant site on catalyst surface

e = electron

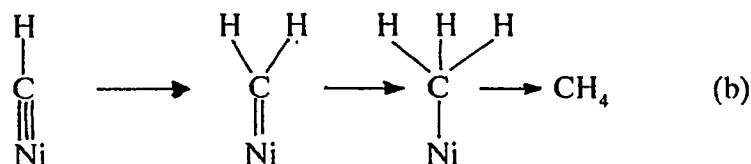
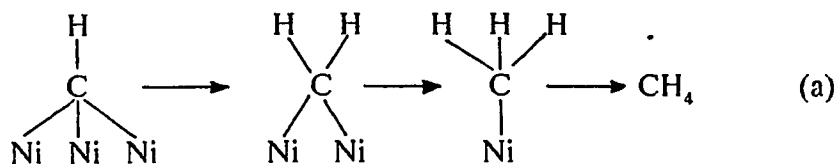
Zagil et al. [39] studied the methanation reaction on supported Ni catalyst using temperature programme heating. They concluded that H_2 was not involved in the rate determining step, but rather splitting of C-O bond was the likely rate determining step. The following elementary steps were proposed:



Fujimoto et al. [40] investigated the hydrogenation of adsorbed CO on supported platinum group metals by IR spectroscopy and temperature programme desorption methods. They proposed the following steps describing the methanation reaction:

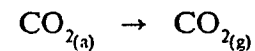
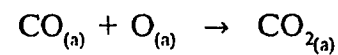
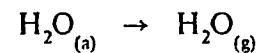
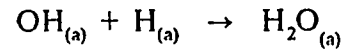
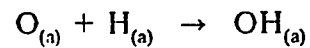
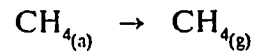
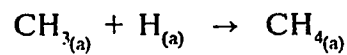
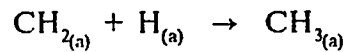
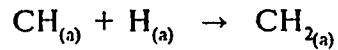
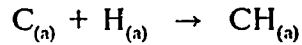
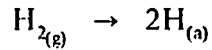
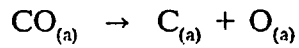
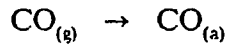


Hays et al. [41] studied methanation reaction mechanism on $\text{Ni}/\gamma\text{Al}_2\text{O}_3$ using multiple reflectance infrared spectroscopy (MIRS). They observed that reaction takes place via a surface nickel carbide route. They also considered the reaction intermediate found in their previous publication [42], and observed that two catalytic routes are possible. In the first step, CO chemisorbs dissociatively and then adsorbed C is hydrogenated in one of the two ways as follows:



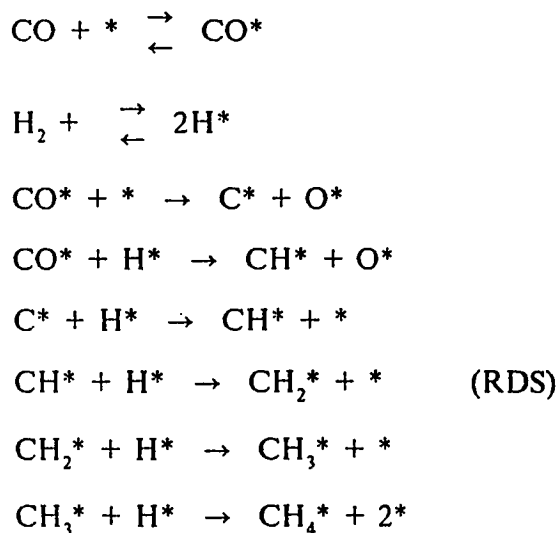
The mechanism (a) was not observed in the previous infrared experiments [42]. This was due to difference in the metal preparation, as the plates in the previous investigation were mechanically polished prior to use.

Vandervell et al. [43] carried out methanation reaction on a nickel catalyst in a plug flow reactor using temperature programme synthesis (TPS). They concluded that there is a competition between H_2 and CO for surface oxygen. It was found that for low CO level ($H_2/CO=24$), H_2 was the main oxidized product. While at high CO level ($H_2/CO=1.24$), CO_2 was prominent. The detailed reaction mechanism is given as follows:



Similar schemes were proposed by Sughrue et al. [44] and Underwood et al. [45], but in their mechanisms the last two steps of the above mentioned scheme were omitted.

Yadav et al. [95] have recently studied a transient behavior of methanation in a Berty type gradientless reactor by making step changes in feed composition from CO/H₂ to H₂ reactor. From step responses they found that for higher H₂/CO ratios the abundant species on Ni/Al₂O₃ catalyst surface is CH. For lower H₂/CO ratios C was found as an intermediate species. They also observed that for stoichiometric ratio, which is close to optimal steady-state operation, both intermediates are important i.e. CO is adsorbed on the Ni surface directly as well as dissociatively. On the basis of results, they have suggested a following mechanism for methanation:

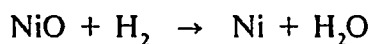


where * represents an active site.

2.5 CHEMISTRY AND THERMODYNAMICS OF REDUCTION OF NICKEL CATALYST

The reduction of nickel catalyst involves the conversion of NiO in the catalyst matrix to metallic Ni which is the active component of the catalyst. Several publications have appeared in recent years which describe the reduction of Ni catalyst [46-48].

The reduction of nickel oxide by hydrogen is given by following equation:



The thermodynamic properties i.e., heat of reaction (ΔH), free energy of reaction (ΔG), and equilibrium constant (k) of the above reaction are shown in Table 2.3.

Over the temperature range of 300-800 °K it can be seen from Table 2.3 that (ΔH) varies from -2.56 to -9.82 kJ/mol indicating that the reaction is nearly thermoneutral [49]. Ross et al. [50] obtained values of (ΔG) of -34.81 kJ/mol at 873 °K which is consistent with Table 2.3. The values of (ΔG) in Table 2.3 indicate that reduction of NiO by hydrogen is thermodynamically feasible over the temperature range of interest.

2.6 KINETICS OF REDUCTION OF NICKEL CATALYST

Gambaro et al. [51] studied the reaction kinetics of NiO/Al₂O₃ catalyst with different NiO percentages. All samples were outgassed at 450 °C for 15 hours and then reduced for 16 hours at 420 °C with 300 mmHg of H₂. The

Table 2.3 Thermodynamic Properties of NiO Reduction [49]

Temp. (K)	Heat of Reduction (ΔH)	Free Energy (ΔG)	Equilibrium Constant
300	-2.56	-12.27	137.0
350	-3.45	-13.82	115.4
400	-4.31	-15.24	97.8
450	-5.13	-16.56	83.5
500	-5.91	-17.78	72.1
550	-6.66	-18.93	62.8
600	-7.37	-20.02	55.3
650	-8.04	-21.05	49.1
700	-8.67	-22.02	44.0
750	-9.26	-22.96	39.7
800	-9.82	-23.85	36.1

extent of reduction (α) was taken as the weight change of the catalyst with time (t), defined as:

$$\alpha_t = \frac{\Delta M_e}{\Delta M_t}$$

Where, ΔM_e is the experimental weight change for a given time and ΔM_t is the expected theoretical change for the total reduction of NiO to Ni. It was found that for low contents of NiO (1 and 4wt%), S-shape isotherms were observed, but for higher contents (8 and 15 wt%) hyperbolic type isotherms were observed. The same degree of reduction was observed after 16 hours of reduction for all cases. The large difference in initial reduction was due to the presence of a difficult-to-reduce phase for low NiO contents.

Sannomiya et al. [52] compared the reduction rates of supported NiO and unsupported NiO. They reported an overall activation energy of 47kcal/mol for the initial stage of reduction of NiO. The stage after the induction period was described by a shrinking core model and is represented by following relationship:

$$1-(1-\alpha)^{\frac{1}{3}} = kt$$

where, k is rate constant

They reported an activation energy of 13.3kcal/mol for the reduction of pure NiO. This value is close to 12.4kcal/mol obtained by Bandrowski et al. [53].

Bandrowski et al. [53] suggested that reduction of NiO has two rates, first is a reaction between NiO and H_2 adsorbed on nickel oxide and the second is an interfacial surface reaction between NiO and H_2 adsorbed on

nickel. The first reaction (r_1) was rapid but short lived and is described as follows:

$$r_1 = k_1(1-x)p_{H_2}^{m-1}$$

where,

k_1 = surface reaction velocity constant

x = fractional reduction of NiO to Ni

The values of m and activation energy were found to be -0.57 and 14.4 kcal/mol, respectively. The second reaction (r_2) started from an initial value of zero and increased progressively, and took over first reaction. Second reaction is described as follows:

$$r_2 = k_2(1-x)p_{H_2}^{n+1}$$

where

k_2 = surface reaction velocity constant

The values of n and activation energies were found to be ~0.95 and 12.4 kcal/mol, respectively.

A recent data on the reduction of supported NiO was published by Chen et al. [48]. Their data indicates that initially there is rapid increase in the reduction of NiO to Ni but increase in reduction slows down at the final period of reduction. This is consistent with work of previously mentioned workers. Chen et al. [48] found a rate expression shown as follows:

$$-r_{NiO} = 5.83 \times 10^{-3} e^{\frac{-26.4}{RT}} [NiO]^2$$

2.7 MECHANISMS OF REDUCTION OF NICKEL CATALYST

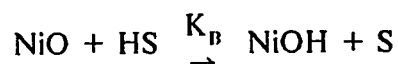
In an early study on the reduction of NiO using hydrogen as a reducing gas by Bandrowski et al. [53], following factors influenced the reduction process:

1. Method of preparation of NiO has a significant influence on its kinetic behavior.
2. The rate of reduction decreases with increase in temperature level of NiO preparation.
3. Reduction is retarded by water vapours.

Gambaro et al. [51], observed certain factors which are involved in reduction of NiO. These factors are:

1. An induction period in which the formation of reduction of nuclei is hindered by high dispersion of NiO.
2. With higher NiO content, a fast process is observed which can be assigned to a nucleation phenomenon on small crystallites of metal oxide.
3. A decaying period corresponding to the last stage of the reduction process is observed after the nucleation is progressed through NiO crystallites.

Hurst et al. [54] used contracting sphere model for the reduction of supported NiO and found that the reduction isotherms are characterized by constantly decreasing rate of reaction, which is consistent with the results of Bandrowski et al. [53]. Chen et al. proposed the following reaction mechanism for the reduction of nickel oxide:



Nickel oxide reacts with adsorbed hydrogen to form nickel hydroxide after hydrogen is dissociatively adsorbed on active site (S). The step, in which nickel hydroxide reacts with the neighbouring nickel hydroxide, is rate determining.

2.8 METHANATION CATALYSTS

Various investigators in early 1920s have compared the methanation properties of various metals at temperatures up to 800 °C. The decreasing order of methanation activity was Ru, Ir, Rh, Ni, Co, Os, Pt, Fe, Mo, Pd, Ag. In terms of metal which is more important for methanation, the list is known shorten to Ru, Ni, Co, Fe, and Mo. The history of these developments is mentioned in more detail in Greyson's chapter on methanation [55]. Later studies were carried out for improvement in the activity and selectivity of the catalysts.

2.8.1 *Ruthenium*

Ruthenium was early recognized as a very active methanation catalyst, but its high cost made it unfavorable for commercial use. Ruthenium can produce methane at 300 °C and at atmospheric pressure. By increasing pressure,

higher molecular weight products are formed. Traces of sulfur compounds rapidly deactivate the ruthenium catalyst.

2.8.2 *Nickel*

Nickel is majorly used for methanation reaction because of its many advantages; it is relatively cheap, very active because of having high surface and most selective to methane as compare to other metals. However, it is easily poisoned by sulfur compounds. Although nickel is less active than ruthenium, it commercially used in processes where traces of CO in H_2 are required to be removed. Nickel supported on kieselguhr or alumina is widely used.

2.8.3 *Cobalt and Iron*

Experiments in 1950s revealed that cobalt was very active for methanation. However, this catalyst tends to deposit carbon more rapidly than nickel catalyst under same set of operating conditions.

Iron catalyst produces small yields of methane and readily promotes carbon deposition even at higher H_2/CO ratios. The iron catalyst maintains its activity very well, but ultimately carbon deposition leads to bridging and plugging of the reactor.

2.8.4 *Molybdenum and Tungsten*

Molybdenum and tungsten catalysts for methanation possess resistance to sulfur poisoning, because they are made sulfided before use. Molybdenum shows a selectivity of about 79-94% for methane. Presence of H_2S in low level declines the activity of molybdenum catalyst, which leads to the production of C_3-C_5 compounds. Ni-Mo catalyst, in comparison to Ni catalyst, exhibits slightly greater methanation activity and a significant improvement in the sulfur resistance [56].

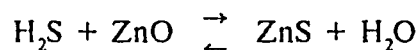
Tungsten catalysts in sulfided form are quite active for methanation, but they require high temperatures such as 475 °C and high pressures such as 1000 psig for producing methane. The selectivity to methane is about 90% and is unaffected by the presence of sulfur.

2.9 COMMERCIAL AND LABORATORIES PROCESSES FOR METHANATION

Methanation is used to remove relatively small amounts of harmful CO from synthesis gas and convert it to harmless methane in ammonia synthesis unit. This reaction is essential because CO in the feed (synthesis gas) once enters into ammonia reactor, it rapidly deactivates the catalyst (Fe) by making a permanent chemisorption on the surface of catalyst. In recent years, methanation is also considered for large scale production of "high BTU" or pipe line gas.

From commercial point of view, it is easy to acquire high selectivity to methane. In doing so some problems regarding the reaction are encountered. They are: deactivation of catalyst by sulfur and carbon deposition, excessive heat generation arising from highly exothermic nature of the reaction. The severity of reaction can be imagine that for every 1%CO in the feed the rise in temperature due to methanation is about 100 °F. Such rise in temperature not only decompose methane but also causes sintering of catalyst which gives rise to deactivation of catalyst.

For nickel catalyst it is usual to limit sulfur in the feed gas less than 1ppm by rigorous purification. This is achieved by either reacting ZnO with feed gas through following reaction:



or by placing a layer of spent nickel catalyst on the top of the catalyst bed, which act as a trap and chemisorbs sulfur compounds. Sometimes both options are used at a time.

Carbon deposition can be avoided by either operating with a sufficiently high H_2/CO ratios ($>3:1$) under the conditions given in Figure 2.1 or supplying extra steam into the system which prevents the carbon deposition. The gases produced from coal gasification have low H_2/CO ratios. This ratio can be altered by water-gas shift reaction, which involves conversion of CO to CO_2 , preceding methanation reaction.

Excessive temperatures in methanation are avoided either by limiting the

content of CO in feed gases or by supplying a rapid heat removal apparatus. Generally the rapid heat removal is obtained by placing a heat exchanger at the outlet of reactor. Recycling of product stream, and the supply of steam along with the feed gas keep the reactants in diluted form. The heat generated during reaction is therefore, carried away by steam.

In removing traces of CO by methanation, the treatment is limited to feed gases containing oxides of carbon not more than 2 mol% [57]. Under proper operating conditions, the reaction goes to almost completion and the exit gas contains only few ppm of carbon oxides. The inlet temperature may vary from 350-750 °F % however, due to unfavorable equilibrium at elevated temperatures, the exit gas should not exceed 825 °F. The system can be operated at pressures ranging from atmospheric to 1200 psi. The space velocities of 1000-2000 hr⁻¹ are typical for operation at atmospheric pressure, and for 20-30 atm. pressure these are about 3 to 5 times higher.

For methane production from coal, The feed gases obtained by Synthane gasifier, contain high percentage of CO (24%). The feed gases first pass through shift converter to reduce CO to about 16% and then it enters into methanator where a low percentage of CO (2-10%) is maintained by recycling the product through the system.

The criteria of design of methanator includes rapid heat removal and temperature control, and type of reactor used e.g., fixed bed, gas recycle, fluidized bed, slurry catalyst, or a combination of aforesaid systems. Some of the commercial reactors are discussed by Mills [23] and are discussed as follows:

Lurgi-Ruhrchemie Process [58]

It consists of a fixed bed reactor which is a vertical tube heat exchanger. The catalyst is placed inside the tubes and water circulates in the shell. The heat released is absorbed by boiling the water. The reactor contains about 40 m³ of catalyst in 2000 tubes, which are 40 ft long and 1/8 in. in diameter. The maximum temperature reached in the reactor is 450 °C.

Kellog Process [23]

It consists of a fluidized bed system which circulates about 7000 tons of catalyst per hour through a 120 ft high reactor. The main part of generated heat is removed by heating the combined (fresh & recycled) feed gas from 150-300 °C before entering the reactor, and residual heat is extracted by two oil-cooled coolers built in the reactor.

BI-GAS Process [59]

This system uses two types of reactors fluidized and fixed bed. Fluidized bed operates at 800 °F and 1000 psia. Space velocities ranges between 1000 to 2000 standard volume of feed per bulk volume of catalyst per hour. A minimum of 80% of CO and H₂ are converted to CH₄ in fluidized bed while fixed bed completes the conversion.

BGC Combined Shift-Methanation System [60]

This system is used for those gasifiers which produce H₂/CO in low ratios. It is a direct methane producer in which CO shift-conversion and methane synthesis occur simultaneously on a single catalyst. It consists of steam

addition followed by direct methane synthesis. Its major advantages are: low cost, low steam requirements, and no need of a separate water-gas shift stage. Some other pilot processes including cold gas recycle (HYGAS), tube wall reactor (TWR), and hot gas recycle (SYNTHANE) are discussed by Mills et al. [23].

HICOM Process [96]

HICOM process (High CO methanation) is a direct high temperature methanation route with operating temperature around 700 °C. The process gas from gasifier in this process, after cooling and desulfurization, is passed through a series of high temperature methanation units without adjusting the H_2/CO ratio to 3.0. Split-stream operation is used to recycle each of these stages, and high-grade heat is recovered after each of them. A key feature of HICOM process is the use of recycle gas to control the temperature of first methanator. Each stage is operated at a temperature which is tolerable by the catalyst. Excess steam is added to prevent carbon deposition. The product from high temperature methanation stages, after removal of recycle gas, passes through low-temperature methanators to convert remaining CO and H_2 to methane. The final product contain mainly methane and some carbon dioxide.

2.9.1 *Laboratory Reactors for Methanation*

Laboratory studies of heterogeneous catalysis are focussed on developing kinetic models of the reaction system or the evaluation of catalysts. In order to develop rate equation required in the design of any chemical reactor, it is

essential that mass and heat transfer effects should be eliminated from kinetic data. Generally, catalytic studies are performed on flow systems (such as fixed bed) which are close to commercial processes. Kinetic studies are difficult with fixed bed systems because of the possibilities of film concentration and temperature gradients between solid catalyst and fluid. It is important in design of a gas-solid reactor the effects of turbulent and molecular diffusion are eliminated and it ensures that reactor performance reflects only chemical reaction. One such design is called continuous stirred tank catalytic reactor (CSTCR), in which the contents are thoroughly stirred in order to keep uniform composition and temperature throughout the reactor. Some of the advantages of CSTCR mentioned by Lee [61] are described as follows:

- a) It permits intrinsic kinetics which is free from mass and heat transfer effects. Such effects are encountered in packed bed reactors.
- b) It minimizes the temperature and concentration gradients between the bulk fluid and catalyst surface, thus provides a perfect mixing.
- c) Fast and highly exothermic reactions can be studied at nearly isothermal conditions and about complete conversion is possible.
- d) Rates can be easily and accurately determined by material balance equation,

$$R = \frac{Q_i C_i - Q_o C_o}{W}$$

where, R = reaction rate, g-mol/hr-g of cat.

Q = Flow rate, ml/hr

C_i = concentration of feed, g-mol/ml

C_o = concentration of product, g-mol/ml

W = weight of catalyst, g

Some major applications of CSTCR are as follows:

- a) It is the most suitable system for the screening of different catalysts by making comparison among them under same operating conditions for the selection of a suitable catalyst.
- b) The intrinsic kinetics of reaction can be determined.
- c) The effects of different parameters on the rate of reaction can be studied.

There are two types of recycle reactors available: external and internal recycle. For laboratory purpose, external recycle reactors are nonattractive because they require mechanical pumps for circulation and reheating of recycle stream.

Reactors with internal circulation are mainly of two types:

a) Stationary Basket

In this type, catalyst is packed in a fixed basket and the reactants are circulated by an internal turbine pump.

Chaudhri et al. [62] used a stationary basket-type continuous stirred reactor. The catalyst was placed in a stationary cylindrical basket which was provided with a fine stainless steel wire mesh and a thermocouple. The stirred tank performance was obtained by rotating a special impeller around the cylindrical basket.

Berty [63] with the cooperation of Autoclave Engineers Inc. designed the first commercial CSTCR gas solid reactor, called Berty reactor, which can be operated at elevated temperatures and pressures. In Berty reactor, catalyst is held in a fixed basket and reactant gases are circulated through it by using a

magnedrive impeller. Berty reactors are available with a catalyst handling capacity of 100 to 300 ml. A 100 ml catalyst handling capacity reactor is used in this study.

b) Spinning Basket

The spinning basket reactor was developed by Prof. J.J.Carberry [64] and his coworkers in 1966 at the University of Notre Dame. In this reactor, catalyst is contained in four baskets of approximately one particle thickness located right-angle to each other. The baskets are mounted on a rotating shaft, driven by a motor, thereby reduces the film diffusion effects.

2.10 STUDIES ON THE ACTIVITY OF NICKEL CATALYSTS

The actual development of methanation process using nickel as a catalyst began in 1939 by the British Research Board [65,66], who studied different metals precipitated on kieselguhr. Their work was completed in 1945 with the findings that nickel and ruthenium are selective to methanation. Dirkson and Linden [67] found that Rancy Ni was much more active than Ni supported on kieselguhr, but it showed a tendency to deactivate by carbon deposition.

White et al. [25] studied the methanation of a mixture of CO, H₂, CO₂, CH₄ and steam for pressure and temperature ranging from 1 atm. to 1000 psig and 900 to 1200 °F, on a ring type Ni catalyst (5/8" by 1/4"). They experimentally verified their predictions about carbon deposition at high steam

gas ratio of 1:1. Lee et al. [68] also reported the formation of carbon on crushed Ni-catalyst with feed mixtures containing 4-13% CO.

Malladi [26] used 58% Ni-catalyst, supported on Kieselguhr (Harshaw Catalyst Co.), in a Bertly Reactor. A feed mixture of CO, varying from 2.95 to 9.64%, and balance being H_2 was used. Operating temperature and pressure varied from 315 to 593 °C and 14.50 kg/sq.cm to 71.30 kg/sq.cm respectively. His measurements indicated that the intrapellet resistances were minimal. The interphase resistances were minimal, when interphase temperature difference was less than 6.5 °C. The interphase mass transfer resistances were significant at 426 °C and at a recycle ratio below 150. Rise in reaction rate was noticed in the temperature range of 315 to 426 °C, but it dropped from 426 to 593 °C because of the sintering effect on catalyst at higher temperatures.

Doesburg et al. [69] used 40% Ni/ Al_2O_3 catalyst, prepared by coprecipitate technique, and reduced it with H_2 at 10 kN/m² for 3 hrs after outgassing at 1 mN/m² for 1 hour at the same temperature. The reduction temperature varied from 573 to 973°K. It was found that degree of reduction increased with reduction temperature, which caused increase in the activity of catalyst. Initially, selectivity dropped for lower reduction temperatures, then it increased for higher reduction temperature. Such change in selectivity was due to the formation of higher hydrocarbons on unreduced surface of catalyst at lower reducing temperatures. Rise in activity and selectivity was due to the formation of massive nickel crystallites.

Vannice [9,70] studied methanation over a series of group VIII metals supported on alumina (Al_2O_3) and silica (SiO_2). He compared the specific activities by normalizing the methane production to the number of metal sites available on surface. Subsequent work has suggested that the specific activity of the catalytic metal is not a fixed quantity. Evidence suggests that both the nature of support and the particle size are important in methanation activity [71,72]. It has been indicated by Bartholomew [47] that reduction conditions tend to change the dispersion of $\text{Ni}/\text{Al}_2\text{O}_3$ catalysts.

Bhatia et al. [73] compared some laboratory prepared Ni-catalysts (Ni-content 5-21%) with commercially available catalysts, namely, Girdler G-87 (40% Ni), Houdry NI-6109 (17% Ni) and Harshaw HSC-102 (42% Ni). They found that conversion increased with laboratory catalysts and only G-87 gave higher conversion. It was due to the reason that high Ni-content could block the catalyst pores which indicated that Ni was poorly dispersed on the support which corresponded to a less surface area. Dalla Betta et al. [72] have observed similar behavior that poorly dispersed Ni-catalyst were not only inactive for CO conversion but also they chemisorbed hydrogen poorly. Bhatia [73] observed that 5%- $\text{Ni}/\text{Al}_2\text{O}_3$ displayed highest turnover number, because of high Ni dispersion, among all catalysts under study. It was also found that activity increased with crystallite size, but for a very large crystallite size, activity decreased because of very strong adsorption of CO and hydrogen on the surface. Therefore, Bhatia [73] reported an crystallite size of 14nm. In his further studies [74], he compared three different types of Ni-catalysts, namely, $\text{Ni}/\eta\text{Al}_2\text{O}_3$ and $\text{Ni}/\text{zeolite Y}$ (Exchanged & Impregnated). It was reported that for larger reduction times of 12-18 hours, the turnover number

for Ni-Y catalyst was higher than $\text{Ni}/\eta\text{Al}_2\text{O}_3$. It is also reported that the activity is found to be lower with higher acidic support because of the formation of carbonaceous residues, which is due to the surface group migration to the Ni-surface [75].

Jarvi [76] compared $\text{Ni}/\text{Al}_2\text{O}_3$ and monolithic 25% $\text{Ni}/\text{Al}_2\text{O}_3$. It is reported that monolithic catalyst, in the pressure range of 10-25 atmosphere with a temperature range of 450- 700 °K and a space velocity from 30000/hr to 50000/hr, has turnover number 100% to 500% higher than $\text{Ni}/\text{Al}_2\text{O}_3$ spheres. It is due to the smaller pore diffusion and high mass transfer rates in monolithic catalyst. Monolithic catalyst showed higher yield of methane under higher and lower conditions of temperatures and pressures, which makes it possible to operate it under less severe conditions in order to avoid sintering and thermal stresses on the catalyst. Commercially monolithic catalyst was found uneconomical because of its high cost. Reucroft et al. [77] studied the effects of reducing temperature and time on the surface area of $\text{Ni}/\text{Al}_2\text{O}_3$ catalyst by N_2 -BET method. They found that metal surface increases as the temperature increases from 400 to 500 °C, but decreases from 500 to 600 °C. The possible reason suggested that sintering of support takes place at high temperatures.

Sinfelt [78] reported that due to very high hydrogenolysis activity of nickel, carbon deposition takes place. Bond et al. [79] and Elliot et al. [80] reported that by adding copper to $\text{Ni}/\text{Al}_2\text{O}_3$ results in a decrease in the turnover number, which is due to dilution of multicentered catalytic sites by copper atoms. Bajpai et al [8] studied on the idea of Bond et al. [79] by

adding copper to $\text{Ni}/\text{Al}_2\text{O}_3$ catalyst and tested the activity in comparison to Ni-catalyst. The activity of $\text{Ni}/\eta\text{Al}_2\text{O}_3$ was found to be lower initially but it acquired same rate as Ni-catalyst after some time on stream. These studies concluded that $\text{Ni}/\eta\text{Al}_2\text{O}_3$ has a longer life because: it deactivates slowly, show less sintering and a very low carbon deposition. This is due to the addition of copper which has an effect on sintering tendency of Ni-particles.

In another study of Bajpai et al. [82], they used four laboratory prepared catalysts ($\text{Ni}/\text{Al}_2\text{O}_3$, NiNaY -uncalcined, NiNaY -calcined, NiCaY -calcined) and a commercially available catalyst (G-87). The deactivation behavior was studied over a period of 24 hours at 573 °K for various H_2/CO ratios (3.1, 3.8, 6.4, 24.5). The results indicated that the activities did not change much with time at H_2/CO ratios of 3.8 and higher. Carbon deposition took place for H_2/CO ratio of 3.1. It was found that excess carbon on the surface of G-87 converted in to bulk carbide (graphite) whose activity was low [16,14], and it covered some of the metal sites making them unavailable for reaction. This behavior was confirmed in the regeneration of catalysts, in which all catalysts were recovered nearly to their initial activities except G-87. Due to crystallite growth, it was found that G-87 catalyst, because of high Ni-content (40%), lost 90% of its activity (H_2/CO ratio of 3.1) in 24 hours. Whereas, NiCaY and $\text{Ni}/\text{Al}_2\text{O}_3$ lost only 50-80% of their initial activities and appeared to be the best catalysts showing least deactivation.

Becker et al. [33] studied deactivation of Ni-catalyst at a temperature of 440 °C, H_2 -pressure at 22.5 bar and CO -pressure ranging from 7.5 to 22.5 bar. At a constant conversion of 20% CO , it was found that increase in CO -

pressure, deactivation of catalyst was rapid. When pressure raised to 60 bar with temperature from 320 to 520 °C and H_2/CO ratio of 3:1, the results showed that deactivation increased by decreasing temperature from 440 to 320 °C. Above 440 °C, deactivation was not influenced by the temperature. This behavior was due to the crystallite size growth by nickel transport via nickel tetracarbonyl ($NiCO_4$) and it was confirmed by SEM (Scanning Electron Microscopy) of fresh and deactivated catalyst. Henkel et al. [83] have also studied the similar change in the deactivation behavior of Ni/Al_2O_3 catalyst at 520-540°K.

Richard et al. [84] studied the deactivation of three different types of nonuniform Ni/Al_2O_3 catalysts. The types used were: 1) uniform catalyst (Active metal uniformly deposited throughout the particle), 2) egg shell catalyst (the metal is deposited in a layer on the exterior of pellet), 3) egg yolk catalyst (the metal is concentrated in the core of pellet with almost no metal on the outer edge). All runs were conducted at 643 °K and 140 kPa. when runs for uniform and core were conducted with a feed gas composition of 5%CO, 10% H_2 , 85%He and H_2/CO of 2, the deactivation was found to be negligible. When H_2/CO with a ratio of 1.1 was used, the shell catalyst totally deactivated in 3 hours. For the same time other two catalysts lost only 20 to 35% of there initial activity. It was found experimentally that shell catalyst was not completely reduced in H_2 due to high dispersion at 643°K. However, it acquired same degree of reduction at 753°K. Gakuska et al. [85] have suggested that reduction of low loading Ni becomes difficult because of high dispersion. It happens, because Al_2O_3 (support) stabilizes the energy of NiO

during reduction, which suppresses reduction.

Hays et al. [35] used different Ni/ γ -Al₂O₃ catalysts, among them, one was commercial 9% Ni/ γ -Al₂O₃ (ICI). The gas to the tubular reactor, 3.1% CO, 9.3% H₂ and balance being N₂, fed at a flow rate of 410 cu.cm/min. at STP with a total pressure of 131 kPa. Commercial catalyst showed higher conversion because of high Ni-content, and strongly influenced by the temperature of reduction. Effects of promoters were also investigated. Platinum and ruthenium, when added, improved the activities and life of the catalysts. For longer periods of deactivation, the activity of catalyst could only be restored by treatment with hydrogen at about 725 °K.

Munteanu et al. [86] have performed an investigation on a temperature-programmed-desorption of Ni/Al₂O₃ catalyst (Ni particle size > 20nm) for CO methanation at 473 °K. They found that methanation of adsorbed CO exhibited a structure sensitivity at 473- 673 °K. At 673 °K, methanation became structure insensitive. It was also found that activity of catalyst with large particles decreased with increasing temperature and it increased with small Ni particles by increasing temperature.

Twigg et al. [87,patent] studied the methanation of synthesis gas containing H₂ (74.7%), N₂ (24.9%), CO₂ (0.2%), and CO (0.2%) over Ni/Al₂O₃ catalyst containing NiO (94.8%), CeO₂ (1.8%), Al₂O₃ (2.9%), and other oxides (0.5 mass%) (BET surface area 229.6 m²/g). The synthesis gas was preheated and passed over a bed of catalyst at 350°C, 1 atm. and a flow rate of 3000 L/h, produced CH₄ with high conversion of carbon oxides.

Fujita et al. [88] proved in their studies on methanation that kinetics under transient condition are quite different. The hydrogenation of surface carbon species is strongly inhibited by reversibly adsorbed CO in methanation of carbon monoxide, where adsorbed CO_2 does not inhibit carbon dioxide hydrogenation to methane. It is generally accepted [15,45,89-92] that CO dissociates to surface carbon species and adsorbed oxygen, which are then hydrogenated to CH_4 and H_2O . In these respects, it was concluded that hydrogenation of adsorbed oxygen to water proceeds more rapidly as compare to carbon species to methane. It was also found that production of methane formation enhanced when CO supply was cut off, because the presence of CO at the catalyst surface was resisting the hydrogenation.

In a recent study by Rajiv et al. [93], they investigated the methane yield on a commercial Ni-catalyst (BASF R1-10 Ni- Al_2O_3), in a Berty reactor. They used 10% CO- H_2 mixture and switched it to a pure H_2 after some time. It was found that methanation rate increased 10 times higher than the steady-state rate observed with 10% CO- H_2 mixture. It is likely that, during steady-state methanation, preadsorbed CO inhibits the adsorption of H_2 . It is conceivable that under cycling conditions the catalyst surface is periodically "cleaned", during the H_2 -rich part of the cycle, leading to high methanation rates.

Ahmed et al. [94] studied the sintering effects on 20% Ni/ $\gamma\text{Al}_2\text{O}_3$ under hydrogen flow at various temperatures. All samples were reduced in situ at 600 °C for 16 hours. It was found after reduction that possibly the large crystallite size particles caused physical blockage of the pores, making them

ink-bottle shape pores.

CHAPTER 3

EXPERIMENTAL INVESTIGATION

3.1 INTRODUCTION

The experimental setup consists of a high pressure reactor system (Fig. 3.1) which includes gas feed equipment, Berty catalytic reactor, heat exchanger to cool the product, product separator and a product discharge equipment.

The gases pass through mass flow meters to acquire the desired feed composition, and then enter into the Berty reactor system after passing through the dryer. The reaction products leave the reactor and are cooled after passing through a water cooled heat exchanger. The water vapors are condensed and separated in a separator. Product gases pass through a dry test meter (DTM) which measures the flow rate and then they are vented off through a vent. A pressure control valve is located on the down-stream of DTM to maintain the back-pressure in the system. A line, from feed and product gas lines, branches out to the Perkin-Elmer gas chromatograph to analyse the composition of feed and product gases.

3.2 EXPERIMENTAL EQUIPMENT

The important sections of the experimental setup are discussed in detail in the following sections:

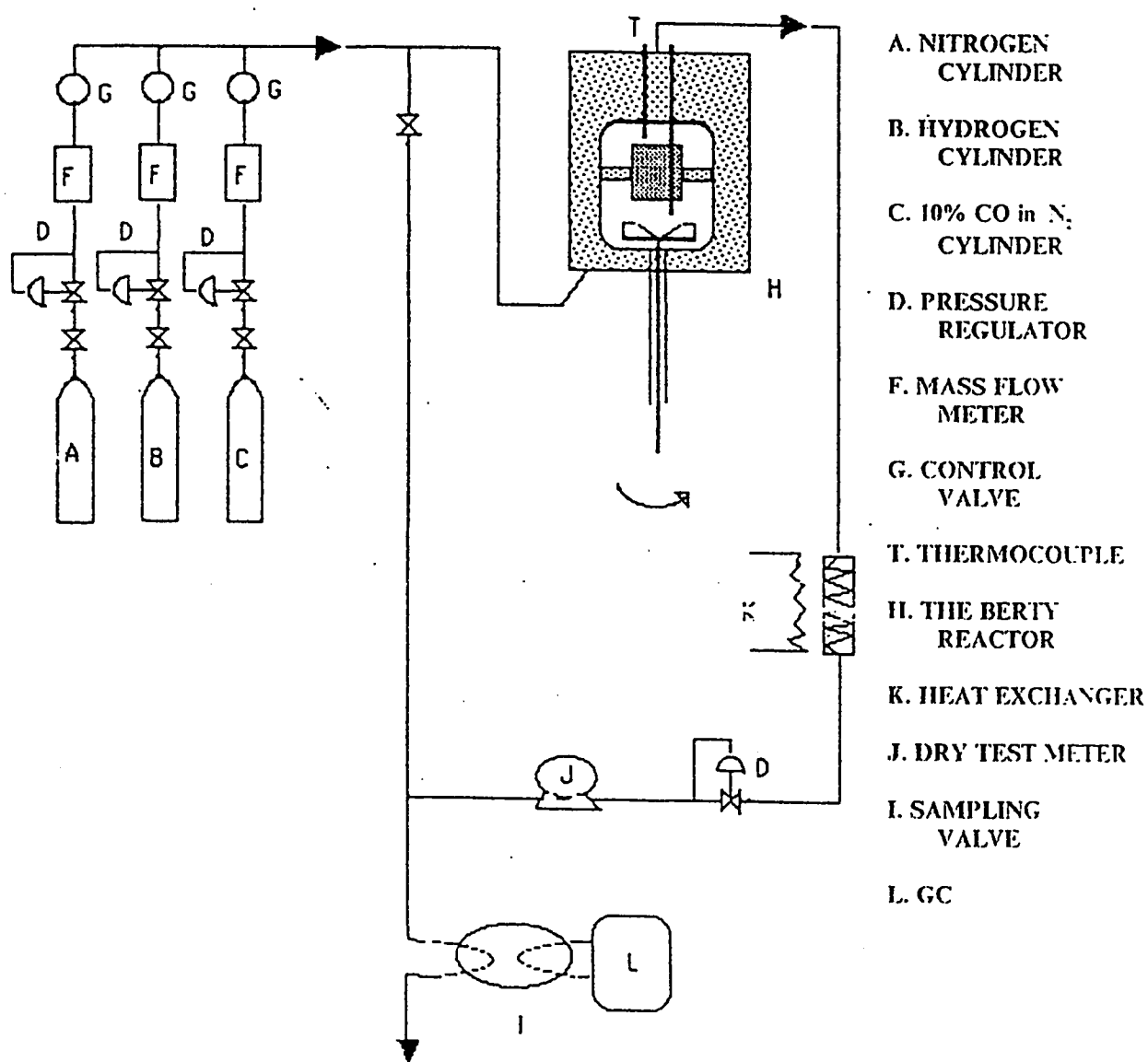


FIGURE 3.1 THE METHANATION REACTION UNIT FLOW-SHEET

3.2.1 *Feed Metering System*

The feed metering system consists of three Brooks mass flow meters. They are used to control the mass flow rate and the composition of feed gases. The feed gases consist of: N_2 (99.99%), H_2 (99.99%) and 10% CO in N_2 . The H_2 (99.99%) is supplied to adjust the H_2/CO ratio to the desired level.

3.2.2 *High Pressure Reactor System*

The gradientless reactor is designed by Berty of Union Carbide, built and supplied by Autoclave Engineers, Inc.. The design of the reactor is shown in Figure 3.1 & 3.2. The reactor consists of the following main parts:

Body & Cover Assembly

The body and cover are made up of stainless steel (S.S.316), Which can be used up to a maximum allowable pressure of 5800 psi with a limiting temperature of 616 °K. This temperature limitation is due to the teflon bearing used in the magne drive assembly (impeller). However, the operating temperature limitations can be increased to 866 °K by using Purebon or Vulon bearings with a water-cooled jacket between the magne drive and the reactor. In present study, the second option was used. The cover is provided with two connections to introduce a pencil type thermocouple from the top and reaches the bottom of the catalyst bed. The thermocouple is connected to a PID temperature controller to control the temperature of reactor.

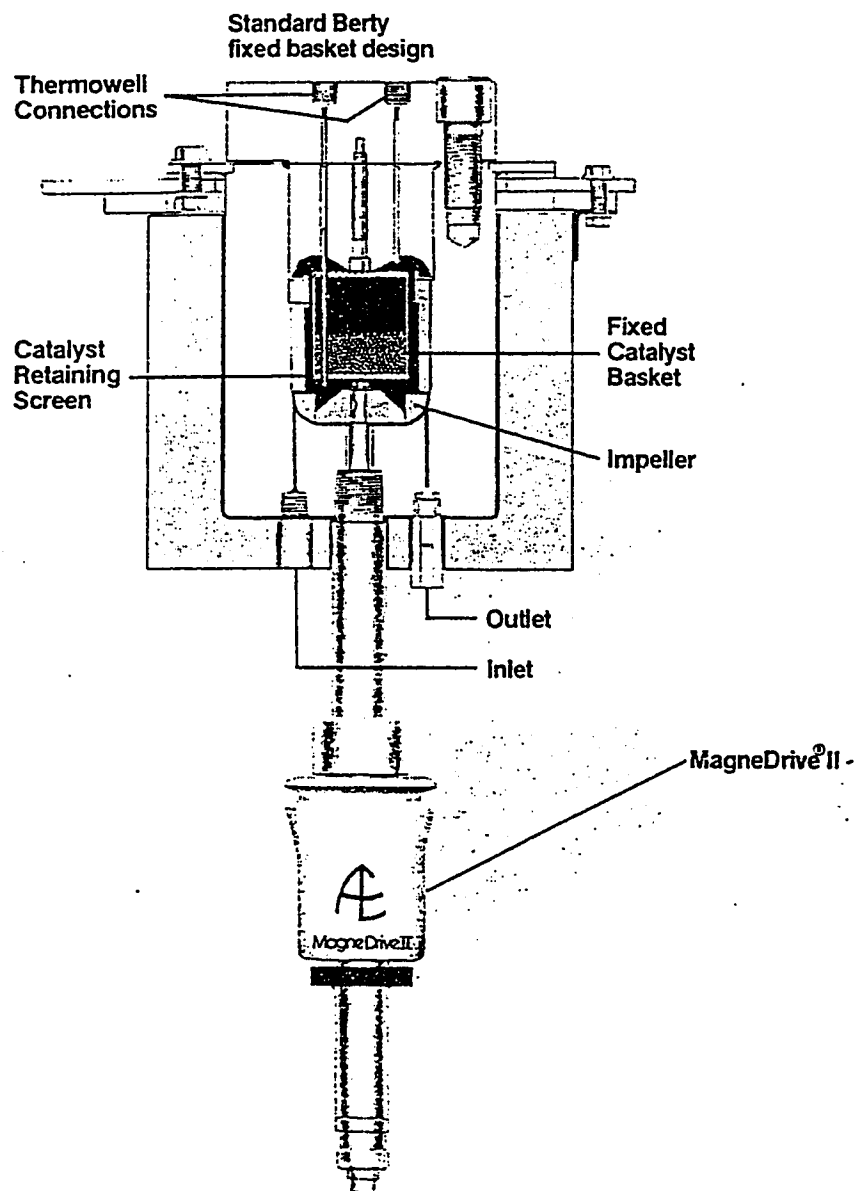


Figure 3.2 A Descriptive View of Berty Reactor

Agitator Assembly

The agitation assembly (called magne drive) is designed for a maximum allowable pressure of 5800 psi and is operated by a 1/4 horsepower d.c. motor. The maximum allowable shaft speed is 2500 rpm. The assembly is especially designed to eliminate packing heat generation and leakage. High speed rotation is obtained by rotating the external magnets mounted on the magne drive, which actuates internal magnets fastened to the shaft. A solid-state silicon rectifier-controller, mounted on the control box, rotates the d.c. motor and controls the speed of outer magnet drive (impeller). Table 3.1 shows the calibration of rpm controller vs. measured rpm.

Furnace

The furnace which is electrically operated, is divided in to three heated zones: top zone, middle zone and bottom zone. The controllers to operate the furnace are located on the control box.

Catalyst Basket

The catalyst basket has a total volume of 100 cu.cm. and is perforated. The basket is provided with outside latches, which hold it firmly in the reactor assembly.

3.2.3 Control Box

The control box has the following components:

- * Magne drive motor speed controller with digital tachometer.

Table 3.1 Calibration of rpm Controller vs Measured rpm

<i>Setting on Potentiometer</i>	<i>rpm Measured</i>
1.0	140
2.0	525
3.0	786
3.1	830
3.2	859
3.3	882
3.4	920
3.5	946
3.6	963
3.7	980
3.8	1001
3.9	1032
4.0	1053
5.0	1264
6.0	1508
8.0	2229

- * Three ammeters to indicate and control the current load to each of the furnace zones.
- * Temperature indicator and controller (TIC) to indicate and control the temperature of reactor. There are three other digital temperature indicators which indicate the temperatures of three zones of furnace.
- * Push buttons to open and close the air operated valves (operated @ 60 psi).
- * Audible warning system in case of unaccounted temperature or pressure rise.
- * Emergency shutdown buttons which cut off all gas supplies and open the nitrogen purge line.

3.2.4 *Power Supply*

Power is supplied by six-independent 120-volt lines. One line supplies power to the control box. Three lines supply power to three zones of the furnace. Two independent 234-volt lines are supplied to the gas chromatograph (GC) and data console.

3.2.5 *Analytical Section*

Both feed and product streams are continuously analyzed by a Perkin-Elmer Sigma 115 gas chromatograph (GC), which is equipped with a thermal conductivity detector (TCD) and a flame ionization detector (FID). An automatic sampling valve continuously takes samples of 10cc each. The gases

in the sample (i.e. CO, CO₂, H₂, N₂, CH₄) are separated by a 100/120 Carbosieve S-II (10 ft x 1/8" ID, SS) packed column which is fitted in the oven of analyzer. The separated gas components are detected by the TCD and are analysed in a data console which is attached to the GC. A description of GC is given in the subsequent section as follows:

Gas Chromatograph System

The Perkin-Elmer Sigma 115 gas chromatograph (GC) consists of two equipments: a laboratory data system called console, and a Sigma series analyzer. The keyboard of the console is used for directives and conversations, and it can operate console to collect data from chromatograph and prints out analysis report. The console establishes the conditions of analyzer and initiates operations of auxiliary devices, such as automatic sampling device, at the desired time. The console is also equipped with accessories which allow the user to write his own programs in BASIC language and can be connected to teleprinter, data modem etc. The storage capacity of console can be increased by using magnetic tape cassettes.

All functions of GC system are controlled by a built-in software package called analysis method which has three subsections; namely, analyzer control, data processing, and event control (appendix B). The analyzer control section operates and controls the desired conditions of analyzer. The data processing and event control sections govern data acquisition and operation of time dependent functions, such as operation of automatic sampling device, in the analyzer.

The analysis method is generated on console by using the Generate directive. After the analysis method generation, a setup conversation is carried on console through Setup directive in order to control the functions of the analyzer under the instructions of analysis method. The method sets up the initial chromatographic conditions for the analyzer e.g., temperatures of oven, column, detectors etc. The operating condition of GC which are used in this investigation are shown in Table 4.1. When the required conditions in the analyzer are stabilized, a "Ready" indicator located on the analyzer is lighted on. the Data collection and processing begin when a sample is injected through an injection port and the "Ready" button is pressed. Use of automatic sampling device does not require the condition of pressing the "Ready" button, because the system operates automatically as soon as the desired conditions of the method are stabilized.

A report, obtained from collected data, is printed out automatically on the console printer/plotter. In addition, the printer/plotter can be linked to data source by using Plot directive through console in order to obtain annotated chromatogram (appendix B).

The obtained data is stored in files in the console memory. These files contain peak area and peak retention time for each stored run. Three types of standards; namely, internal standard, external standard, or normalization analysis are used to identify the relative retention time of components and their concentrations. The concentration of a sample is obtained from the peak area of each component which is calculated by calibration against a known sample. The calibration procedure is described in section 4.2.

At the end of each run, initial chromatographic conditions are reset automatically for next run, and the "Ready" light turns on again when the preset conditions are stabilized. In case of automatic sampling device, The system starts again automatically for the next run without the ready button being pressed. The DATA STOP and RESET keys can be depressed in sequence to terminate a run at any stage and to return the system to its preset initial conditions. The VOID key can be pressed instead of RESET releases the system from the control of analysis method; however, the initial conditions of chromatograph remain the same as established by that method.

The stored analysis method can be modified by means of Modify directive. Also, response factor which relates the peak area with a standard component concentration is calculated automatically and can be incorporated into a method by means of calibration conversation, as described in section 4.2.

3.3 MATERIALS

The catalyst used in this investigation is C13-4-04 (20%Ni / γ Al₂O₃), manufactured by UCI (United Catalyst Inc.) and supplied by SAMAD (Al-Jubail). The catalyst consists of sphere of about 1/4 in. in diameter. A typical analysis of the catalyst is given in Tables 3.2 and 3.3.

3.4 EXPERIMENTAL PROCEDURE

In order to load the Ni/ γ Al₂O₃ catalyst, thermocouple which is fitted through the cover is disconnected and very carefully pulled up. Any bending

Table 3.2 Catalyst Analysis*

COMPOUND	Wt. %
Ni	20.3
Al_2O_3	69.1
CaO	4.9
Na	0.1

*Analyzed by Research Institute (RI), KFUPM

Table 3.3 Fresh Catalyst Analysis*

Physical Properties	Amount
B.E.T. Surface Area (m ² /g)	82.3
Pore Volume (cc/g)	0.52
Avg. Pore Radius (Å)	126.4
Carbon Content (wt%)	-

*Analyzed by Research Institute (RI), KFUPM

can break the thermocouple. The cover is removed by loosening the bolts. Catalyst basket is taken out, and filled with the required amount of catalyst. After filling the basket, it is placed back at the same position in order to match the opening in the cover with the thermocouple case inside the basket. This allows thermocouple to pass through and reach the bottom of the catalyst basket. An insulation cap is mounted on the cover to avoid heat losses. The system is pressurized with N_2 through N_2 -purge line up to 800 psi to detect any leakage through the system.

The following procedure for the operation of system was adopted:

- * Connect the Brooks flow meters to the power supply, and warm them for 15 minutes.
- * Obtain feed composition by GC.
 - Open feed line to GC.
 - Close feed line to reactor.
 - Adjust the Brooks flow meters to the desired composition.
 - Obtain feed composition by GC.
 - Close the Brooks flow meters
- * Pressurize the system
 - Open feed line to reactor.
 - Close nitrogen purge line.
 - Close feed line to GC
 - Introduce nitrogen to pressurize the system by opening Brooks flow meters.
 - Adjust the back pressure by pressure control valve (PCV-81) to the desired level.

- * Set the reactor temperature to the desired level by the temperature controller
- * Adjust the desired speed of impeller.
- * When the temperature is stabilized at the desired level (about $\pm 1^\circ\text{C}$), allow hydrogen and CO into the system.
- * Analyze the product composition (in GC) by opening a valve on the branching loop from the outlet pipe .

3.5 REDUCTION PROCEDURE FOR Ni-CATALYST

In view of the investigations on the reduction of Ni-catalyst by KACST [4], following method was adopted for this study:

The reduction of 20% Ni/ $\gamma\text{Al}_2\text{O}_3$ catalyst was carried out in a Berty reactor in situ. A sample of 10 gm. was loaded in the reactor for each set of experiment. The reduction temperature was kept between 250 and 500 $^\circ\text{C}$, because, thermal sintering of the catalyst was not observed up to 500 $^\circ\text{C}$ [4]. Pure hydrogen (99.99%) was used as a reducing gas. The space velocity was kept constant at 3000 hr^{-1} . The heating rate from room temperature to the reducing temperature was kept between 1 $^\circ\text{C}/\text{min}$ and 5 $^\circ\text{C}/\text{min}$. The duration of reduction was kept from 2 to 16 hours. After the reduction, H_2 supply was stopped and flow of inert gas (N_2) was continued at 50 ml/min until the sample cooled down to room temperature.

3.6 GAS SAMPLE ANALYSIS

The gas sample analysis was performed by gas chromatograph (GC). The GC was provided with a carbosieve S-II packed column which separates H_2 , O_2 , N_2 , CO , CH_4 , and CO_2 gases in 25 minutes. The following steps were taken for sample analysis:

- Two carbosieve column were fitted in the oven of GC
- He gas was allowed to pass continuously through the column at 30 ml/min. The pressures at the inlet gauge of GC and at the discharge of He-cylinder were kept at 75 psig and 80 psig, respectively.
- Calibration of GC was performed by injecting a gas sample of calibration gas of known composition through an automatic sampling device in order to acquire the correct response factor of each component (Table 4.3).
- The calculated response factors were incorporated in the main program of sample analysis in order to analyse feed and product gas samples (Appendix B).

CHAPTER 4

RESULTS

4.1 OVERALL VIEW

This study involves the reduction of a commercial $\text{Ni}/\gamma\text{Al}_2\text{O}_3$ (C13-4-04;20%Ni) catalyst at various conditions and investigates the effects of reduction on the activity and selectivity of the catalyst for a methanation reaction. Methanation reaction involves the reaction of CO with H_2 in order to produce CH_4 . The reactor used to investigate this reaction is the Berty reactor which is a CSTCR with internal recycling. Berty reactor provides several advantages such as ease of interpretation of data. Internal recycling facility provides high mass velocity which eliminates physical resistances (e.g. diffusion resistance) around catalyst bed.

The reduction variables for Ni-catalyst are temperature, duration, space velocity, and heating rate of catalyst bed. It has already been found in a report by KACST [4] that among above mentioned variables only two are important. They are temperature and duration of reduction. Where, space velocity and heating rate have effects of less significance on reduction as compare to other variables. The temperatures of reduction employed during this study were 250,300,350,400,450, and 500 °C. The durations of reduction were 2,4,8,12, and 16 hours. The space velocity was kept constant at 3000 hr^{-1} . The reduction pressure was kept at 30 psig and also the weight of

catalyst charge per run was kept constant at 10 gm. Methanation reaction was carried out after reduction in order to investigate the effects of reduction conditions on the activity and selectivity of Ni/ γ -Al₂O₃ catalyst. The reaction was carried out at temperature of 350 °C and a pressure of 30 psig. The space velocity was kept between 3600-3900 hr⁻¹.

The activity of Ni-catalyst was calculated by determining the rate of reaction. A material balance was made at the inlet and outlet of the reactor system, and is shown as follows:

$$\text{Rate} = \frac{F_{\text{in}} Y_{A_{\text{in}}} - F_{\text{out}} Y_{A_{\text{out}}}}{W}$$

where,

F_{in} = Total molar flow rate In (g-mol/hr)

F_{out} = Total molar flow rate Out (g-mol/hr)

$Y_{A_{\text{in}}}$ = Mole fraction of compound A In

$Y_{A_{\text{out}}}$ = Mole fraction of compound A Out

W = Weight of catalyst (g)

Above equation determines both rates of carbon monoxide conversion and methane production.

The selectivity is defined and calculated as follows:

$$S_{\text{CH}_4} = \frac{\text{Desired-Product}}{\text{Consumed-Reactant}} = \frac{r_{\text{CH}_4}}{-r_{\text{CO}}} = \frac{F_{\text{out}} Y_{\text{CH}_4}}{F_{\text{in}} Y_{\text{CO}_0} - F_{\text{out}} Y_{\text{CO}}} \times 100$$

Another term, called turnover number (N_A), defined as number of molecules

reacting per site of catalyst per unit time, was also employed to calculate the normalized or specific activity (independent of Ni-content of catalyst) of Ni/ γ -Al₂O₃ catalyst. The N_A was used to compare the activity obtained during this study with activities, in terms of N_A , obtained for Ni-catalyst by other researchers. The turnover number is calculated as follows:

$$N_A = \frac{r_A}{H_2\text{-Uptake} \times 2}$$

Where,

H_2 -uptake = Amount of H_2 chemisorbed on metallic Ni (g-mol/g-catalyst)

The subscript "A" represents CO or CH_4

The run employing different reduction conditions was started with a fresh catalyst. Initially, a deactivation run was carried out to ensure the stability of the catalyst. A number of runs were carried out at different speeds of impeller to ensure the absence of mass transfer limitation around the catalyst's spheres. After obtaining the optimal reduction conditions, some other runs were carried out (e.g. reaction at different space velocities, pressures, and H_2 /CO ratio) and their effects on the activity and selectivity on Ni-catalyst were investigated.

4.2 CALIBRATION OF GAS CHROMATOGRAPH

Calibration of gas chromatograph (GC) was carried out as an initial step. In all experimental runs H_2 , N_2 , CO, CH_4 , and CO_2 were determined as reaction products. Traces of O_2 were also found in reactant and product

composition. No other organic compound was detected.

The GC results were obtained on dry-basis. Calculation were performed to convert results from dry-basis to wet-basis, and it was found that values of reaction rates remained unaffected by using either of two. For simplicity, dry-basis was chosen for calculating rate of reaction. Table 4.1 shows the conditions of GC employed.

The compounds from GC analyzer evolved in the following order; H_2 , O_2 , N_2 , CO , CH_4 , and CO_2 . All compounds were identified by their retention times. For this purpose, pure sample of each compound was injected into GC, and the time at which a compound evolved was determined as retention time for that compound. Table 4.2 represents the retention times for each of the compounds.

The GC normally takes response factor equal to 1.0 to calculate gas composition. The response factor is varied from 1.0 to compute correct peak area which is essential in determining the true composition of gas. Correct response factor is obtained by injecting a gas sample of known composition in GC and comparing the composition obtained by GC with the known composition of sample gas. The correct response factors are then inserted in the main program for computing sample composition. Table 4.3 represents the correct response factors for each compound of interest, which are helpful to correct the peak area obtained by GC for each compound. All the experimental results and the GC sample output are shown in appendix D and appendix A, respectively.

Table-4.1 Operating Conditions of GC

Gas Chromatograph	Perkin-Elmer Sigma 115
Integrator	Perkin-Elmer
Columns	Carbosieve S-II 100/120, 10' x 1/8" SS
Column Temperature	35°C for 7min, heating @ 32°C/min upto 120°C, hold at 120°C for 15 min.
Detector Temperature	60°C
Injector Temperature	50°C
Carrier gas	He, 30 cc/min
He cylinder discharge pressure	74 psig

Table 4.2 Retention Times of Compounds

<i>Compound</i>	<i>Time (min)</i>
H_2	1.41
O_2	5.20
N_2	5.50
CO	8.00
CH_4	12.20
CO_2	19.40

Table 4.3 Response Factors Obtained by GC Calibration

<i>Compound</i>	<i>Time (min)</i>
H_2	30.636
O_2	0.809
N_2	0.841
CO	0.800
CH_4	0.912
CO_2	0.744

4.3 REACTION RATES VS SPEED OF IMPELLER

Methanation reaction was carried out at different speeds of impeller. Figure 4.1 shows the reaction rates of CO conversion and CH_4 production vs. rpm. The speed of impeller varied from 150 to 860 rpm. The run#3 to run#7, as shown in appendix D, were carried out to examine the external physical transport resistances.

4.4 DEACTIVATION

Figure 4.2 shows the results obtained for deactivation run in which reaction rates are plotted vs. time. The temperature of reaction was 350 °C. The plot shows that initial rate of CH_4 is slow but it progresses very rapidly and oscillates for about four hours before reaching the steady-state. On the other hand, rate of CO conversion is very fast from the beginning but it slows down minutely till it reaches the steady-state after about four hours. After four hours, both reactions sail steadily. A similar behavior is also cited in literature [37,88]. Figure 4.2 shows reproduced runs. For this purpose, feed gases to the reactor were cut-off and the reactor was shut-down. The entire system brought into operation again under identical conditions, as used before, in order to collect new set of data. The purpose of deactivation test and reproducing runs is to ensure the stability of the catalyst.

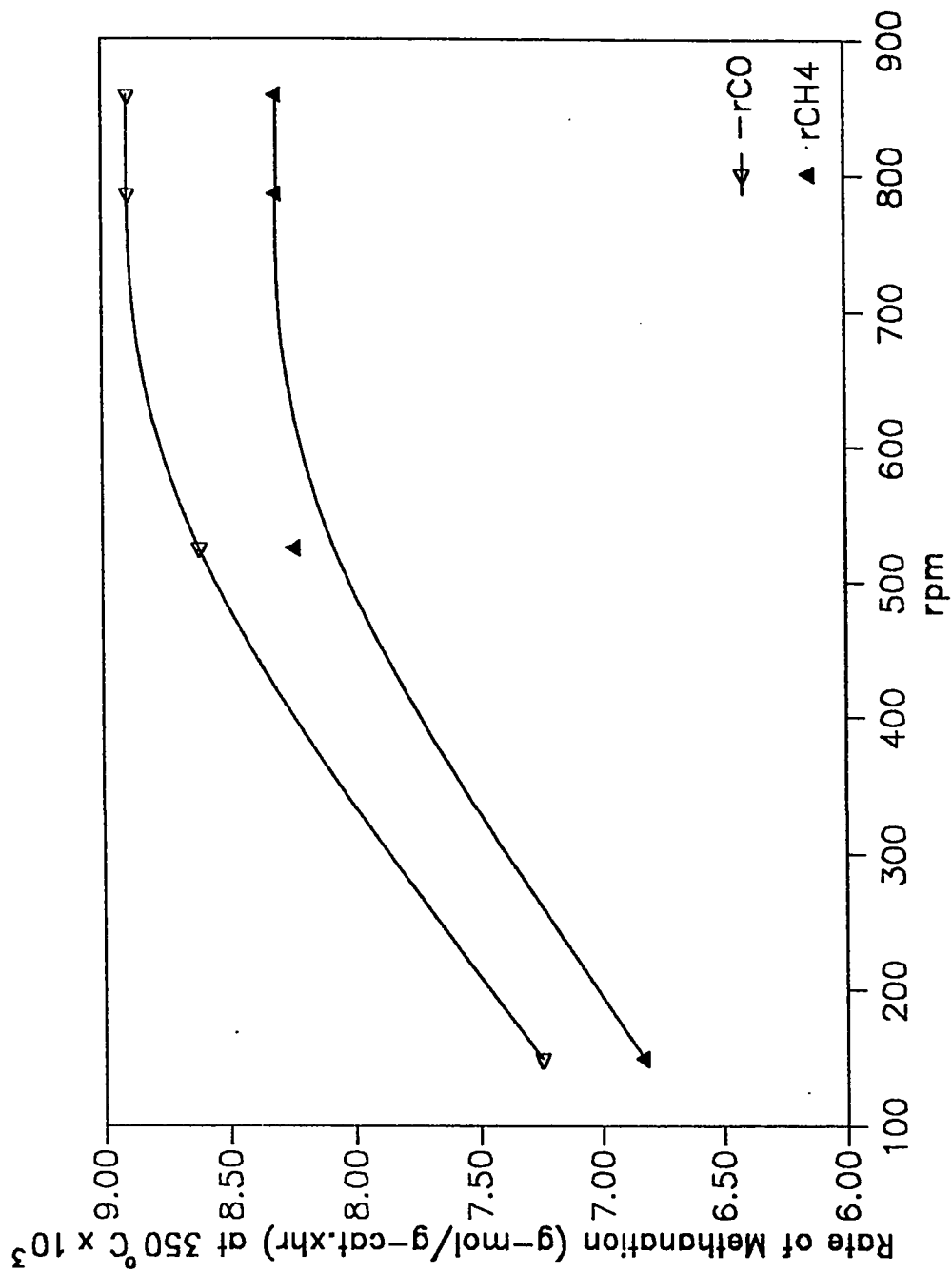


Figure 4.1 Effects of Speed of Impeller on the Methanation Reaction Rates of Ni-catalyst

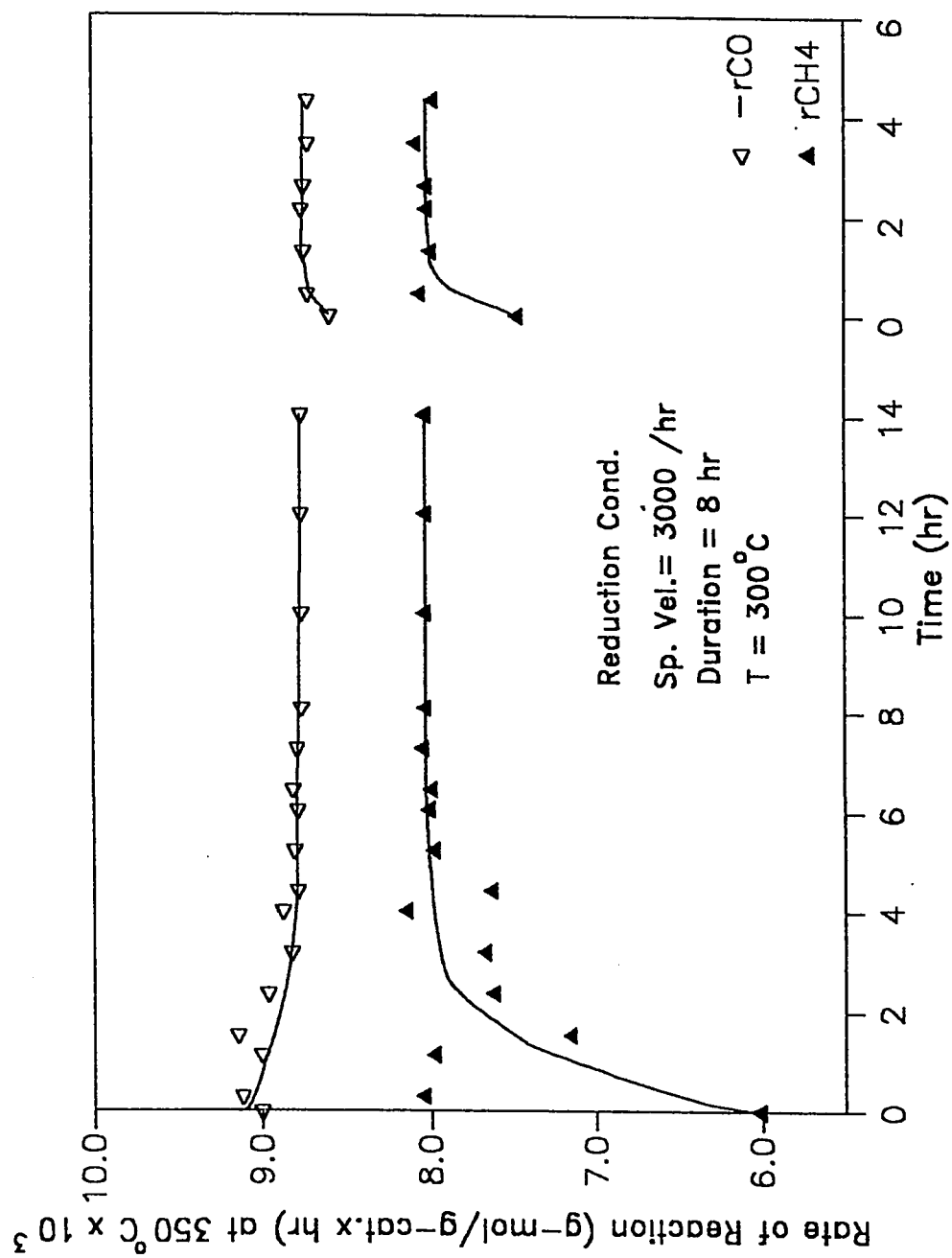


Figure 4.2 Activity and Reproducibility of Ni-catalyst

4.5 REPRODUCIBILITY OF DATA

The reproducibility of data was tested by repeating a number of runs at identical conditions. It was found that data was reproducible within 2% error. No initial increase in activity was observed except with fresh catalyst. Table 4.4 and Figure 4.2 shows some of the reproduced runs. For reproducibility of data another test was made in which two runs (run#9-10 and run#20-21) were carried out using two different catalyst samples. Both samples were reduced at same conditions and then for both rates of reaction were determined. The results show that rates in both runs are very similar to each other, which improves the confidence in reproduction of runs from scratch. Figure 4.3 represents the reproducibility of runs from scratch.

4.6 TEMPERATURE DIFFERENCE ACROSS THE CATALYTIC BED

The Berty reactor is provided with two thermocouples which indicate the temperature of catalytic bed. One thermocouple is located on the top of the bed and the other is in the bottom. This arrangement of thermocouples is useful in determining the isothermal operation of reactor. The temperature difference across the bed in this work ranged from 1 to 2 °K indicating an isothermal operation.

4.7 ACTIVITY OF Ni-CATALYST AT DIFFERENT REDUCTION CONDITIONS

Run#7 to run#19 in appendix D show the rates of reaction which were

Table 4.4 Reproducibility of Data

Run#	Compound	T (°C)	$r \times 10^3$	$r_{rep} \times 10^3$
1-2	CO	350	8.9	8.7
1-2	CH ₄	350	8.2	8.2
7-8	CO	250	8.3	8.5
7-8	CH ₄	250	7.2	7.4
9-10	CO	300	8.9	8.9
9-10	CH ₄	300	8.4	8.3
20-21	CO	300	8.8	8.8
20-21	CH ₄	300	8.1	8.1

* T is reduction temperature

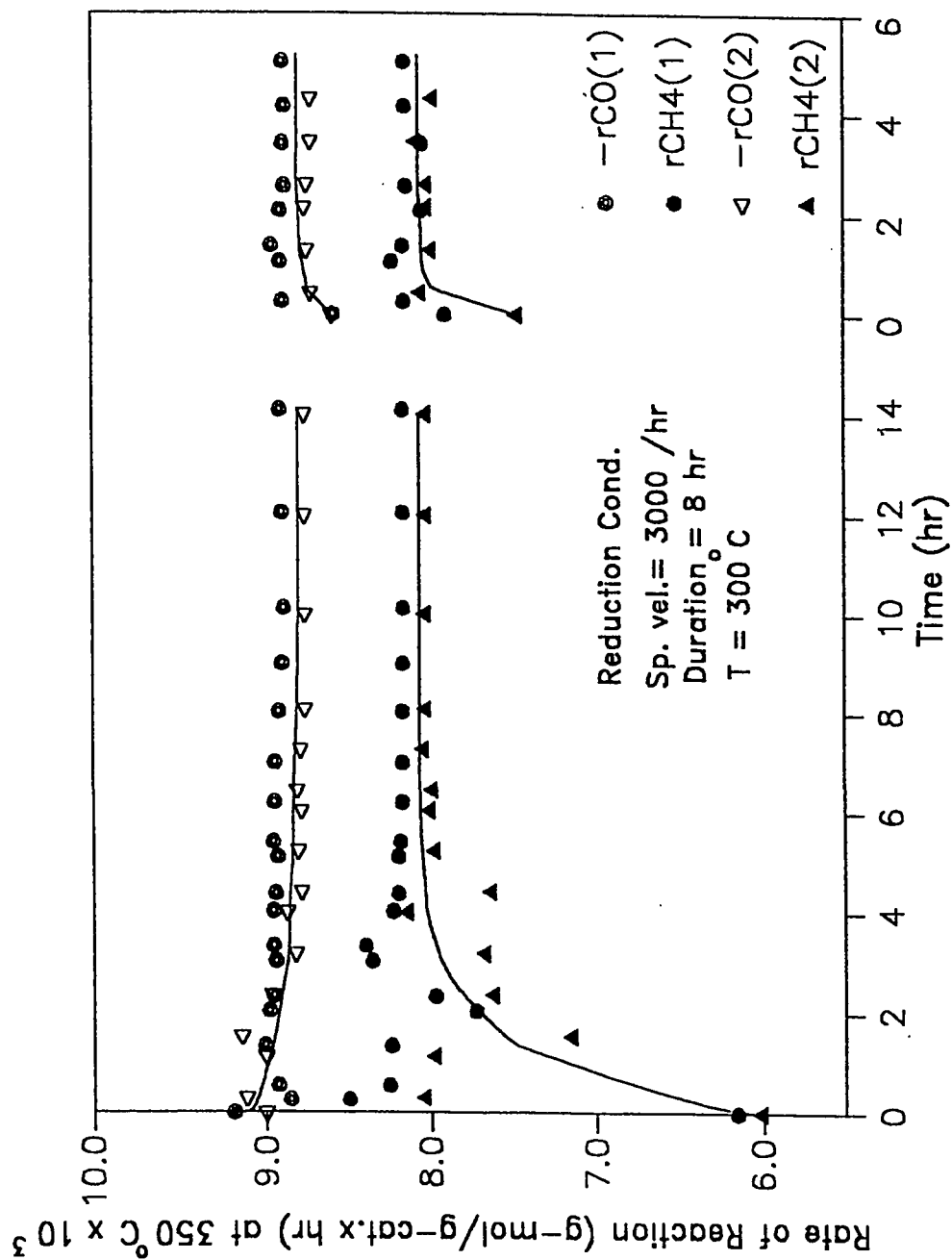


Figure 4.3 Reproducibility of Two Runs Over Ni-catalyst

obtained at several conditions of reduction. The data was measured for reduction temperatures ranged from 250 to 500 °C and for duration of reduction ranged from 2 to 16 hours.

4.8 REACTION RATE VS SPACE-VELOCITY (flow rate)

Run#22 to run#27 in appendix D represent the runs in which rate of reactions was measured at different space-velocities of feed gas. The data was measured at space-velocities ranged from 1760 to 8500 hr⁻¹

4.9 REACTION RATE VS PRESSURE

Run#9 and from run#28 to run#30 in appendix D were used to measure the rate of reaction at different pressures of reactor. Pressures ranged from 30 to 70 psig were used to collect the data.

4.10 REACTION RATE VS H₂/CO RATIO

Run#31 to run#37 were used to measure the rate of reaction at different H₂/CO ratios. The data was collected by varying the ratios from H₂/CO = 1.0 to H₂/CO = 6.5.

4.11 SELECTIVITY FOR METHANE

The selectivity for methane formation was calculated for a variety of

operating conditions. These operating conditions are: reduction temperatures and durations, space-velocities, reaction pressures, and H_2/CO ratios. Each operating condition has some effects on selectivity.

CHAPTER 5

DISCUSSION

5.1 THE EFFECT OF SPEED OF IMPELLER

The effects of different speeds of impeller on the rate of reaction are shown in Figure 4.1. The Figure 4.1 shows that rates of reaction are low at lower speed of impeller, and increase gradually with increment in the speed. This behavior indicates that external mass transfer resistances are very small and a perfect mixing is obtained at a speed of 786 rpm and above. It has been experimentally proved by Berty [63] that for a perfect mixing, a minimum recycle ratio of 20 is recommended. In this study, we have calculated recycle ratio equal to 125 (shown in appendix A). These observations are further strengthened by using mass and heat transfer correlations as shown in appendix C. These correlations produce reliable results because Reynolds no. is relatively large.

The Reynolds no. is the main factor which controls the external mass and heat transfer. This means higher speed of impeller provides higher velocities of gases across the bed, making Reynolds no. high which gives minimal mass and heat transfer resistances.

5.2 DEACTIVATION

Fresh catalyst was used for the deactivation test. Reaction rates are shown in Figure 4.2. The temperature of reaction was 350 °C. The Figure 4.2 represents a lower rate of reaction for CO and is unstable for about 5 hours. The rate of CH₄ is initially higher but it lowers down after some time, and then remains steady. After 5 hours of operation both reactions proceed steadily with 2% of experimental error.

Figure 4.2 also represents reproduced run in which the flow of the feed was interrupted for some time and reinjected. It is observed that initial behavior of fresh catalyst is not repeated. Such behavior is also cited in literature but explanation is still vague [37,81].

A definite explanation for transition state in Figure 4.2 is difficult because all studies are performed at steady-state. However, one can say that after the reduction of catalyst with flowing H₂, some of the H₂ is remained trapped in the pores of the catalyst and occupies most of the active sites of the surface. When feed is injected, CO finds few active sites for dissociative adsorption. The adsorbed CO then starts reacting with neighboring adsorbed H₂ which is previously available in abundance on the active surface of catalyst. That is why a low rate of CO conversion is observed because of low occupancy of CO on the surface. On the other hand, a high rate of CH₄ production is observed because of the availability of H₂ in abundance on the surface of catalyst. As times passes, CO occupies more active sites because of its more affinity toward active site as compare to H₂. Therefore, rate of CO conversion increases

while rate of CH_4 production decreases to some extent. A time reaches when both rates of reaction acquire steady-state, because at that time H_2/CO ratio becomes same on the surface as it is in the feed.

In a transient study on methanation, Fujita et al. [88] observed that as reaction starts, CO adsorbs dissociatively on catalyst surface. The incoming H_2 was found to have more affinity for adsorbed O than for C. Therefore, the production of H_2O is more rapid as compare to carbon species to form methane. Also, strong bonding of adsorbed CO gives slower rate of methane formation. For these probable reasons whenever fresh catalyst is charged in the reactor, it repeats the same phenomenon as shown in Figure 4.3.

5.3 EFFECTS OF REDUCTION CONDITIONS ON THE ACTIVITY OF $\text{Ni}/\gamma\text{Al}_2\text{O}_3$ CATALYST

5.3.1 *Reduction Temperature*

Different samples (10 grams each) of commercial $\text{Ni}/\gamma\text{Al}_2\text{O}_3$ (C13-4-04;20%Ni) catalyst were reduced at different conditions of temperatures starting from 250 °C to 500 °C. The other conditions like: duration of reduction, space velocity, and heating rate of catalyst bed were kept constant throughout the reduction temperature study. The duration was kept for 8 hours, and space-velocity and heating rate were kept at 3000 hr^{-1} and 5 °C/min, respectively. The reduction conditions are taken from a technical report of KACST project [4] and are presented in Table 5.1.

Table 5.1 Reduction Conditions of Ni/ γ -Al₂O₃ (C13-4-04;20%Ni) Catalyst
at Different Temperatures [4]

Run#	Temperature of Reduction (°C)	Heating Rate (°C/min)	Reduction Time (hr)	Space Velocity (hr ⁻¹)	H ₂ Flow cc/min
7	250	5	8	3000	490
9	300	5	8	3000	490
12	350	5	8	3000	490
13	400	5	8	3000	490
14	450	5	8	3000	490
15	500	5	8	3000	490

After reduction, methanation reaction was carried out using H_2 and CO as reactants. Balance being the N_2 which was acting as a diluent. The additional supply of N_2 was due to the highly exothermic nature of methanation reaction. Excess N_2 not only dilutes the reactants but also immediately takes away the generated heat during the reaction. Therefore, the temperature of reactor stays at the preset temperature with the exception of $\pm 1-2^\circ C$. The reaction conditions were kept constant throughout reduction study. The temperature was kept at $350^\circ C$, and pressure and space-velocity were kept at 30 psig and 3700 hr^{-1} , respectively.

Figure 5.1 shows that activity of $Ni/\gamma Al_2O_3$ is quite low at a reduction temperature of $250^\circ C$ for both rates of reactions (i.e. $-r_{CO} = 8.2 \times 10^{-3} \text{ g-mol/g-cat.xhr}$, $-r_{CH_4} = 7.2 \times 10^{-3} \text{ g-mol/g-cat.xhr}$). It is understandable that at low reduction temperatures, the percentage of reduced Ni is low as has been studied and proved by KACST report [4] and is represented in Table 5.2. When temperature of reduction was increased from $250^\circ C$ to $300^\circ C$, a sudden rise in rates of both reactions was observed (Figure 5.1). This shows that percent of reduced Ni is increased as can be seen in Table 5.2 and as a result more active sites are available for reaction. This logic is further strengthened by the results obtained from the analysis of spent $Ni/\gamma Al_2O_3$ catalyst samples, as shown in Table 5.3.

Comparing Run#7 and Run#9 in Table 5.3, it can be observed that the surface area and the pore volume of Run#7 are less than Run#9. This shows that %reduction of Ni (available active sites), Ni-surface area, and pore volume of catalyst are playing key role in describing the behavior of

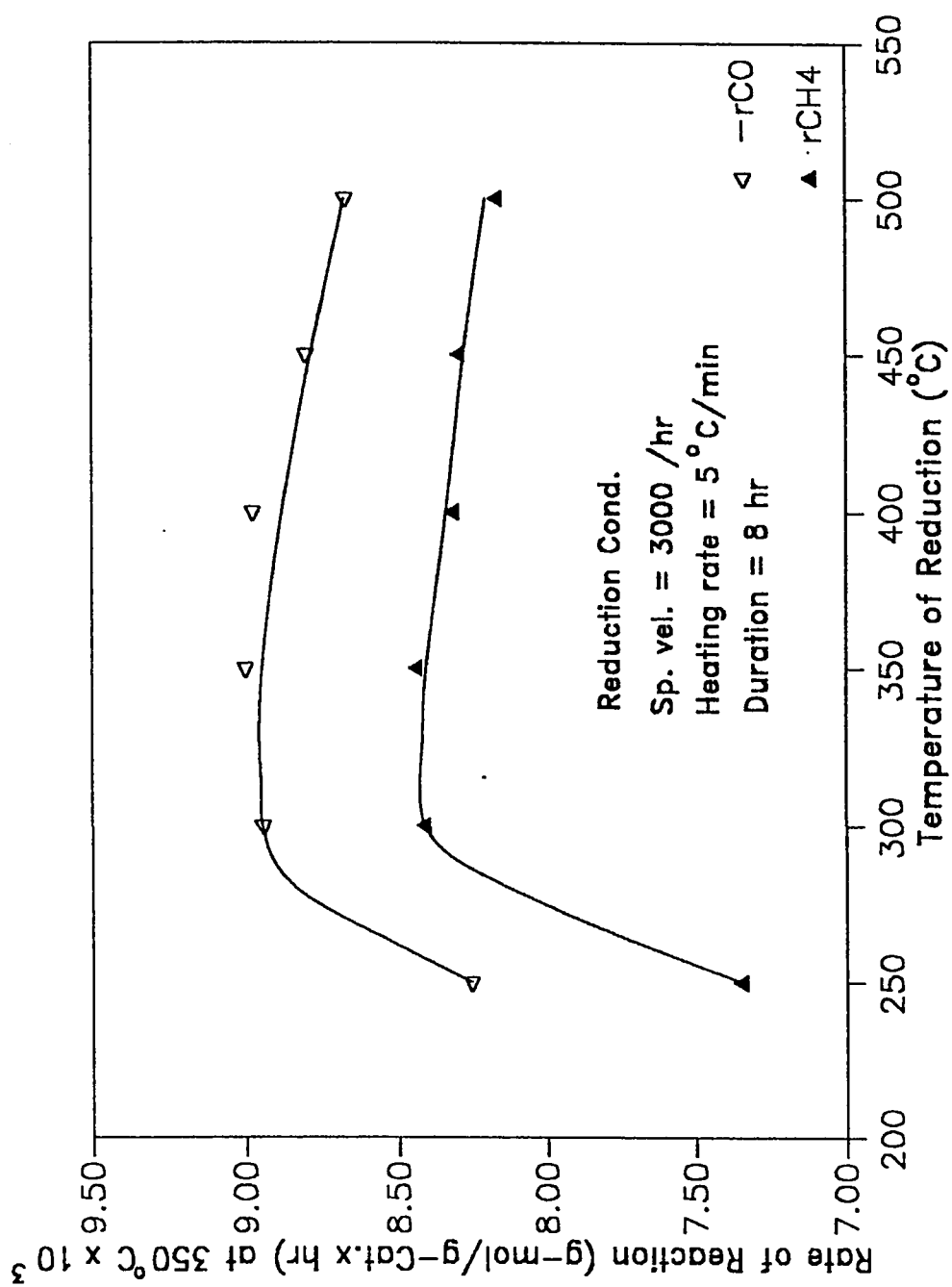


Figure 5.1 Effects of Reduction temperature on the Activity of Ni-catalyst

**Table 5.2 Percentage of Reduced Ni Obtained by Reducing Ni/ γ Al₂O₃
(C13-4-04;20%Ni) Catalyst at Different Temperatures [4]**

Run#	Temperature of Reduction (°C)	% Ni Reduced
7	250	17.2
9	300	39.40
12	350	64.1
13	400	82.30
15	500	97.3

Table 5.3 Analysis of Spent $\text{Ni}/\gamma\text{Al}_2\text{O}_3$ (C13-4-04;20%Ni) Catalyst

Run#	Temperature of Reduction (°C)	Ni-Surface Area (m ² /g)	Pore Volume cc/g	Avg. Pore Radius (Å)	Carbon Content (wt%)
7	250	0.41	0.47	214	1.25
9	300	2.42	0.51	175	0.96
12	350	3.93	0.48	160	0.90
13	400	5.33	0.50	155	0.87
15	500	7.26	0.48	144	0.80

* Analysis performed by Research Institute (RI), KFUPM.

Ni/ γ -Al₂O₃ for the two runs.

When the reduction temperature was increased from 300°C to 500°C, it can be seen in Figure 5.1 that the rates of reactions for CO conversion and CH₄ formation were all lying in the same region as it was obtained for reduction at 300°C. Figure 5.1 also shows a slight decrease in both rates of reactions as temperature increases. Since a sudden change in rate of reaction is not found as was observed between 250°C and 300°C, therefore it can be said that rates of reactions at 300°C and above are identical and are within 3% experimental error.

A question arises why both rates of reactions lie in same region with increasing reduction temperature? Answer can be found by looking at the Table 5.2 that the number of active sites (%reduced Ni) is increasing with the temperature of reduction. Under these conditions rates of reactions should increase with increasing reduction temperature but it is not observed. Table 5.3 shows that the Ni-surface area is also increasing with increased reduction temperature, but pore volume remains almost constant. It can be seen from Table 5.3 that average pore radius is decreasing with rise in reduction temperature. This could be because of some of the pores are blocked or narrowed due to thermal sintering. It has been predicted by Flynn et al. [99] that a catalyst with a broad pore-size distribution sinters rapidly than the catalyst with a narrow pore-size distribution. It can be observed from Table 5.3 that as reduction temperature increases, the average pore-size starts to decrease and causes a decrease in the rate of reaction in the sense that further increment in the rate is not observed at higher reduction temperature.

Another possibility of constant rates of reactions is the conversion of CO which is about 90% in each set of data. Although, more sites are available at higher reduction temperature but less reactants are further available for reaction after such a high conversion. One possibility of constant rate of reaction at higher reduction temperature is the structural change i.e. the transformation of active site in to a passive site. Such possibility is also discussed by Satterfield [98]. Table 5.3 also shows carbon content in samples which is constant at about 1.0 wt% for all samples. It has been cited by Menon et al. [97] that the activity catalyst, containing 6-10 wt% carbon, does not change appreciably. Bajpai et al. [81] have also found about 1wt% of carbon deposition on Ni-catalyst after 16 hours of operation, which did not affect the activity of catalyst. It can be said that 1 wt% carbon content does not affect the activity of $\text{Ni}/\gamma\text{Al}_2\text{O}_3$ catalyst.

For the above mentioned reasons, no observable change in activity of $\text{Ni}/\gamma\text{Al}_2\text{O}_3$ is observed at higher reduction temperatures. Therefore, it can be said that 300 °C is the optimal reduction temperature among the various applied temperatures. Reduction at higher temperatures somehow affects the life of catalyst and is also not feasible economically. In subsequent sections, reduction temperature is kept constant at 300°C along with other variables.

The reduction procedure which was adopted in the technical report of KACST project [4] employed a 50/50 mixture of H_2 & He as reducing gas. It has been mentioned [4] that the ratio of H_2 & He does not change with percent reduction of Ni metal. To prove this statement, two runs (Run#9 & Run#11) were carried out. In Run#9, pure H_2 was used as a reducing gas

and a 50/50 mixture of H_2 & He was used for reduction in Run#11. Figure 5.2 shows that both rates of reactions are identical for Run#9 and Run#11, and are within 5% experimental error. This shows that He acts as a diluent and does not affect the extend of reduction.

5.3.2 *Duration of Reduction*

The reduction of $Ni/\gamma Al_2O_3$ (C13-4-04;20%Ni) catalyst was carried out for different durations at $300^\circ C$. The other conditions i.e. heating rate and space velocity were kept constant at $5^\circ C/min$ and $3000 hr^{-1}$, respectively. The conditions of duration of reduction are taken from the technical report of KACST project [4] and are shown in Table 5.4.

After reduction, methanation reaction was carried out using H_2 and CO as reactants with N_2 being an inert gas. The reaction conditions were kept same as discussed in previous section.

Figure 5.3 shows that the activity of $Ni/\gamma Al_2O_3$ is low when it was reduced for only 2 hours. A rapid rise in activity was observed with 4 hours of reduction. This change in reaction rate could be understood that less active sites are available for 2 hours of reduction than the active sites obtained from the reduction for 4 hours. When the duration of reduction increased from 4 hours to 8 hours, a small rise in activity was observed. After 8 hours up to 16 hours, further rise in activity was not observed (Figure 5.3). This behavior could be explained with the help of the technical report of KACST project [4] which is shown in Table 5.5, and Table 5.6. The Table 5.5 represents that by

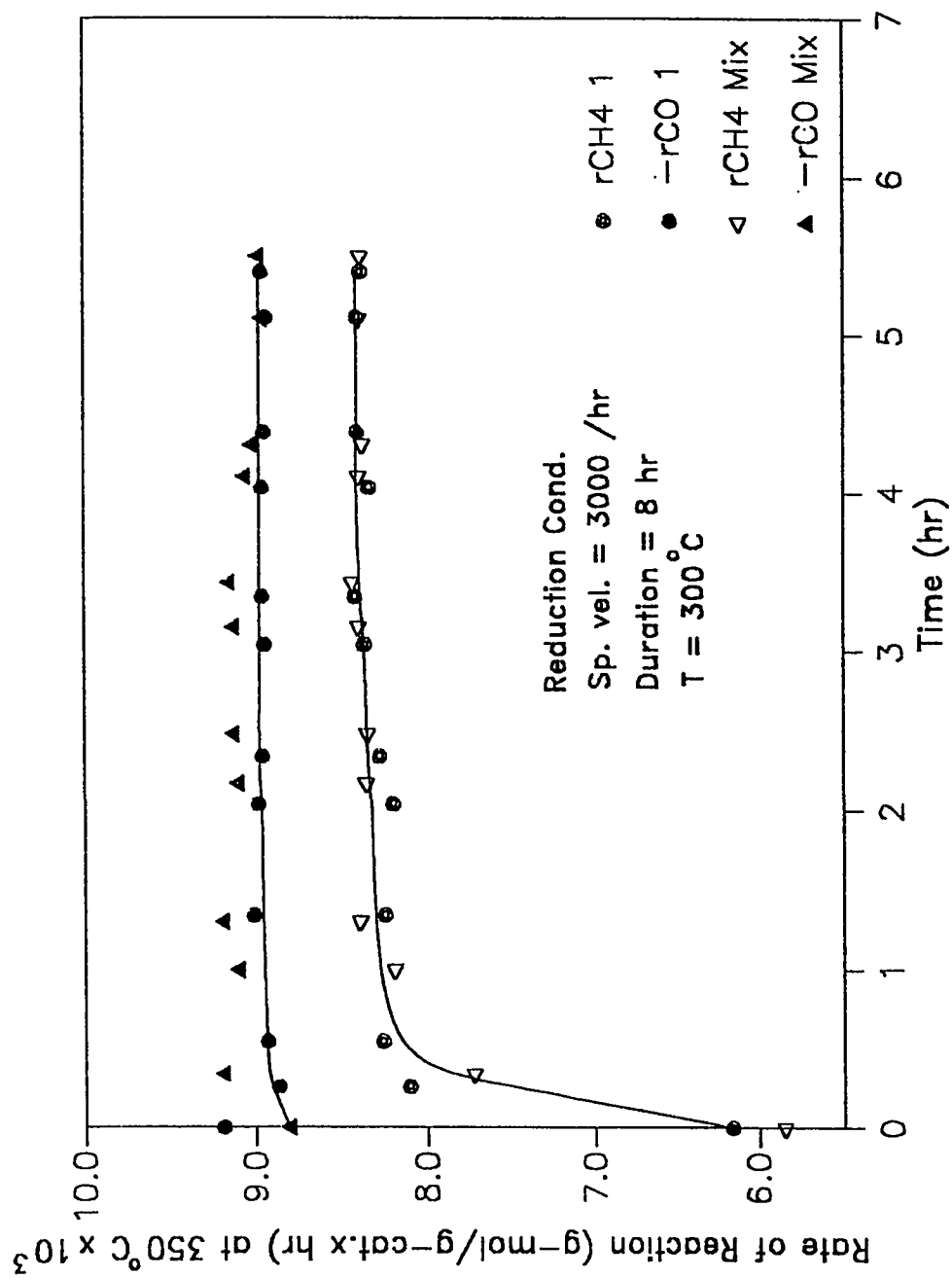


Figure 5.2 Comparison of Activity Between Two Samples of Ni-cat. reduced in H₂ and H₂:He Mix.

**Table 5.4 Reduction Conditions of Ni/ γ -Al₂O₃ (C13-4-04;20%Ni) Catalyst
for Different Durations [4]**

Run#	Duration of Reduction (hr)	Temperature of Reduction (°C)	Heating Rate (°C/min)	Space Velocity (hr ⁻¹)	H ₂ Flow cc/min
19	02	300	5	3000	490
16	04	300	5	3000	490
9	08	300	5	3000	490
17	12	300	5	3000	490
18	16	300	5	3000	490

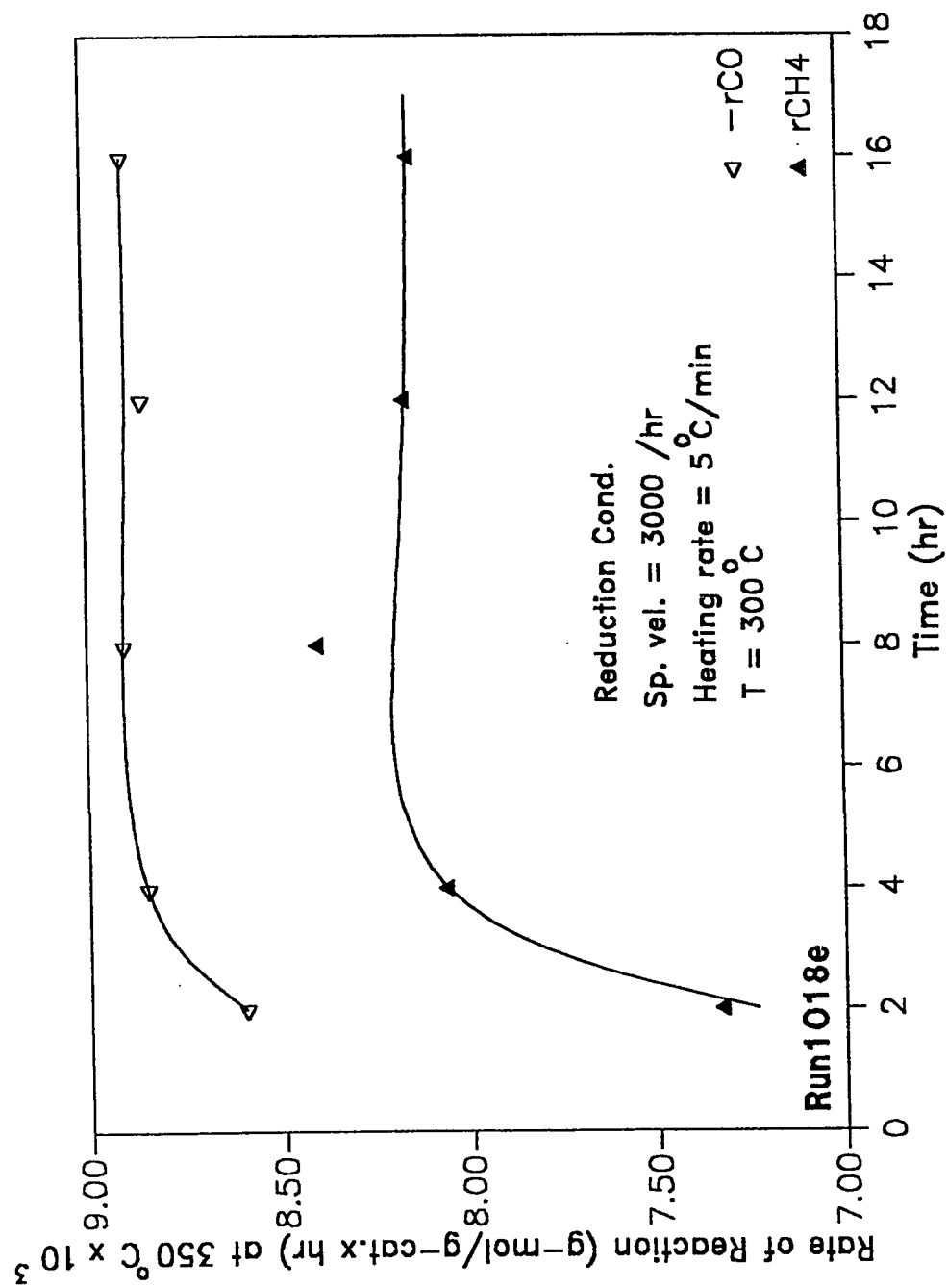


Figure 5.3 Effects of Reduction time on the Activity of Ni-catalyst

**Table 5.5 Percentage of Reduced Ni Obtained by Reducing Ni/ γ -Al₂O₃
(C13-4-04;20%Ni) Catalyst For Various Durations [4]**

Run#	Duration of Reduction (hr)	% Ni Reduced
16	04	27.80
9	08	39.9
17	12	61.20
18	16	47.90

Table 5.6 Analysis of Spent $\text{Ni}/\gamma\text{Al}_2\text{O}_3$ (C13-4-04;20%Ni) Catalyst

Run#	Duration of Reduction (hr)	Ni-Surface Area (m^2/g)	Pore Volume cc/g	Avg. Pore Radius (\AA)	Carbon Content (wt%)
19	02	-	0.46	208	1.21
16	04	1.24	0.50	192	1.05
9	08	2.42	0.51	175	0.96
17	12	3.74	0.48	192	1.05
18	16	3.92	0.49	177	1.00

* Analysis performed by Research Institute (RI), KFUPM.

increasing the duration of reduction, percentage of reduced Ni increases but this rise is gradual. It can be seen from Table 5.5 that the difference between two percentages of reduced Ni are small for two sets of duration of reduction. Table 5.6 represents a somewhat similar picture. The Ni-surface area is increasing gradually with increment in duration of reduction. A similar behavior is also cited by Bhatia et al. [74] and is shown in Figure 5.4. Pore volume and average pore diameter are almost same for all durations of reduction. Since carbon content is 1wt% therefore, it seems to pose no effect on the activity of $\text{Ni}/\gamma\text{Al}_2\text{O}_3$ catalyst.

From above observations, it could be said that by increasing the duration of reduction a rapid rise in percentage of reduced Ni is obtained which causes a rise in the activity of $\text{Ni}/\gamma\text{Al}_2\text{O}_3$. After 8 hours of reduction (Run#9), further rise in the number of active sites is very slow. Thus, the activity for 8,12, and 16 hours remains almost constant. As a result it could be said that duration of 8 hours of reduction (Run#9) is the optimal duration in which highest rates of reactions are observed.

5.3.3 *Effects of Heating Rate And Space Velocity*

It has been already proved experimentally by the technical report of KACST project [4] that by changing the heating rate of catalyst bed from 1°C to 5°C and space velocity from 480 hr^{-1} to 4800 hr^{-1} , no observable change in reduction of $\text{Ni}/\gamma\text{Al}_2\text{O}_3$ catalyst is observed. Keeping these views in mind, effects of heating rates and space velocity were not studied.

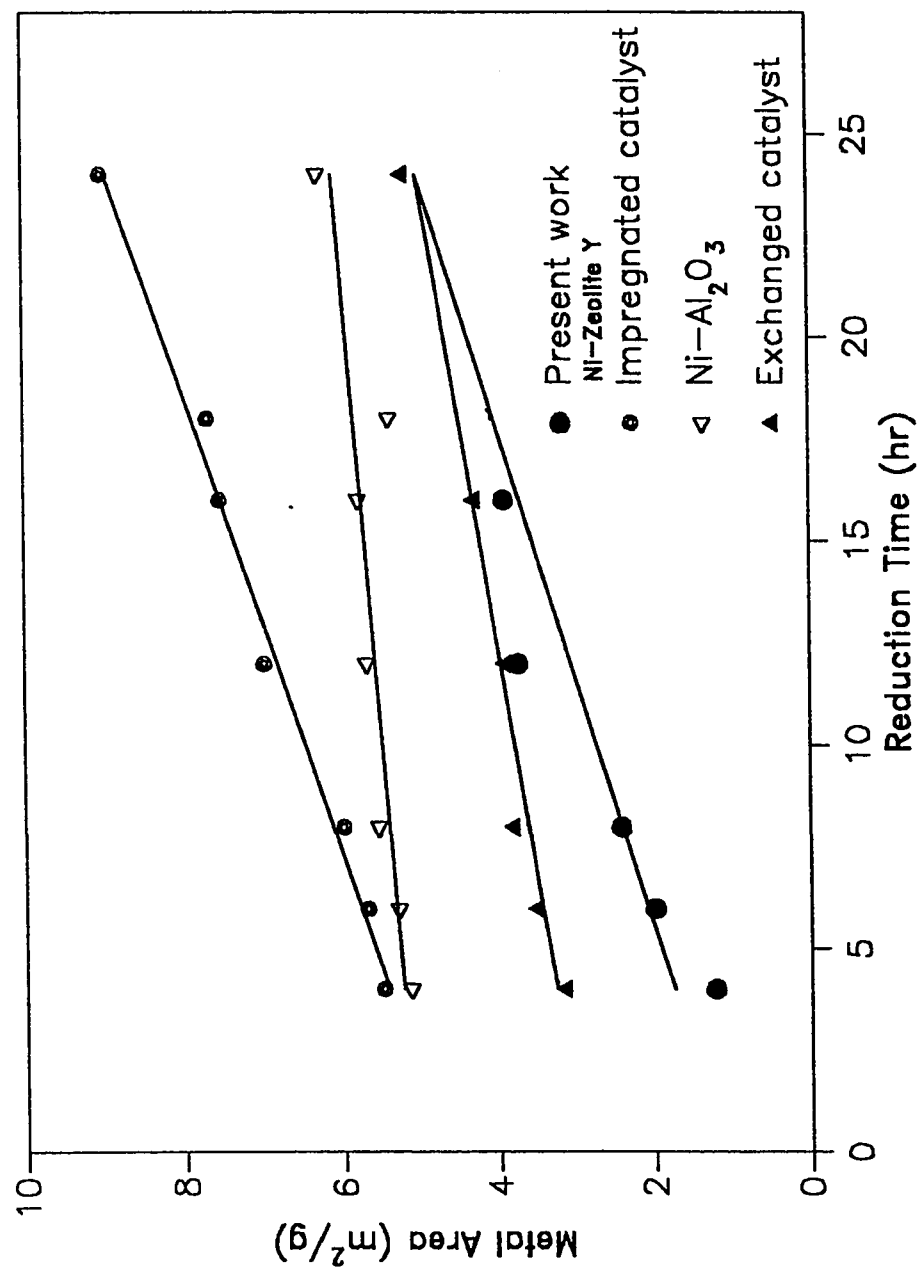


Figure 5.4 Effect of Reduction Time on Nickel Metal Area[74]

By the study of all factors of reduction which influence the activity of $\text{Ni}/\gamma\text{Al}_2\text{O}_3$ catalyst, it is being finalized that the optimal reduction conditions in order to obtained optimal rates of reactions are as follows: temperature of reduction is 300°C , duration of reduction is 8 hours, space velocity is 3000 hr^{-1} , and heating rate is $5^\circ\text{C}/\text{min}$.

This is from best of our knowledge that this work is conducted for the first time. There is no data available in the literature which can be compared with this data.

The optimal reductions, which are obtained from the effect of reduction conditions on the activity of catalyst, are used in subsequent sections in order to investigate the effects of different operating parameters on the activity and selectivity of $\text{Ni}/\gamma\text{Al}_2\text{O}_3$ catalyst.

5.4 THE EFFECTS OF SPACE-TIME ON THE ACTIVITY OF $\text{Ni}/\gamma\text{Al}_2\text{O}_3$ CATALYST

A study was carried out to observe the effects of space-time on the activity of $\text{Ni}/\gamma\text{Al}_2\text{O}_3$ catalyst for a methanation reaction. The space-time ranged from $1.1 \times 10^{-4}\text{ hr}$ to $5.6 \times 10^{-4}\text{ hr}$. Figure 5.5 shows that both rates of CO conversion and CH_4 formation increase as the space-time decreases, and vice versa. For a small space-time of feed in the reactor, the concentration of reactants remains higher than the concentration of product. Thus, more reactants are available all the time giving higher rate of formation of product. On the other hand, large space-time of feed in the reactor increases the

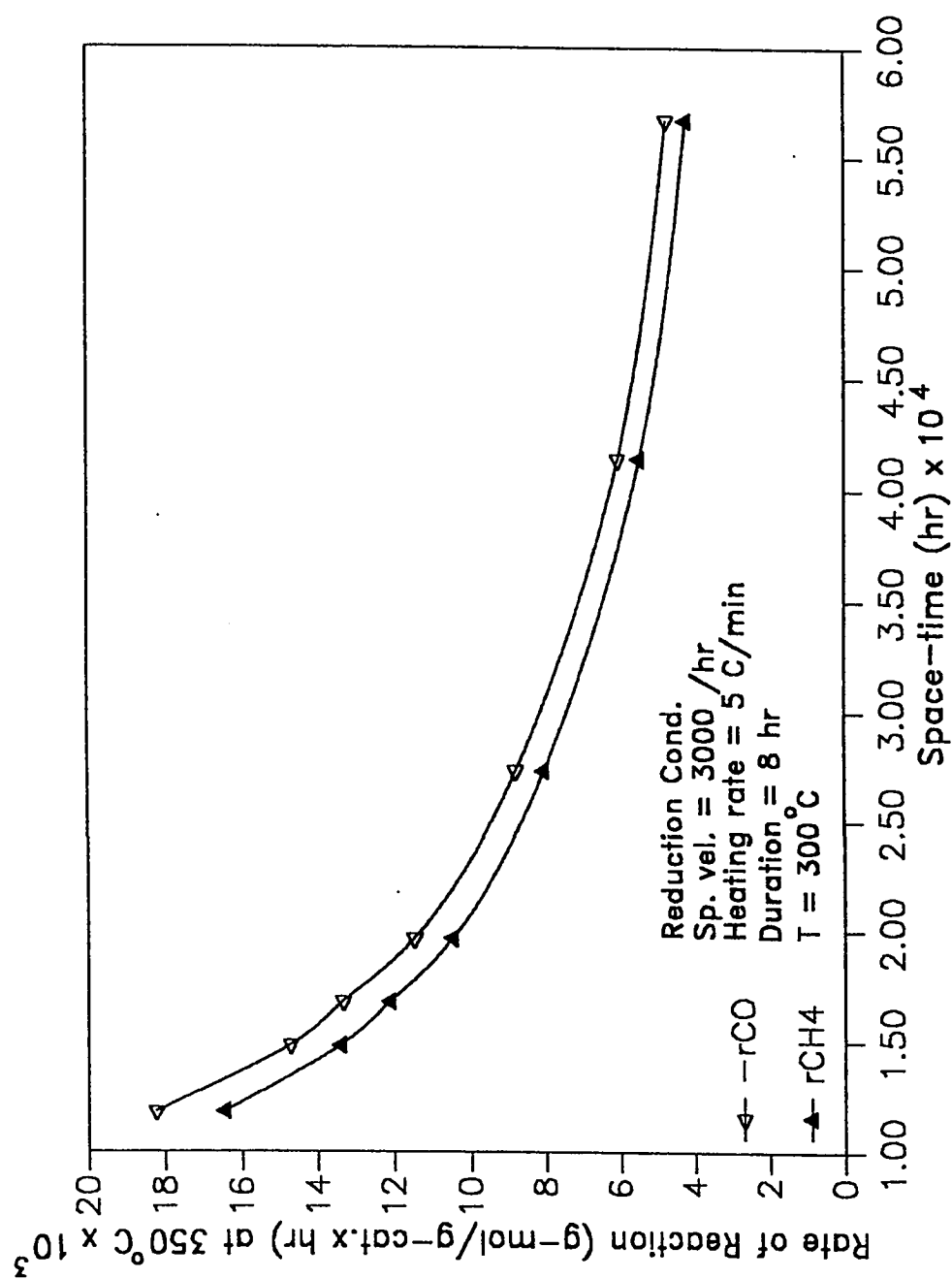
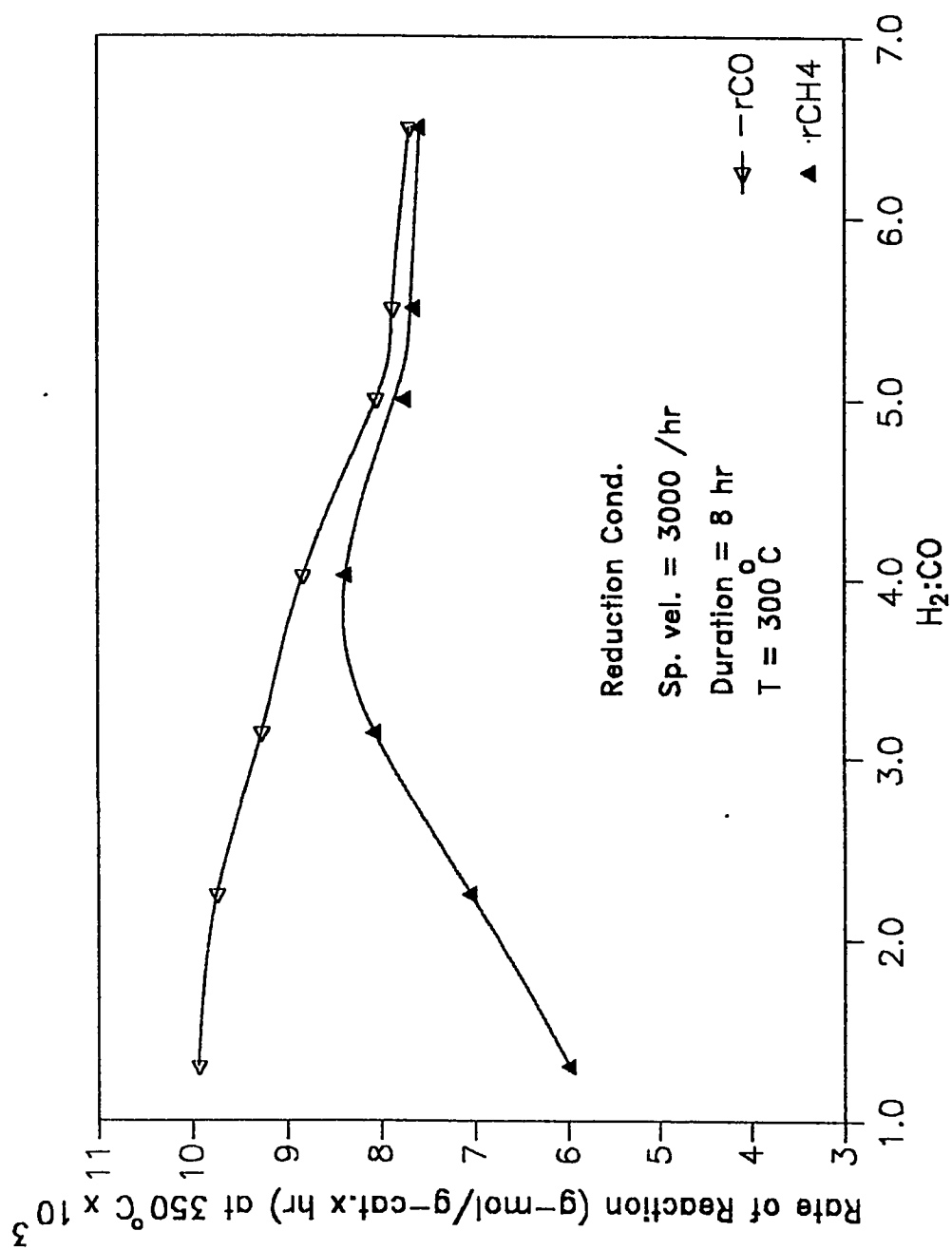


Figure 5.5 Effects of Space-time on the Activity of Ni-catalyst

concentration of product in the reactor which inhibits the reactants to be adsorbed on catalyst surface for reaction. Also, concentration of reactants drops down in the reactor because of lower feed rate providing more time for reactants to stay in reactor for reaction. Thus, the decreased concentration of reactants in the reactor reduces the rate of product formation. A similar behavior is also cited by Jarvi et al. [76]. They not only discussed that drop in rate of reaction at higher space-time is due to decrease in reactants concentration, but also mentioned that rise in rate at lower space-time is due to high mass transfer coefficient of catalyst. Therefore, in order to acquire higher rates of reactions, the space-time should be kept low.

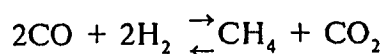
5.5 THE EFFECTS OF $H_2:CO$ RATIO ON THE ACTIVITY OF $Ni/\gamma-Al_2O_3$ CATALYST

Different ratios of $H_2:CO$ were tried to observe their effects on the rate of reaction. In Figure 5.6, as $H_2:CO$ is increased from 4.0 to 6.5, there is a slight decrease in the rate of CO conversion. The rate of CH_4 formation almost remains the same. This is due to rise in concentration of H_2 which occupies more active sites and leaves less sites for CO to be adsorbed and to react. In a similar study Bajpai et al.[81] used higher H_2/CO ratio (3.1 to 24.8) and found that for higher H_2/CO ratio of 24.8 the rate of reaction dropped down as compared to lower ratio of 3.8. No definite explanation was mentioned by them for this behavior. Vandervell et al. [43] have also performed studies on higher H_2/CO ratio. They found that H_2 more readily reacts with adsorbed O than CO because of its higher concentration, therefore,

Figure 5.6 Effects of H₂:CO ratio on the Activity of Ni-catalyst

more water is formed than CH_4 . For this reason we observe a decrease in the rate of reaction at higher ratios.

An almost reverse behavior is observed when lower ratios of H_2 :CO were tried. Figure 5.6 shows that rate of CO conversion increases gradually as H_2 :CO is lowered from 4.0 to 1.0, and at the same time production of CH_4 is decreased. The reason is quite understandable that at lower H_2 :CO ratios, the side reaction is promoted.



Due to above dominant reaction more CO_2 is produced than CH_4 . The percentage of C deposition on the catalyst surface did not increase from 1%, that is why a decrease in CO conversion was not observed. The domination of above reaction has also cited by Vandervell et al. [43]. They have reported that at low H_2 /CO ratio, there is a competition between CO and H_2 for adsorbed O for oxidation. Since CO has more affinity for surface, therefore, it readily reacts with surface and forms CO_2 . This could be a probable reason that a higher rate of CO conversion is obtained at lower H_2 /CO ratio. On the other hand, more conversion of CO to CO_2 decreases the rate of CH_4 formation.

5.6 THE EFFECTS OF PRESSURE ON THE ACTIVITY OF $\text{Ni}/\gamma\text{Al}_2\text{O}_3$ CATALYST

The rates of reactions were studied by changing the pressure of the reaction system from 30 psig to 72 psig. Figure 5.7 shows that no appreciable change is observed in the rates of CO conversion and CH_4 production. It seems that change in pressure, while operating the system at low pressures, has insignificant effect on the rate of reaction. It has been reported by Jarvi et al. [76] that a rise in reaction was observed at a higher pressure (7-18 atm) which is in accordance with Le Chatelier's principle. The maximum pressure obtained in this study was 5 atm. A probable reason could be that at such a pressure, effect on rate is negligible.

5.7 THE EFFECTS OF DIFFERENT OPERATING CONDITIONS ON THE SELECTIVITY FOR CH_4 FORMATION OVER $\text{Ni}/\gamma\text{Al}_2\text{O}_3$ CATALYST

5.7.1 *The Effects of Temperature of Reduction*

Figure 5.8 shows that the selectivity for CH_4 formation is about 87% at a reduction temperature of 250 °C. This indicates that less number of active sites are created during reduction. The water-gas shift reaction is also initiated as a side reaction by which CO_2 is produced. Same reaction is also observed when $\text{Ni}/\gamma\text{Al}_2\text{O}_3$ catalyst was reduced at higher temperatures but its effect was not prominent as it appears in catalyst reduced at 250 °C. The reason is that the reduction at higher temperatures generates more active sites. Production of CO_2 also takes place with the catalyst reduced at higher

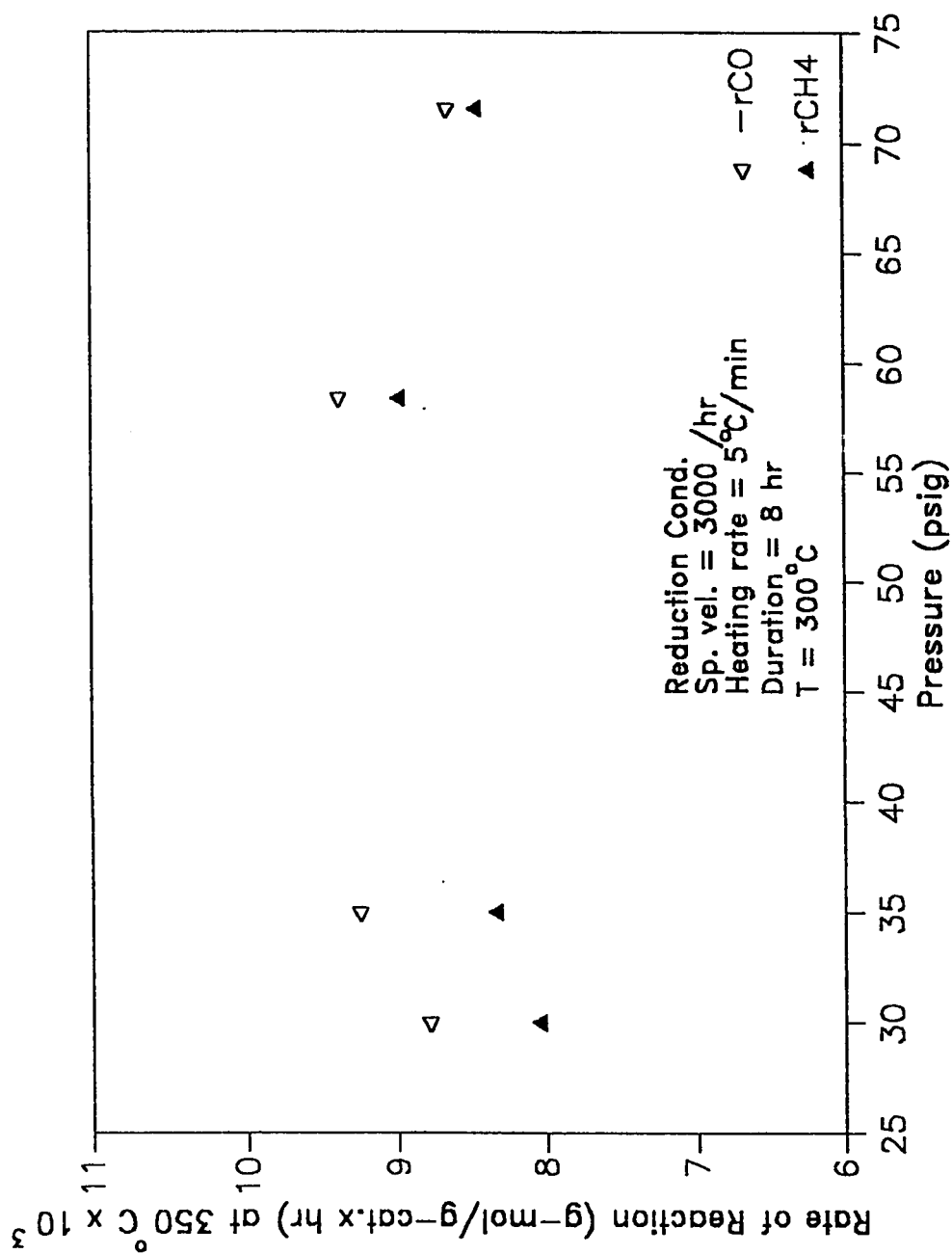


Figure 5.7 Effects of Pressures on the Activity of Ni-catalyst

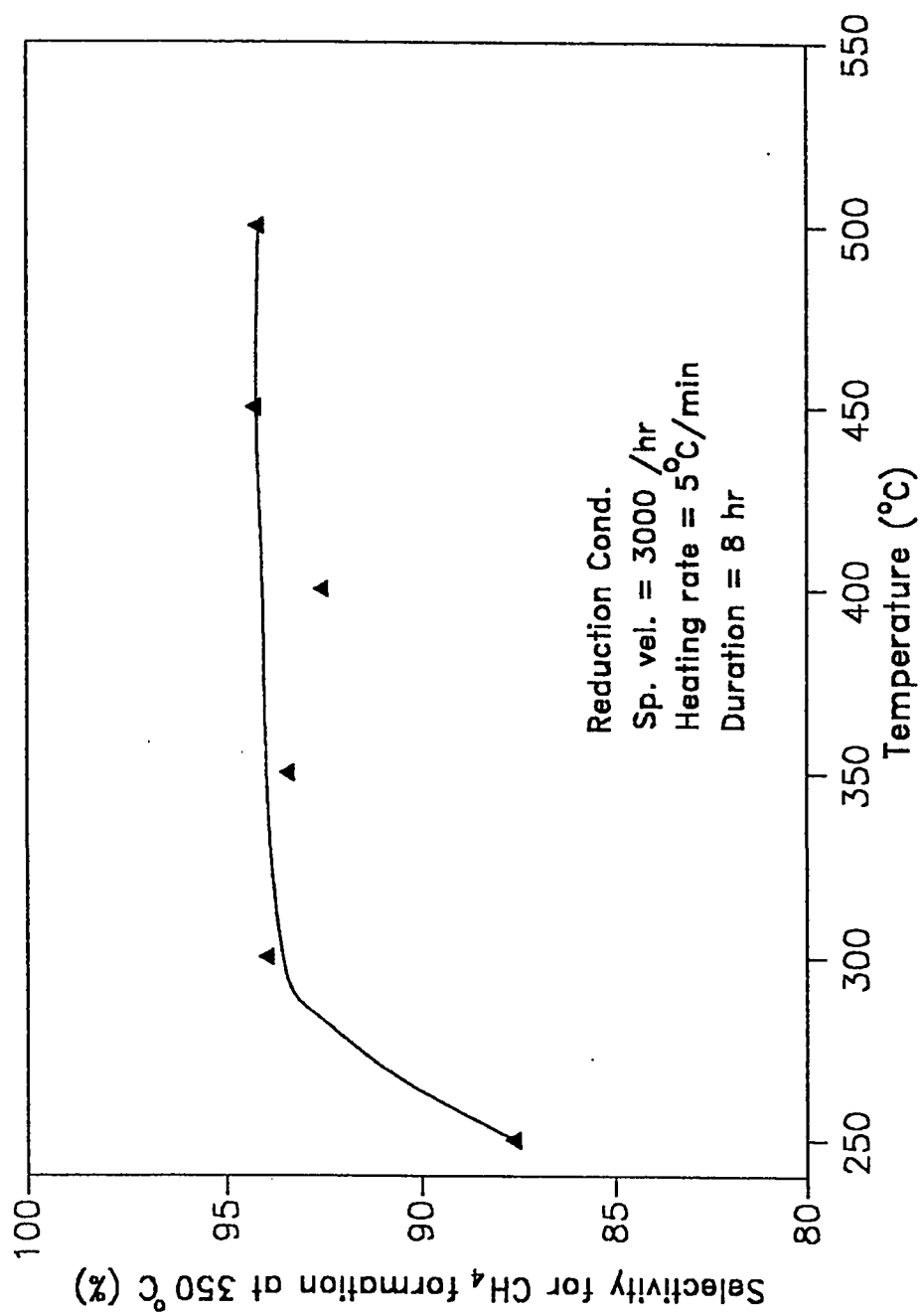


Figure 5.8 Selectivity for CH₄ formation as a function of Reduction Temperature

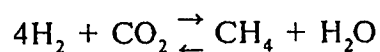
temperature, but it does not significantly affect the selectivity because the catalyst surface occupies more active sites. It can be seen in Figure 5.8 that selectivity remains constant for reduction temperatures ranging from 300-500 °C.

5.7.2 *The Effects of Duration of Reduction*

Figure 5.9 shows a similar behavior for selectivity as has been observed in Figure 5.8. It is found that for a lower duration of reduction, less active sites are generated. For larger duration of reduction the rise in active sites is gradual. That is why an almost constant but higher selectivity is observed for a duration of 8 to 16 hours of reduction. Selectivity, for lower duration of 2 to 4 hours of reduction, is found to be low. The explanations to above behavior are similar to those which are discussed in section 5.7.1.

5.7.3 *The Effects of Space-Time*

Figure 5.10 shows that as the residence time of the reactants in the reactor is increased, the selectivity to CH₄ formation is increased. The side reaction, as shown below, is taking part in addition to methanation reaction.



Since CO₂ has less affinity towards surface chemisorption than CO; therefore, higher residence time drops the concentration of CO through reaction and allows CO₂ to chemisorb and to react with H₂ in order to give more selective product.

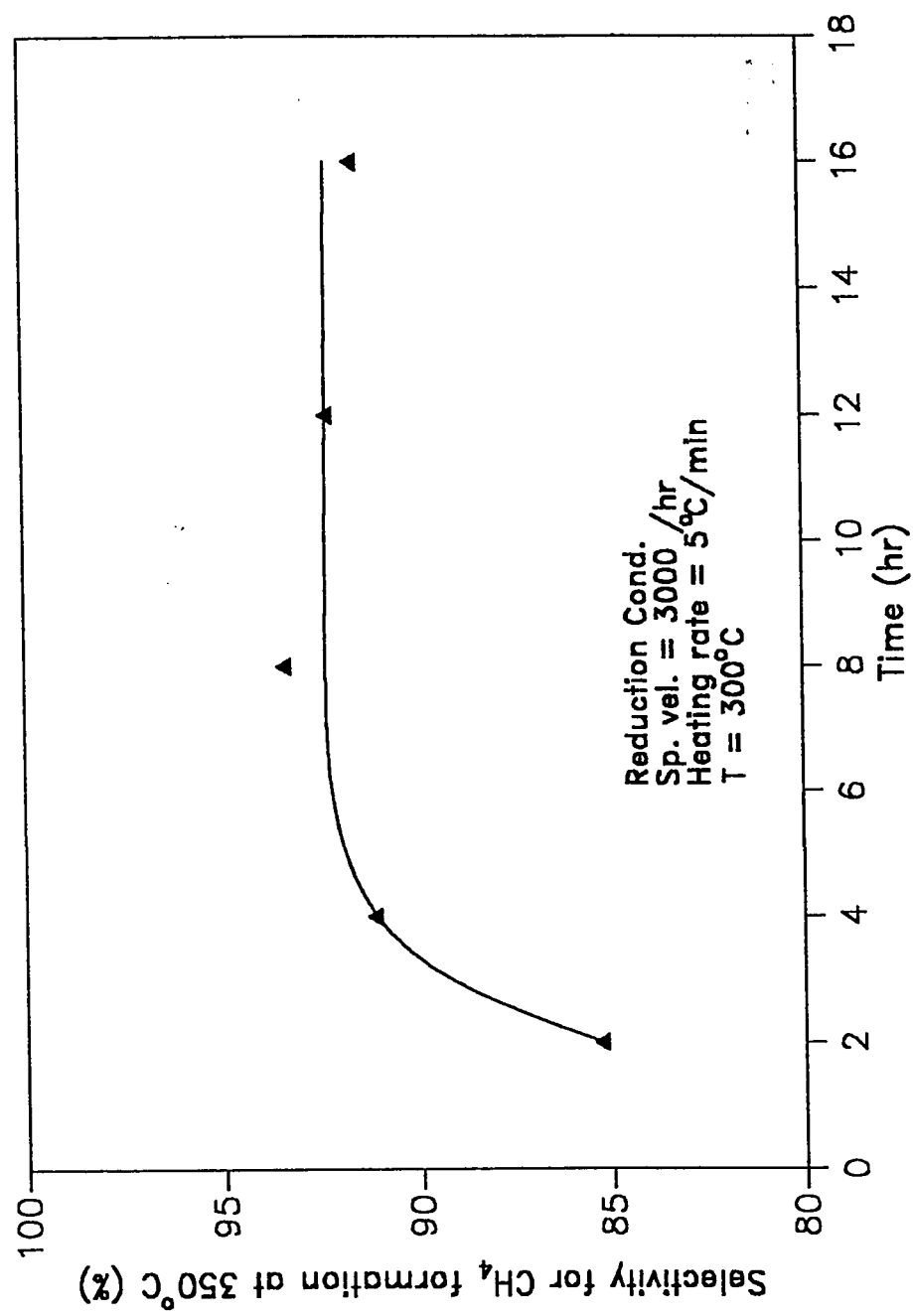


Figure 5.9 Effects of Time of Reduction on the Selectivity of CH₄ formation

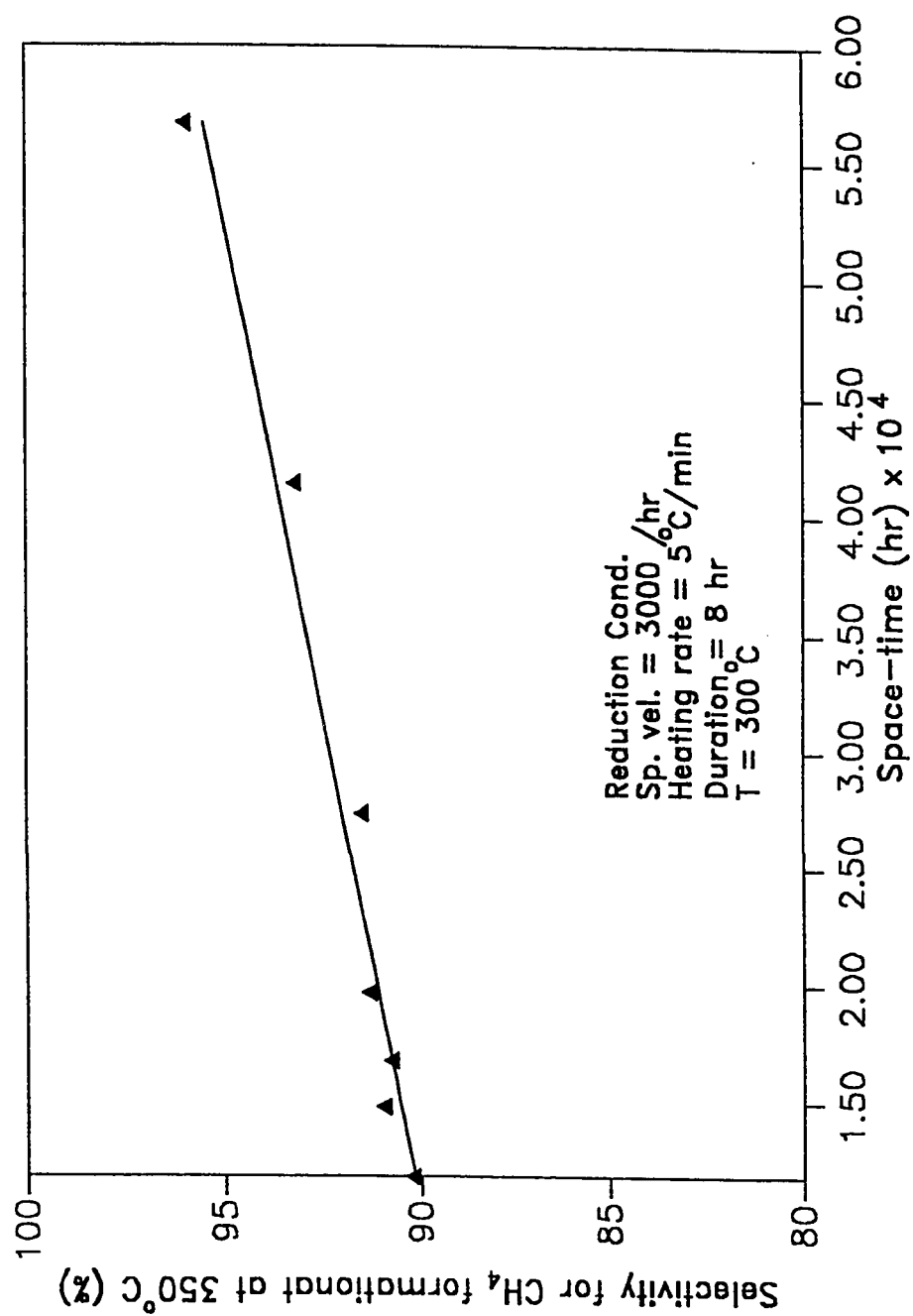


Figure 5.10 Effects of Space-time on the Selectivity of Ni-catalyst

There are normally three types of active sites available on the surface of catalyst [98]. They are: very active sites which holds the reactants strongly on the surface, normal active sites at which reaction takes place at a normal pace, and the less active sites which hold the reactants weakly and cannot proceed the reaction to completion [98]. When residence time is increased, then normal active sites and some of the less active sites take part in the reaction. Therefore, more adjacent sites are available to adsorb H_2 in the neighborhood of CO. Thus provides higher selectivity to CH_4 . Also, for lower space-time the reactants do not find enough time to sit on a proper site in a desired composition in order to give selective product.

5.7.4 *The Effects of H_2 :CO Ratio*

The stoichiometric ratio of H_2 :CO for methanation reaction is 3.0. In this study a slightly higher ratio of about 4 was used to avoid carbon deposition on the surface of $Ni/\gamma Al_2O_3$ catalyst. It can be observed from Table 5.3 and Table 5.6 that carbon on the catalyst surface for all samples is around 1wt%. As H_2 :CO ratio is increased from 4.0 to about 6.5 in Figure 5.11, there is a gradual increase in selectivity for CH_4 formation; because, more H_2 is available on the neighboring site of CO for reaction. When H_2 :CO ratio was dropped from 4 to 1, it can be seen from Figure 5.11 that there is a steeper drop in the selectivity for CH_4 formation. The side reaction, as discussed in section 5.5, is causing the drop in selectivity. The reasons are discussed in section 5.5.

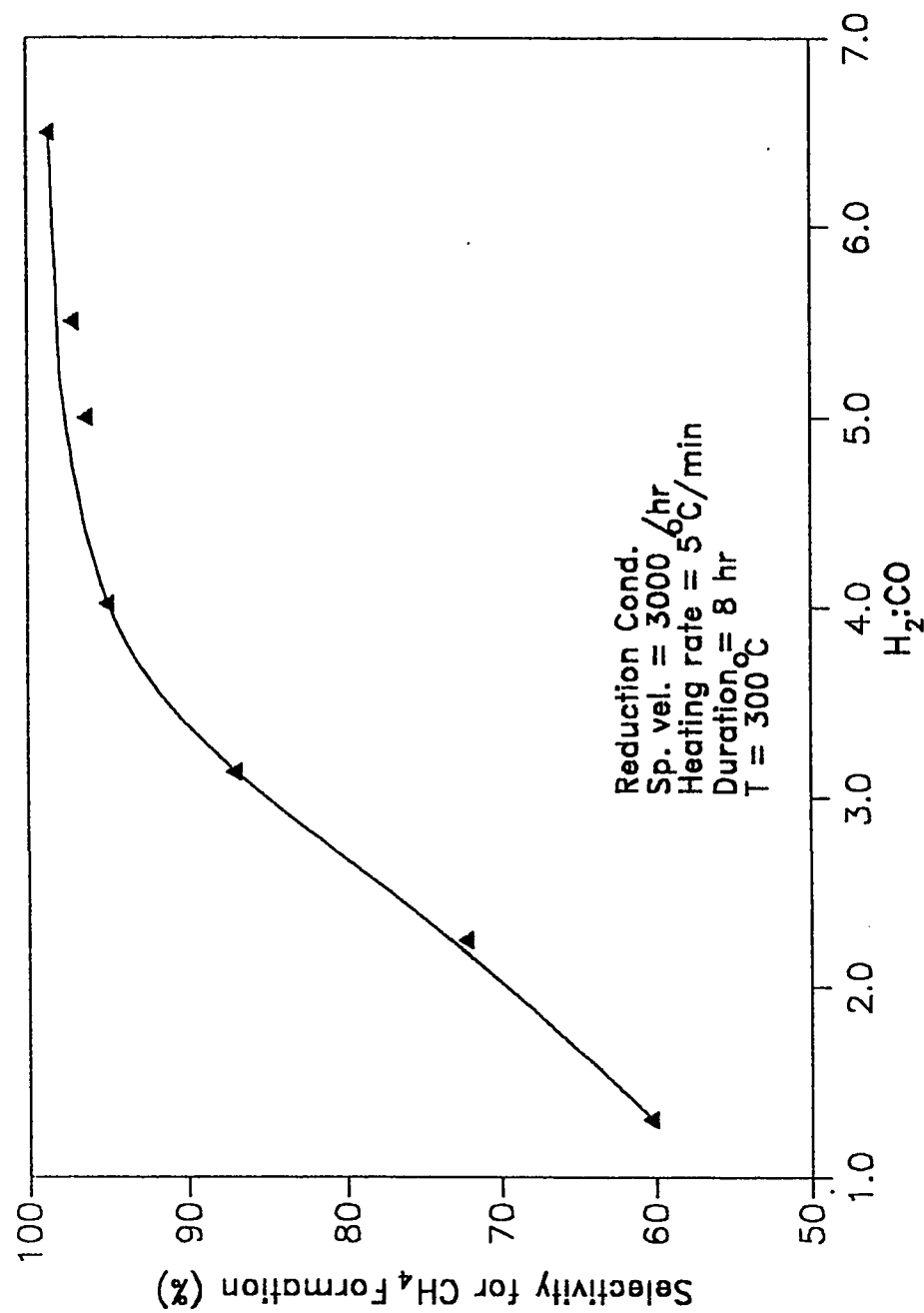


Figure 5.11 Effects of $\text{H}_2:\text{CO}$ ratio on the Selectivity of Ni-Catalyst

5.7.5 *The Effects of Pressure of Reactor System*

When pressure of reactor system is increased, more reactants are pumped into the catalyst therefore, more reactants are available on the surface of catalyst for methanation. Such type of behavior is observed in Figure 5.12 in which a gradual rise in selectivity for CH_4 formation is observed. Jarvi et al. [76] have also found that the rate of CO_2 production (due to water-gas reaction) is suppressed at higher pressure.

5.8 A COMPARISON OF SPECIFIC ACTIVITIES FROM DIFFERENT STUDIES

In this investigation the rate of reaction, obtained after reducing the catalyst under optimal reduction conditions, is converted into turnover number which is also called as specific activity. The turnover number, in terms of CO and CH_4 , is compared with the turnover number obtained for different types of Ni-catalysts by different researchers. Table 5.7 represents the work of some of the authors and compares with the activity obtained in this study. These activities are taken from the turnover rate expression and adjusted to temperature close to or equal to 350°C .

It can be seen from the Table 5.7 that the temperature of most of the specific activities are below 350°C . It is due to the reason that the turnover rate expressions in these studies are limited by the temperature. For this reason a true comparison among these activities is difficult. However, it can be said that most turnover numbers are comparable with this study with the

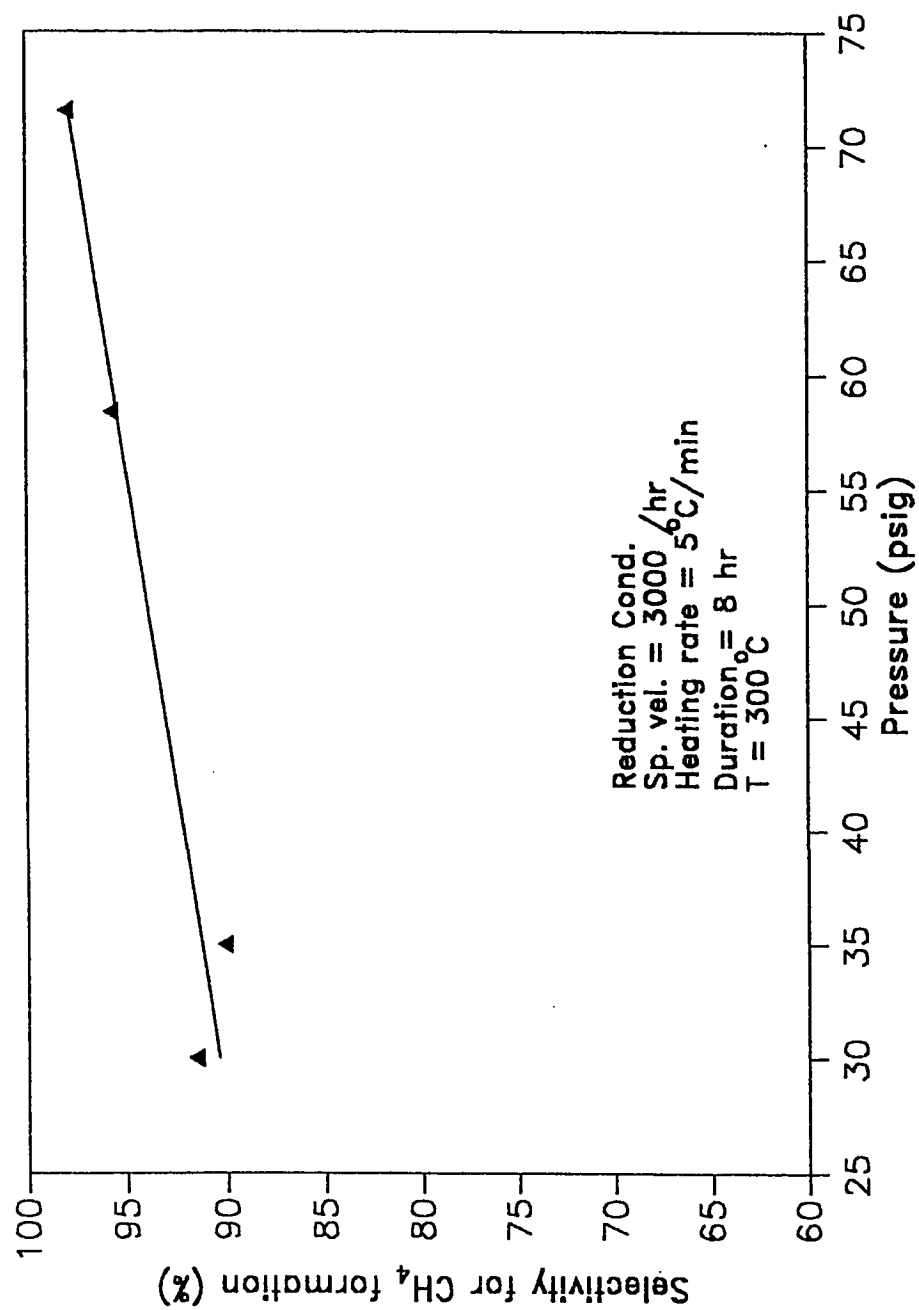


Figure 5.12 Effects of Pressures on the Selectivity of Ni-catalyst at 350°C

Table 5.7 Comparison of Specific Activity from Different Studies

Catalyst	Temperature (°C)	H ₂ uptake (μmol/g)	N _{CH₄} (mol/site.s)	N _{CO} (mol/site.s)	Reference
8.8% Ni/ηAl ₂ O ₃	275	19	85 x 10 ⁻³	128 x 10 ⁻³	Vannice et al.[70]
16.7% Ni/SiO ₂	275	121	1.7 x 10 ⁻³	-	"
42% Ni/αAl ₂ O ₃	275	65	43 x 10 ⁻³	109 x 10 ⁻³	"
30% Ni/αAl ₂ O ₃	275	318	18 x 10 ⁻³	35 x 10 ⁻³	"
21% Ni/ηAl ₂ O ₃	275	-	164 x 10 ⁻³	-	Bhatia et al.[73]
17% Ni(NI-6109)	350	-	72 x 10 ⁻³	-	"
40% Ni(G-87)	275	-	87 x 10 ⁻³	-	"
42% Ni(IISE-102)	275	-	75 x 10 ⁻³	-	"
18% Ni/γAl ₂ O ₃	254	44	491 x 10 ⁻³	-	Al-Saleh [27]
19% Ni/20% Al ₂ O ₃ / monolith	252	75	12.5 x 10 ⁻³	-	Jarvi et al.[76]
20% Ni/20% Al ₂ O ₃ / monolith	252	65	11.7 x 10 ⁻³	-	"
25% Ni/Al ₂ O ₃ / monolith	252	179	7.4 x 10 ⁻³	-	"
40% Ni/Al ₂ O ₃ (G-87)	252	167	4.4 x 10 ⁻³	-	"
20% Ni/γAl ₂ O ₃	350	29.6	38.4 x 10 ⁻³	41.7 x 10 ⁻³	Present Work

exception of few.

CHAPTER 6

CONCLUSIONS AND RECOMMENDATIONS

6.1 CONCLUSIONS

- a) The optimal reduction conditions for a commercial $\text{Ni}/\gamma\text{Al}_2\text{O}_3$ (C13-4-04;20%Ni) catalyst (manufactured by UCI; supplied by SAMAD Fertilizer Co.) are obtained by reducing the catalyst at different operating conditions and studying their effects on the activity and selectivity of a methanation reaction. The obtained optimal reduction conditions are in agreement with the reduction conditions recommended by the technical report of KACKST project [4]. The optimal reduction conditions are as follows:

Reduction temperature: 300 °C

Duration of reduction: 8 hr

Space velocity: 3000 hr^{-1}

Heating rate of bed: 5 °C/min

- b) The interphase mass and heat transfer resistances are minimal in Berty reactor.
- c) The activity of fresh catalyst increases initially then remains steady

showing stability of catalyst.

- d) The rate of CO conversion decreases by increasing the residence time. On the other hand, selectivity to CH_4 formation increases from 90 to 96%.
- e) The rate of CO conversion increases by decreasing the residence time. On the other hand, selectivity to CH_4 formation slightly decreases.
- f) Using higher H_2/CO ratio (3.0-6.5), the selectivity to methane improves up to 98% but the rate of methanation is decreased.
- g) Lower H_2/CO ratio (3.0-1.0) increases the rate of CO conversion, but both the selectivity and rate of CH_4 production are decreased.
- h) Reaction pressure does not affect the rate of methanation. However, it improves the selectivity of methanation.

6.2 RECOMMENDATIONS

- a) A Kinetic study can be performed for the same catalyst to estimate methanation rate expression free from transport resistances.
- b) Different types of Ni-catalysts can be reduced under identical reduction conditions, and can be screened by studying their activities and deactivation.
- c) Introducing CO_2 with the feed to observe its behavior on the activity of catalyst.
- d) High pressure of reaction system could be helpful in observing its effect on the activity and selectivity of $\text{Ni}/\gamma\text{Al}_2\text{O}_3$.

NOMENCLATURE

A	: equilibrium constant
a_t	: external surface area per unit mass of catalyst, m^2/kg
C_b	: bulk concentration, $g\text{-mol}/l$
C_p	: specific heat, $cal/g\text{-mol}^\circ K$
C_s	: surface concentration, $g\text{-mol}/l$
$D_{A,B}$: Diffusivity of A into B , m^2/hr or m^2/s
D_p, d_p	: diameter of particle, mm or m
E	: activation energy, $kcal/mol$ or $J/g\text{-mol}$
ΔE_a	: apparent activation energy, kJ/mol
e	: electron
F_{in}	: total flow rate In, $g\text{-mol}/hr$
F_{out}	: total flow rate Out, $g\text{-mol}/hr$
F_o	: measured flow rate, ml/s
f_m	: modified friction factor
G	: mass flux = ρV , $kg/m^2.s$
ΔG	: Gibb's free energy, $kcal/mol$
ΔH	: heat of reaction, $kcal/g\text{-mol}$ or kJ/mol
Δh	: pressure head
J_D	: J-factor for diffusion
K	: specific reaction rate constant
K_f	: thermal conductivity, $cal/cm.s.^\circ K$

k	: equilibrium constant
ΔM_e	: experimental wt. change for a given time
ΔM_t	: theoretical wt. change for a given time
m	: order of reaction
N_A, N_{CH_4}	: turnover number, molecules/site-s
n	: order of reaction
P	: pressure; psig, bar, or MPa
P_b	: pressure in bulk phase, atm or psia
P_{CO}	: partial pressure of CO, bar
P_{H_2}	: partial pressure of H_2 , bar
P_s	: pressure on surface, atm or psia
Q_o	: flow rate in side the reactor, cm^3/s
R	: gas constant = $1206 \frac{psia.cm^3}{g-mol.hr}$
R	: recycle ratio, Q_o/F_o
Re	: Reynolds number = $\frac{D_p G}{\mu}$
r	: rate of reaction, g-mol/g-cat.hr
r_{CH_4}	: rate of CH_4 formation, g-mol/g-cat.hr
$-r_{CO}$: rate of CO conversion, g-mol/g-cat.hr
S_{CH_4}	: selectivity of methane formation, $\frac{r_{CH_4}}{-r_{CO}}$
SEM	: Scanning Electron Microscopy
T_b	: temperature in bulk phase, °K
T_s	: temperature on surface, °K
t	: time, hr or sec.
TBD	: Temperature Programme Desorption

<i>TPR</i>	:	<i>Temperature Programme Reaction</i>
<i>TPS</i>	:	<i>Temperature Programme Synthesis</i>
<i>V</i>	:	<i>velocity, m/s</i>
<i>W</i>	:	<i>weight of catalyst, g</i>
<i>x</i>	:	<i>fractional reduction of NiO to Ni</i>
$Y_{A_{in}}$:	<i>mole fraction of compound A In</i>
$Y_{A_{out}}$:	<i>mole fraction of compound A Out</i>
<i>Z</i>	:	<i>specific reaction rate constant</i>

Greek Symbols

α_t	:	<i>extent of reduction, wt. change of catalyst with time</i>
ε	:	<i>void fraction of bed</i>
η	:	<i>effectiveness factor of mixedness</i>
θ	:	<i>dimensionless time</i>
λ	:	<i>lag time</i>
μ	:	<i>viscosity, kg/m.s</i>
ρ	:	<i>density, kg/m³</i>
τ	:	<i>residence time</i>
φ	:	<i>Shape factor, or Thiele modulus</i>

REFERENCES

- [1] Sabatier, P. and Senderens, J.B. *C.R. Acad. Sci., Paris*, 134, 514 (1902).
- [2] Strelzoff, S., *"Technology and Manufacture of Ammonia"*, Wiley, New York (1981).
- [3] Watson, G.H., *"Methanation Catalysts"*, IEA Coal Research Report, London (1980).
- [4] Yeboah, Y.Y., Maadhah, A.G., Al-Saleh, M.A. and Shalabi, M.A., *KACST Research Project No. AR-9-064* (1989).
- [5] Hair, M.L., *Infrared Spectroscopy in Surface Chemistry*, Book, p.217-266.
- [6] Joint Army-Navy-Airforce Thermochemical Tables, *NSRDS-Nat. Bur. Stand.-37*, 2nd ed., June (1966).
- [7] Bienstock,D.,Forney,A.J. and Field,J.H., *Ibid*, 6194 (1966).
- [8] Field,J.H.,and Forney,A.J., *Procedings of the Synthetic Pipeline Gas Symposium*, American Gas Association, Arlington, Virginia, p.83 (1966).
- [9] Vannice, M.A., *J. Catal.*, 37, 462-473 (1975).
- [10] Yates,J.T. and Garland,C.W., *J. Phy. Chem.*, 65, p.617 (1961).
- [11] Vlasenko,V.M.,Kukhar,L.A.,Rusov,M.T., and Sanchenco,N.P., *Kinetika Kataliz*, 5(2),301-306 (1962).
- [12] Fischer,F. and Tropsch,H., *Brennst.-Chem.*, 7, p.92 (1926).
- [13] Vannice,M.A., *Catal. Sci. Tech.* Vol.3, Springer-Verlag, Berlin, Heidelberg, (1982).
- [14] Wentreck,P.R.,Wood,B.J.,Wise,H., *J. Catal.* 43, p.363 (1976).
- [15] Araki,M. and Poncc,J., *J. Catal.* 44, p.439 (1976).
- [16] McCarty,J.G. and Wise,H., *J. Catal.* 57, p.406 (1979).
- [17] Shuit,G.C.A. and Reijen,L.L.V., *Adv. in Catal.* 10, 245-315 (1958).

- [18] Beeck,O., *Adv. in Catal.* 11, 171-176 (1950).
- [19] Vannice,M.A. *Cat. Rev.-Sci. Eng.*, 14(2), 153-191 (1976).
- [20] Wedler,G.,Papp,H.,Schroll,G., *J. Catal.* 38, 153-165 (1975).
- [21] Farrauto,R.J., *J. Catal.* 41(3), 482-485 (1976).
- [22] Zagli,E.A.,Falconer,J.L.,Keenan,C.A., *J. Catal.* 56, p.453 (1979).
- [23] Mills,G.A. and Steffgen,F.W., *Catal. Reviews* Vol.8, Marcel Dekker Inc. (1973).
- [24] Greyson,M.,Demeter,J.J.,Schleisinger,M.D.,Johnson,G.E.,Jonakin,J. and Myers,J.W., *Bu. Mines RI* 5137 (1955)
- [25] White,G.A.,Roszkowski,T.R.,Stanbridge,D.W., *A.C.S Fuel Div. Reprints*, 19(3), 57-69 (1974).
- [26] Madhava, M., *Ph.D. Thesis*, Illinois Institute of Tech., USA, (1977).
- [27] Al-Saleh,M.A. *Ph.D. Thesis*, Colorado School of Mines, USA, (1981).
- [28] Nicolai,J.,Dhont,M. and Jungers,J.C., *Bull. Soc. Chim., Belgium*, 55, 160-176 (1946).
- [29] Schoubyc,P., *J. Catal.*, 14, p.238 (1969).
- [30] Van Herwijn,T.,Van Doesburg,H. and De Jong,W.A., *J. Catal.*, 28, 391-402 (1973).
- [31] Tajbl,D.J.,Feldkirchuner,H.L. and Lee,A.L., *ACS Div. Fuel Chem. Prep. No.4*, 235-245 (1966).
- [32] Hausberger,A.L.,Knight,C.B. and Atwood,K., *Adv. Chem. ser. No. 146*, p.47 (1975).
- [33] Becker,J.,Cheng,Y.H. and Hedden,K., *International Gas Research Conference* (1983).
- [34] Saha,N.C. and Wolf,E.E., *Appl. Catal.* 13, 101-112 (1984).
- [35] Hayes,R.E.,Thomas,W.J. and Hayes,K.E., *J. Catal.* 92, 312-326 (1985).

- [36] Lowe,A. and Tanger,U., *Chem. Eng. Technol.*, 10, 361-367 (1987).
- [37] Levi,T.T. and David Curtis,M., *AIChE J.*, 35(1), 109-119 (1989).
- [38] Vlasenko,V.M. and Yuzefovich,G.E., *Russian Chem. Rev.(English)*, 38(9), 728-739 (1969).
- [39] Zagil,A.E.,Falconer,J.L. and Keenan,C.A., *J. Catal.*, 56, 453-467 (1979).
- [40] Fujimoto,K.,Kameyama,M. and Kungi,T., *J. Catal.*, 61, 7-14 (1980).
- [41] Hayes,R.E. and Ward,K.J., *J. Catal.*, 61, 7-14 (1980).
- [42] Hayes,R.E.,Thomas,W.J. and Hayes,K.E., *Appl. Catal.*, 6, p.53 (1983).
- [43] Vandervell,N.D. and Bowker,M., *Appl. Catal.*, 30, 151-158 (1987).
- [44] Sughrue,E. and Bartholomew,C.H., *Appl. Catal.*, 2, p.239 (1982).
- [45] Underwood,R. and Bennett,C., *J. Catal.*, 86, p.245 (1984).
- [46] Holm,V.C.F. and Clark,A., *J. Catal.*, 11, p.305 (1968).
- [47] Bartholomew,C.H. and Farrauto,R.J., *J. Catal.*, 45, 41-53 (1976).
- [48] Chen,I. and Shiue,D.W., *IEC Research*, 27, 429-434 (1988).
- [49] Rostrup-Nielsen,J.R., *Catalytic Steam Reforming*, Springer-Verlag, N.Y., 30-46 (1984).
- [50] Ross,J.R. and Steel,M.C.F., *JCS Far. Trans. I.*, 69, p.10 (1973)
- [51] Gambaro,L.A.,Fierro,J.L.G.,Agedo,A.L.,Tejuca,L.G., *Sur, & Interface Analysis*, 4, 234-239 (1982).
- [52] Sannomiya,A.Ichimara,K.,Yano,M.,Harano,Y., *Mem. Fac. Eng.*, Osaka U., 24, p.161 (1983).
- [53] Bandrowski,J.,Bickling,C.R.,Yang,K.H.,Hougen,O.A., *Chem. Eng. Sci.*, 17, p.379 (1962).
- [54] Hurst,N.W.,Gentry,S.J.,Jone,A., *Catal. Rev. Sci. Eng.*, 24, 233-309 (1984).
- [55] Greyson,M., *Methanation*, (Emmett,P.H. ed.) Catalysis Vol.4, Reinhold,

- N.Y., Ch.6, 473-511 (1956).
- [56] Bartholomew, C.H., Weatherbee, G.D., Jarvi, C.A., *J. Catal.*, 60, 257-269 (1979).
 - [57] Kohl, A.L. and Riesenfeld, F.C., *Gas Purification*, McGraw Hill, N.Y., p.463 (1960).
 - [58] Herbert, W. and Tramm, H., *Erdoel Kohle*, 9, p.363 (1956).
 - [59] Graboski, M.S. and Diehl, E.K., *5th Synthetic Pipeline Symposium, Chicago, Ill.*, Oct., p.29-31 (1973).
 - [60] Tart, K.R. and Rampling, T.W., *Hydrocarbon Processing*, Apr., p.114 (1981).
 - [61] Lee, A.L., *IGT*, 341-351.
 - [62] Choudhry, V.R. and Doraiswami, L.K., *I&EC Proc. Des. Dev.*, 11(3), 420-427 (1972).
 - [63] Berty, J.M., *Symp. Acs. Pet. Dev.*, 343-350 (1977).
 - [64] Tajbl, D.J., Simmons, J.B., Carberry, J.J., *I&EC Fund.*, 5(2), 171-175 (1966).
 - [65] Dent, F.J. and Hebden, D., *Gas Journal*, 261, 1949.
 - [66] Dent, F.J. and Hebden, D., *GRB Comm.*, 160-67, 1949.
 - [67] Dirksen, H.A. Linden, H.R., *"Pipeline Gas from Coal by Methanation of Synthesis Gas"*, IGT Research Bulletin No.31, Chicago (USA), July (1963).
 - [68] Lee, A.L., Tajbl, D.J. and Feldkirchner, H.L. *"Clean-up Methanation for Hydrogasification Process"*, ACS div. Fuel Chem. prep. No.4, 235-45 (1966).
 - [69] Doesburg, E.B.M., Orr, S., Ross, J.R.H. and Vonreigen, L.L., *J.C.S. Chem. Comm.* 734-35 (1977).
 - [70] Vannice, M.A., *J. Catal.*, 50, 228 (1977).

- [71] Vannice, M.A., *J. Catal.*, 40, 129 (1975).
- [72] Dalla, B.R.A., Piken, A.G. and Shelef, M., *J. Catal.*, 40, 173 (1975).
- [73] Bhatia, S., Bakhshi, N.N. and Mathews, J.F., *Can. J. Chem. Eng.*, 56(10), 575-81, 1978.
- [74] Bhatia, S., Bakhshi, N.N. and Mathews, J.F., *Can. J. Chem. Eng.*, 59(8), 492-96, 1981.
- [75] Richardson, J.T. and Huang, C.P., *J. Catal.*, 51, 1 (1978).
- [76] Jarvi, G.A., Mayo, K.B. and Bartholomew, C.H., *Chem. Eng. Commun.*, 4, 325-41, 1980.
- [77] Reucroft, P.J. and Park, J.W., *J. Mater. Energy Syst.*, 2(1), 28-33, 1980.
- [78] Sinfelt, J.H., Carter, J.L. and Yates, D.J.C., *J. Catal.*, 24, 283 (1972).
- [79] Bond, G.C. and Turnham, B.D., *J. Catal.*, 45, 128 (1976).
- [80] Elliot, D.J. and Lunsford J.H., *J. Catal.*, 57, 11 (1979).
- [81] Bajpai, P.K., Bakhshi, N.N., Liu Dan-Chu and Mathews, J.F., *Can. J. Chem. Eng.*, 60(10), 613-16 (1982)
- [82] Bajpai, P.K., Bakhshi, N.N. and Mathews, J.F., *Can. J. Chem. Eng.*, 60(2), 4-10 (1982)
- [83] Hankel, K.G. and Duesseldorf, A., *Chem. Ing. Tech.*, 60(12), 1055 (1988).
- [84] Richard, W.R., and Randolph, S.H., *Ind. Eng. Chem. Prod. Res. Dev.*, 23, 208-14, 1984.
- [85] Gakuska, J., Chang, J.R. and Amenomiya, Y., *J. Catal.*, 68, 172 (1981).
- [86] Munteanu, G., Segal, E. and Butucelea, A., *Thermochim. Acta.*, 133, 137-42 (1988).
- [87] Twigg, Martyn Vincent (I.C.I. PLC) (Patent) 1988.
- [88] Fujita, S., Terunuma, H., Kobayashi, H. and Takezawa, N., *React. Kinet. Catal. Lett.*, 33(1), 179-84 (1987).

- [89] Ponec, V., *Catal. Rev. Sci. Eng.* , 18, 151 (1978).
- [90] Bell, A.T., *Catal. Rev. Sci. Eng.* , 23, 203 (1981).
- [91] Gardner, D.W., and Bartholomew, C.H., *Ind. Eng. Chem. Fundam.*, 20, 229 (1981).
- [92] Kasaoka, S., Sasaoka, E. and Misumi, K., *J. Chem. Soc. Japan*, 1246 (1982).
- [93] Kasaoka, S., Sasaoka, E. and Misumi, K., *J. Chem. Soc. Japan*, 1246 (1982).
- [94] Ahmed, K., Kershenbaum, L. and Chadwick, D., *Chem. Eng. Sci.*, 44(4), 999 (1989).
- [95] Yadav, R., Rinker, R.G., *Ind. Eng. Chem. Res.*, 31, 502-508 (1992).
- [96] Twigg, M.W., *Catalyst Handbook*, 2nd Ed., Wolfe Publishing Ltd., Englang, Ch.7 (1989).
- [97] Menon, P.G., *J. Mol. Catal.*, 59, 207-220, (1990).
- [98] Satterfield, C.N., *Heterogeneous Catalysis in Practice*, McGraw-Hill Inc., U.S.A., Ch.2 (1980)
- [99] Flynn, P.C., and Wanke S.E. *J. Catal.*, 37, 432 (1975).

APPENDIX-A
Reactor Performance

Reactor Performance

The degree of mixing in the Berty reactor was determined by Berty [63] by using a helium tracer in nitrogen to carry out step-change experiment. He used a plug-flow reactor in series with an ideal mixer, since the only observable deviation from the ideal behavior was a time delay. The model used is as follows:

$$C/C_s = e^{-\eta(t-\lambda)/\tau}$$

where, C/C_s is the ratio of decaying He-concentration to the steady-state concentration that existed before the helium shut-off. τ is the residence time, η is effectiveness factor for mixing and λ is the lag time.

A close approximation to the ideal mixing and uniformity in the flow was varified experimentally by Berty [63] at a minimum recycle ratio of 20.

Calculations of Impeller

Leva equation for pressure through a fixed bed is represented as follows:

$$\Delta \frac{P}{q} = \Delta h = \left[\frac{4f_m(1-\epsilon)^{3-\eta}}{\theta^{3-\eta}\epsilon^3} \right] \left(\frac{L}{D_p} \right) \left(\frac{V^2}{2g} \right)$$

The η for Leva equation is $1.96 \sim 2.0$, and f_m is close to 1.0. Therefore, Leva equation simplifies to:

$$\Delta h = \left[\frac{4(1-\epsilon)}{\theta\epsilon^3} \right] \left[\frac{V^2}{2g} \right] \quad (1) \quad \text{for } \frac{L}{D_p} = 1 \text{ (sphere)}$$

$$\Delta h = K \left[\frac{V^2}{2g} \right]$$

The specifications of catalyst for this investigation are:

$$D_p = 0.25 \text{ in.} = 6.35 \text{ mm}$$

$$\varepsilon = 0.40$$

$$\eta = 2.0$$

$$f_m = 1.0$$

$$\text{therefore, } \frac{1-\varepsilon}{\varepsilon^3} = 9.38$$

$$\frac{1}{\varphi} = 1.1$$

$$\text{therefore, } \frac{1-\varepsilon}{\varphi \varepsilon^3} = 10.318$$

Applying Leva equation to calculate K

$$K = \frac{4(1-\varepsilon)}{\varphi \varepsilon^3}$$

$$K = 41.272$$

The equation for the bolwer is:

$$\Delta h = 1.1 \left(\frac{\text{rpm}}{1000} \right)^2 \quad (2)$$

since two pressure heads must be equal therefore, Eq.1&2 are combine to give:

$$\Delta h = 41.272 \frac{V^2}{2g} = \Delta h = 1.1 \left(\frac{\text{rpm}}{1000} \right)^2$$

$$\text{rpm} = 1383.57 \text{ V}$$

or

$$V = 0.722 \times \frac{\text{rpm}}{1000}$$

for rpm = 859

$$V = 0.621 \text{ m/sec.}$$

Calculations of Recycle Ratio

$$V = 62.1 \text{ cm/sec at rpm} = 859$$

$$F_o = \text{measured flow rate @} = 600 \text{ cm}^3/\text{min}$$

$$F_o = 10 \text{ cm}^3/\text{sec}$$

$$Q_o(\text{inside}) = AV$$

where,

$$A = \pi \frac{D_o^2}{4}$$

$$A = 20.26 \text{ cm}^2$$

therefore,

$$Q_o = 1258.15 \text{ cm}^3/\text{sec.}$$

$$\text{Recycle Ratio (R)} = \frac{Q_o}{F_o}$$

$$R = 125.58$$

The calculated recycle ratio is > 20 , which is the minimum requirement for complete mixing.

APPENDIX-B

Sample Calculations

Sample Calculations for Run # 9Catalyst: Ni/ γ -Al₂O₃

wt. = 10.013 g

T = 350 °C

P = 30 psig

R (gas constant) = 1206 $\frac{\text{psia}\cdot\text{cm}^3}{\text{g}\cdot\text{mol}\cdot\text{K}}$

Room Temperature = 26 °C

	<i>Feed</i>	<i>Product (dry%)</i>	<i>Product (wet%)</i>
H ₂	27.05	18.75	17.50
O ₂	0.03	0.02	0.018
N ₂	66.81	74.04	69.09
CO	6.73	0.75	0.70
CH ₄	-	6.36	5.937
CO ₂	-	0.43	0.401
H ₂ O	-	-	6.338

Flow out = 530 ml/min

$$C_{\text{CO}_0} = 6.73 \% = y_{\text{CO}_0} = 0.0673$$

$$C_{\text{CH}_4} = 6.36 \% = y_{\text{CH}_4} = 0.0636$$

$$C_{\text{CO}} = 0.75 \% = y_{\text{CO}} = 0.0075$$

$$\text{Moles out } (F_{\text{out}}) = \frac{PV}{RT} = \frac{14.7 \times 530}{1206 \times 299} \times 60$$

$$F_{\text{out}} = 1.296 \frac{\text{g}\cdot\text{mol}}{\text{hr}}$$

Carbon balance

$$\begin{aligned}\text{Carbon in product} &= 1.296(0.0075 + 0.0636 + 0.0043) \\ &= 0.097 \text{ g-mol/hr}\end{aligned}$$

therefore,

$$F_{\text{in}} (\text{mole in}) \times Y_{\text{CO}_0} = \text{Carbon in Product}$$

$$F_{\text{in}} \times 0.0673 = 0.097$$

$$F_{\text{in}} = 1.471 \text{ g-mol/hr}$$

$$\begin{aligned}\text{Feed in} &= \frac{F_{\text{in}} RT}{P} \\ &= \frac{1.471 \times 1206 \times 299}{14.7 \times 60} = 601.4 \text{ ml/min}\end{aligned}$$

Rate of reaction is calculated as follows:

$$\begin{aligned}\text{Rate} &= \frac{F_{\text{in}} y_{\text{CO}_0} - F_{\text{out}} y_{\text{CO}_{\text{out}}}}{W} \\ -r_{\text{CO}} &= \frac{1.471 \times 0.0673 - 1.296 \times 0.0075}{10.013}\end{aligned}$$

$$-r_{\text{CO}} = 8.9 \times 10^{-3} \frac{\text{g-mol}}{\text{g-cat.hr}}$$

similarly,

$$r_{\text{CH}_4} = \frac{1.296 \times 0.0636}{10.013}$$

$$r_{\text{CH}_4} = 8.2 \times 10^{-3} \frac{\text{g-mol}}{\text{g-cat.hr}}$$

$$\text{CO conversion} = \frac{0.0673 - 0.0075}{0.0673} \times 100 = 88.8\%$$

Selectivity (S) for CH_4 is calculated as follows:

$$S_{CH_4} = \frac{\text{Desired-Product}}{\text{Consumed-Reactant}} = \frac{r_{CH_4}}{-r_{CO}} = \frac{F_{out} y_{CH_4}}{F_{in} y_{CO_0} - F_{out} y_{CO}} \times 100$$

$$= \frac{8.2 \times 10^{-3}}{8.9 \times 10^{-3}} \times 100 = 92.1 \%$$

Turnover number for CH_4 is calculated as follows:

$$N_{CH_4} = \frac{r_{CH_4}}{H_2\text{-Uptake} \times 2}$$

$$H_2\text{-Uptake} = 29.63 \mu\text{mol/g-cat.} \quad [4]$$

$$= \frac{8.2 \times 10^{-3}}{29.63 \times 10^{-6} \times 2 \times 3600} \times \frac{6.023 \times 10^{23}}{6.023 \times 10^{23}}$$

$$N_{CH_4} = 38.4 \times 10^{-3} \text{ molecule/site-sec}$$

similarly,

$$N_{CO} = 41.7 \times 10^{-3} \text{ molecule/site-sec}$$

Also,

$$\text{space vel.} = \frac{\text{flow rate}}{\text{vol. of reactor}} = \frac{\text{flow rate}}{\text{wt. of cat.}} \times \text{bulk density of cat.}$$

$$= \frac{601}{10.103} \times 1.02 \times 60 = 3672 \text{ hr}^{-1}$$

Program of Gas Chromatograph

LST1

METHOD 1

ANALYZER CONTROL

INJ TEMP 50
 DET ZONE 1,2 60 60
 AUX TEMP 25
 FLOW A,B 30 30
 INIT OVEN TEMP, TIME 35 7

TEMP RATE TIME
 120 32.0 12

DATA PROC

STD WT, SMP WT 0.0000 1.0000 0
 FACTOR, SCALE 1 0
 TIMES 21.65 0.00 327.67 327.67 327.67 327.67
 SENS-DET RANGE 50 4 0.00 2 0 0
 UNK, AIR 1.000 0.00
 TOL 0.0000 0.050 1.0
 REF PK 1.000 7.50 9.50 8.00
 STD NAME CO

RT	RF	CONC	NAME
1.41	30.636	0.9330	H2
5.20	0.809	1.0000	O2
5.50	0.841	95.0464	N2
8.00	0.800	1.0000	CO
12.20	0.912	1.0100	CH4
19.40	0.744	1.0100	CO2

EVENT CONTROL

ATTN-CHART-DELAY 4 15 0.01

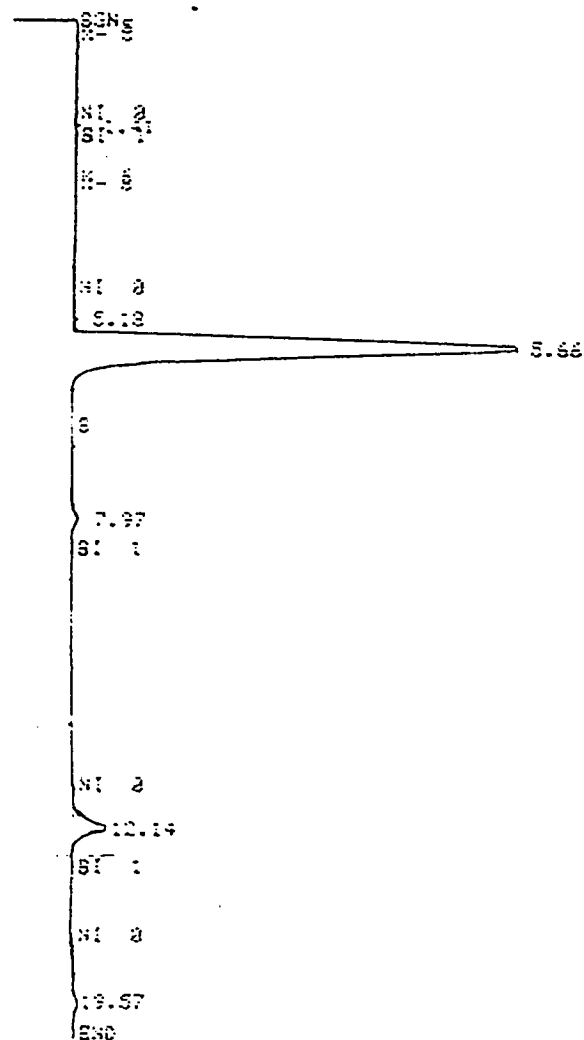
TIME	DEVICE	FUNCTION	NAME
0.00	EXT	X	0
0.00	NO INT	NI	1
0.10	EXT	X	5
0.20	EXT	X	-5
1.25	NO INT	NI	0
1.55	NO INT	NI	1
2.10	EXT	X	6
2.20	EXT	X	-6
4.00	NO INT	NI	0
8.40	NO INT	NI	1
11.60	NO INT	NI	0
12.70	NO INT	NI	1
18.80	NO INT	NI	0
20.30	NO INT	NI	1

Output of Gas Chromatograph

ANAL : DET : METH 2 2 FILE 21

RUN 2 PRODRUN13

SENSITIVITIES 50 4



ANAL : DET : METH 2 2 FILE 21

RUN 2 PRODRUN13 22 : 40.5 11 / 15 / 91

SENSITIVITIES 50 4

TIME	AREA	SC	RT	RF	C	NAME
1.41	0.1114		0.176	30.836	13.1927	H2:
5.13	0.0033	U	0.649	0.809	0.0167	O2:
5.66	18.5289		0.710	0.841	74.0515	H2:
7.97	0.1715		1.000	0.800	0.7314	CO:
10.14	1.3095		1.523	0.912	6.3654	CH4:
19.57	0.1619		2.455	0.744	0.6422	CO2:

TIME FUNC NEW VALUE
20.09 01 20.09

APPENDIX-C

Calculations of Transport Effects

Calculation of Transport Effects

The reaction rates are chosen at:

$$T = 350\text{ }^{\circ}\text{C} = 623\text{ }^{\circ}\text{K}$$

$$P = 30\text{ psig} = 3.04\text{ atm}$$

as

$$Re = \frac{D_p G}{\mu}$$

where

$$D_p = 0.00635\text{ m}$$

$$\mu_{CO} = 3.05 \times 10^{-5}\text{ Pa.s} \quad (\text{Ref. W.W.W. p-102})$$

$$\mu_{H_2} = 1.45 \times 10^{-5}\text{ Pa.s}$$

$$\mu_{N_2} = 2.98 \times 10^{-5}\text{ Pa.s}$$

$$\mu_{mix} = 1.48 \times 10^{-4}\text{ Pa.s} = 6.69 \times 10^{-5}\text{ Kg/m.s}$$

$$\rho_{H_2} = 4.0934\text{ Kg/m}^3 \text{ @ } 600^{\circ}\text{K}$$

$$\rho_{CO} = 0.5687\text{ Kg/m}^3 \text{ @ } 600^{\circ}\text{K}$$

$$\rho_{N_2} = 0.5688\text{ Kg/m}^3 \text{ @ } 600^{\circ}\text{K}$$

$$\rho_{mix} = 1.5\text{ Kg/m}^3 \text{ @ } 600^{\circ}\text{K}$$

$$V = 0.621\text{ m/s} \quad (\text{appendix A})$$

$$G = V\rho = 0.9315 \frac{\text{Kg}}{\text{m}^2 \text{ s}}$$

therefore,

$$Re = 88.41 > 10$$

In order to calculate external mass transfer, the following correlation is used:

$$C_b - C_s = \frac{r_p \left(\frac{\mu_{\text{mix}}}{\rho D} \right)^{2/3}}{a_t \left(\frac{G}{\rho_{\text{mix}}} \right) J_d}$$

$$r_p = \text{rate of reaction per unit mass of catalyst} = 8.33 \times 10^{-3} \frac{\text{g-mol}}{\text{g-cat. hr}}$$

$$a_t = \text{external surface area per unit mass of catalyst} = 0.392 \frac{\text{m}^2}{\text{Kg}}$$

for $Re > 10$

$$J_D = \text{J-factor} = \frac{0.458}{\epsilon_B} \left(\frac{d_p G}{\mu_{\text{mix}}} \right)^{-0.407}$$

taking $\epsilon_B = 0.40$

$$J_D = 0.184$$

$$D_{\text{CO-N}_2, \text{H}_2} = 2.95 \times 10^{-5} \text{ m}^2/\text{s} = 1.77 \times 10^{-3} \text{ m}^2/\text{hr} \quad (\text{Ref. Sherwood p-62})$$

$$\text{Sc. no} = \frac{\mu_{\text{mix}}}{\rho D} = 1.512$$

therefore,

$$C_b - C_s = 6.79 \times 10^{-5} \text{ g-mol/l}$$

or

$$P_b - P_s = R_g T (C_b - C_s) = 3.47 \times 10^{-3} \text{ atm}$$

$$P_b - P_s = 5.1 \times 10^{-2} \text{ psia}$$

Above result proves that external mass transport effects are insignificant.

External Heat Transfer

The following correlation is used:

(Ref. Smith Ch.10)

$$T_s - T_b = \frac{r_p(-\Delta H) \left(\frac{C_p \mu}{K_f} \right)^{2/3}}{a_t J_{11} C_p G}$$

where,

$$-\Delta H = \text{Heat of reaction} = 52084 \frac{\text{cal}}{\text{g-mol } ^\circ\text{K}} \quad @ 623 \text{ } ^\circ\text{K}$$

$$C_p = \text{Specific heat of CO} = 2.88 \times 10^{-3} \frac{\text{cal}}{\text{g-mol } ^\circ\text{K}}$$

$$K_f = \text{Thermal conductivity of CO} = 2.88 \times 10^{-3} \frac{\text{cal}}{\text{cm.s.} ^\circ\text{K}} \quad @ 623 \text{ } ^\circ\text{K}$$

as

$$J_{11} = J_D = 0.184$$

therefore,

$$\text{Pr. no} = \frac{C_p \mu_{\text{CO}}}{K_f} = 0.35$$

Hence,

$$T_s - T_b = 0.121 \text{ } ^\circ\text{K}$$

Thus, the above result indicates the absence of external heat transfer effects.

APPENDIX-D**Data of Runs**

RUN # 1

Catalyst: Ni/ γ -Al₂O₃

wt. = 10.015 g

Reduction Conditions:

T = 350 °C

Time = 16 hr

Space Velocity = 4800 hr⁻¹Reducing gas = H₂H₂ flow = 787 ml/min.

rpm = 859

Reaction Conditions:

T = 350 °C

Pressure = 30 psig

Space Velocity = 3685 hr⁻¹H₂/CO = 4.0

Feed in = 603 ml/min.

Product out = 522 ml/min

Feed Composition (Vol.%)

Time (hr)	H ₂	O ₂	N ₂	CO
0.00	27.31	0.14	65.35	6.89
0.46	27.11	0.07	66.16	6.62
6.20	26.83	0.02	66.43	6.70

Product Composition (Vol.%)

Time (hr)	H ₂	O ₂	N ₂	CO	CH ₄	CO ₂
0.00	41.06	0.05	56.20	0.51	1.89	0.27
0.29	18.49	0.04	73.70	0.61	6.68	0.45
0.56	18.02	0.03	74.20	0.67	6.57	0.48
1.26	17.99	0.02	74.35	0.71	6.55	0.36
2.17	17.94	0.03	73.60	0.53	7.05	0.82
3.09	18.07	0.01	73.50	0.66	7.29	0.41
4.02	18.11	0.03	73.17	0.68	7.46	0.53
4.53	17.96	0.02	74.40	0.72	6.49	0.35
5.20	18.03	0.01	74.20	0.72	6.53	0.46
5.50	17.97	0.01	74.30	0.71	6.51	0.47

RUN # 2

Catalyst: Ni/ γ -Al₂O₃

wt. = 10.015 g

Reduction Conditions:

T = 350 °C

Time = 16 hr

Space Velocity = 4800 hr⁻¹Reducing gas = H₂H₂ flow = 787 ml/min.

rpm = 859

Reaction Conditions:

T = 350 °C

Pressure = 30 psig

Space Velocity = 3599 hr⁻¹H₂/CO = 4.0

Feed in = 589 ml/min.

Product out = 526 ml/min

Feed Composition (Vol.%)

Time (hr)	H ₂	O ₂	N ₂	CO
0.00	26.25	0.16	66.30	7.20
4.00	26.79	0.02	66.49	6.68

Product Composition (Vol.%)

Time (hr)	H ₂	O ₂	N ₂	CO	CH ₄	CO ₂
0.00	20.54	-	74.05	1.30	3.80	0.24
0.37	19.90	-	72.58	0.73	6.36	0.38
1.08	18.89	0.01	73.49	0.72	6.45	0.41
1.37	18.10	0.01	74.05	0.71	6.61	0.49
2.15	18.49	0.03	74.00	0.72	6.64	0.11
2.53	18.16	-	74.10	0.68	6.77	0.24
3.31	17.82	-	74.60	0.71	7.35	0.42

RUN # 3

Catalyst: Ni/ γ -Al₂O₃

wt. = 10.015 g

Reduction Conditions:

T = 350 °C

Time = 16 hr

Space Velocity = 4800 hr⁻¹Reducing gas = H₂H₂ flow = 787 ml/min.

rpm = 150

Reaction Conditions:

T = 350 °C

Pressure = 30 psig

Space Velocity = 3599 hr⁻¹H₂/CO = 4.0

Feed in = 589 ml/min.

Product out = 526 ml/min

Feed Composition (Vol.%)

Time (hr)	H ₂	O ₂	N ₂	CO
0.00	26.25	0.16	66.30	7.20
3.05	26.79	0.02	66.49	6.68

Product Composition (Vol.%)

Time (hr)	H ₂	O ₂	N ₂	CO	CH ₄	CO ₂
0.00	17.34	-	74.90	1.55	5.80	0.37
0.45	16.27	0.03	75.71	2.05	5.46	0.45
1.32	16.47	0.01	75.53	2.00	5.38	0.59
2.19	17.92	0.01	74.29	2.03	5.35	0.37

RUN # 4

Catalyst: Ni/ γ -Al₂O₃

wt. = 10.015 g

Reduction Conditions:

T = 350 °C

Time = 16 hr

Space Velocity = 4800 hr⁻¹Reducing gas = H₂H₂ flow = 787 ml/min.

rpm = 525

Reaction Conditions:

T = 350 °C

Pressure = 30 psig

Space Velocity = 3599 hr⁻¹H₂/CO = 4.0

Feed in = 589 ml/min.

Product out = 526 ml/min

Feed Composition (Vol.%)

Time (hr)	H ₂	O ₂	N ₂	CO
0.00	26.25	0.16	66.30	7.20
1.35	26.79	0.02	66.49	6.68

Product Composition (Vol.%)

Time (hr)	H ₂	O ₂	N ₂	CO	CH ₄	CO ₂
0.00	17.83	0.01	74.37	0.87	6.54	0.36
0.26	18.02	0.02	74.20	0.94	6.40	0.38
0.54	17.90	-	74.35	0.96	6.45	0.31

RUN # 5

Catalyst: Ni/ γ -Al₂O₃

wt. = 10.015 g

Reduction Conditions:

T = 350 °C

Time = 16 hr

Space Velocity = 4800 hr⁻¹Reducing gas = H₂H₂ flow = 787 ml/min.

rpm = 786

Reaction Conditions:

T = 350 °C

Pressure = 30 psig

Space Velocity = 3599 hr⁻¹H₂/CO = 4.0

Feed in = 589 ml/min.

Product out = 526 ml/min

Feed Composition (Vol.%)

Time (hr)	H ₂	O ₂	N ₂	CO
0.00	26.25	0.16	66.30	7.20
1.10	26.79	0.02	66.49	6.68

Product Composition (Vol.%)

Time (hr)	H ₂	O ₂	N ₂	CO	CH ₄	CO ₂
0.00	16.44	-	75.68	0.78	6.50	0.58
0.30	17.46	0.02	74.74	0.74	6.48	0.52

RUN # 6

Catalyst: Ni/ γ -Al₂O₃

wt. = 10.015 g

Reduction Conditions:

T = 350 °C

Time = 16 hr

Space Velocity = 4800 hr⁻¹Reducing gas = H₂H₂ flow = 787 ml/min.

rpm = 859

Reaction Conditions:

T = 350 °C

Pressure = 30 psig

Space Velocity = 3599 hr⁻¹H₂/CO = 4.0

Feed in = 589 ml/min.

Product out = 526 ml/min

Feed Composition (Vol.%)

Time (hr)	H ₂	O ₂	N ₂	CO
0.00	26.25	0.16	66.30	7.20
1.00	26.79	0.02	66.49	6.68

Product Composition (Vol.%)

Time (hr)	H ₂	O ₂	N ₂	CO	CH ₄	CO ₂
0.00	17.57	0.02	74.76	0.72	6.55	0.34
0.22	17.20	-	75.00	0.74	6.51	0.51

RUN # 7

Catalyst: Ni/ γ -Al₂O₃

wt. = 10.014 g

Reduction Conditions:

T = 250 °C

Space Velocity = 3000 hr⁻¹H₂ flow = 493 ml/min.

Time = 8 hr

Reducing gas = H₂

rpm = 859

Reaction Conditions:

T = 350 °C

Space Velocity = 3758 hr⁻¹

Feed in = 615 ml/min.

Pressure = 30 psig

H₂/CO = 4.0

Product out = 545.45 ml/min

Feed Composition (Vol.%)

Time (hr)	H ₂	O ₂	N ₂	CO
0.00	27.23	0.01	66.11	6.63
0.12	27.49	0.02	65.95	6.53
5.00	24.77	-	68.35	6.87
6.00	24.85	0.01	68.27	6.85

Product Composition (Vol.%)

Time (hr)	H ₂	O ₂	N ₂	CO	CH ₄	CO ₂
0.00	21.22	0.03	70.96	1.45	5.09	1.23
0.26	20.08	0.01	72.72	1.17	5.41	0.58
0.56	20.40	0.02	72.01	1.25	5.49	0.81
1.21	20.37	0.02	72.32	1.24	5.29	0.73
1.56	20.26	0.01	72.20	1.23	5.49	0.78
2.26	19.27	0.02	73.04	1.28	5.53	0.84
3.20	16.89	0.01	75.26	1.25	5.56	1.01
4.03	16.94	0.01	75.26	1.24	5.55	0.98
4.48	17.73	-	74.50	1.27	5.49	0.93
5.28	17.90	0.01	74.50	1.25	5.52	0.74

RUN # 8

Catalyst: Ni/ γ -Al₂O₃

wt. = 10.014 g

Reduction Conditions:

T = 250 °C

Space Velocity = 3000 hr⁻¹H₂ flow = 493 ml/min.

Time = 8 hr

Reducing gas = H₂

rpm = 859

Reaction Conditions:

T = 350 °C

Space Velocity = 3795 hr⁻¹

Feed in = 621 ml/min.

Pressure = 30 psig

H₂/CO = 3.92

Product out = 557.62 ml/min

Feed Composition (Vol.%)

Time (hr)	H ₂	O ₂	N ₂	CO
0.00	26.47	-	66.82	6.70
2.00	26.44	-	66.81	6.73

Product Composition (Vol.%)

Time (hr)	H ₂	O ₂	N ₂	CO	CH ₄	CO ₂
0.00	18.54	0.02	75.32	1.38	3.94	0.78
0.29	19.21	-	73.28	1.27	5.46	0.76
0.59	19.02	-	73.35	1.25	5.47	0.90
1.32	19.17	0.01	73.25	1.23	5.48	0.83

RUN # 9

Catalyst: Ni/ γ -Al₂O₃

wt. = 10.013 g

Reduction Conditions:

T = 300 °C

Time = 8 hr

Space Velocity = 3000 hr⁻¹Reducing gas = H₂H₂ flow = 493 ml/min.

rpm = 859

Reaction Conditions:

T = 350 °C

Pressure = 30 psig

Space Velocity = 3673 hr⁻¹H₂/CO = 3.8

Feed in = 601 ml/min.

Product out = 530 ml/min

Feed Composition (Vol.%)

Time (hr)	H ₂	O ₂	N ₂	CO
0.00	27.05	0.02	65.88	6.83
6.00	26.36	0.03	66.81	6.73
14.50	26.36	0.02	66.82	6.73

Product Composition (Vol.%)

Time (hr)	H ₂	O ₂	N ₂	CO	CH ₄	CO ₂
0.00	12.75	0.04	81.26	0.57	4.76	0.31
0.26	18.72	-	73.38	0.82	6.56	0.43
0.55	18.03	0.02	74.26	0.77	6.38	0.47
1.34	17.44	0.02	73.34	0.71	6.37	2.06
2.04	17.92	0.01	74.86	0.73	5.97	0.32
2.34	18.57	0.02	74.09	0.75	6.16	0.35
3.04	18.11	0.03	74.24	0.76	6.46	0.35
3.34	17.75	0.01	73.68	0.75	7.35	0.40
4.03	18.35	0.02	74.04	0.75	6.36	0.43
4.38	17.64	0.05	74.56	0.76	6.49	0.42
5.11	18.15	-	74.01	0.77	6.49	0.52
5.40	17.71	-	74.47	0.75	6.48	0.45
6.20	18.34	0.01	74.07	0.75	6.37	0.43
7.00	18.34	0.01	74.07	0.76	6.36	0.44
8.03	18.39	0.01	74.03	0.77	6.34	0.46
9.00	18.38	0.02	74.09	0.75	6.36	0.44
10.12	18.38	0.02	74.08	0.75	6.37	0.44
12.05	18.33	0.01	74.12	0.76	6.33	0.43
14.09	18.33	0.01	74.12	0.77	6.33	0.44

RUN # 10

Catalyst: Ni/ γ -Al₂O₃

wt. = 10.013 g

Reduction Conditions:

T = 300 °C

Time = 8 hr

Space Velocity = 3000 hr⁻¹Reducing gas = H₂H₂ flow = 493 ml/min.

rpm = 859

Reaction Conditions:

T = 350 °C

Pressure = 30 psig

Space Velocity = 3673 hr⁻¹H₂/CO = 3.8

Feed in = 601 ml/min.

Product out = 525 ml/min

Feed Composition (Vol.%)

Time (hr)	H ₂	O ₂	N ₂	CO
0.00	26.35	-	66.90	6.73
6.00	26.34	-	66.90	6.74

Product Composition (Vol.%)

Time (hr)	H ₂	O ₂	N ₂	CO	CH ₄	CO ₂
0.00	18.40	-	74.06	1.01	6.16	0.32
0.26	16.96	-	75.40	0.77	6.40	0.46
1.05	17.66	0.01	74.61	0.76	6.39	0.45
1.37	17.65	-	74.69	0.72	6.36	0.55
2.07	16.60	-	75.68	0.76	6.35	0.59
2.56	17.62	0.01	74.67	0.75	6.40	0.56
3.40	17.62	0.01	74.68	0.75	6.39	0.51
4.15	17.61	0.02	74.68	0.75	6.41	0.48
5.01	17.61	0.01	74.69	0.74	6.42	0.49

RUN # 11

Catalyst: Ni/ γ -Al₂O₃

wt. = 10.013 g

Reduction Conditions:

T = 300 °C

Time = 8 hr

Space Velocity = 3000 hr⁻¹Reducing gas = H₂/He = 1:1H₂ + He flow = 495 ml/min.

rpm = 859

Reaction Conditions:

T = 350 °C

Pressure = 30 psig

Space Velocity = 3758 hr⁻¹H₂/CO = 3.9

Feed in = 615 ml/min.

Product out = 526 ml/min

Feed Composition (Vol.%)

Time (hr)	H ₂	O ₂	N ₂	CO
0.00	26.41	0.01	66.83	6.73
6.30	26.36	0.03	66.81	6.73

Product Composition (Vol.%)

Time (hr)	H ₂	O ₂	N ₂	CO	CH ₄	CO ₂
0.00	11.79	0.13	80.55	1.03	4.56	-
0.34	18.00	0.05	74.06	0.73	6.02	1.05
1.00	18.28	-	74.48	0.79	6.22	0.32
1.30	18.23	0.02	73.72	0.73	6.53	0.62
2.17	17.90	0.02	73.72	0.80	6.50	1.03
2.48	18.27	0.03	74.16	0.78	6.46	0.30
3.15	18.27	-	74.04	0.78	6.47	0.52
3.43	17.98	0.01	74.33	0.76	6.44	0.48
4.10	17.66	0.03	74.68	0.77	6.33	0.48
4.40	17.67	0.03	74.63	0.78	6.41	0.47
5.15	17.77	0.03	74.53	0.83	6.45	0.47
5.50	17.77	0.01	74.55	0.83	6.47	0.45

RUN # 12

Catalyst: Ni/ γ -Al₂O₃

wt. = 10.014 g

Reduction Conditions:

T = 350 °C

Time = 8 hr

Space Velocity = 3000 hr⁻¹Reducing gas = H₂H₂ flow = 483 ml/min.

rpm = 859

Reaction Conditions:

T = 350 °C

Pressure = 30 psig

Space Velocity = 3673 hr⁻¹H₂/CO = 3.98

Feed in = 602 ml/min.

Product out = 529 ml/min

Feed Composition (Vol.%)

Time (hr)	H ₂	O ₂	N ₂	CO
0.00	26.73	-	66.56	6.70
5.40	26.94	0.02	66.35	6.69

Product Composition (Vol.%)

Time (hr)	H ₂	O ₂	N ₂	CO	CH ₄	CO ₂
0.00	24.77	-	69.43	0.61	4.75	0.41
0.44	18.63	0.01	73.61	0.66	6.75	0.31
1.31	19.05	0.01	73.32	0.64	6.57	0.38
2.18	19.50	-	72.99	0.64	6.52	0.32
3.05	19.34	0.01	73.03	0.63	6.60	0.35
3.53	19.35	0.01	72.32	0.63	6.42	1.25
4.41	19.29	0.01	73.04	0.63	6.67	0.32
5.11	18.15	0.01	74.31	0.67	6.49	0.35

RUN # 13

Catalyst: Ni/ γ -Al₂O₃

wt. = 10.012 g

Reduction Conditions:

T = 400 °C

Time = 8 hr

Space Velocity = 3000 hr⁻¹Reducing gas = H₂H₂ flow = 498 ml/min.

rpm = 859

Reaction Conditions:

T = 350 °C

Pressure = 30 psig

Space Velocity = 3722 hr⁻¹H₂/CO = 4.0

Feed in = 609 ml/min.

Product out = 535 ml/min

Feed Composition (Vol.%)

Time (hr)	H ₂	O ₂	N ₂	CO
0.00	26.97	-	66.31	6.71
3.30	27.56	0.01	65.79	6.63
3.45	27.49	0.02	65.86	6.62

Product Composition (Vol.%)

Time (hr)	H ₂	O ₂	N ₂	CO	CH ₄	CO ₂
0.00	15.05	0.01	78.31	0.58	5.79	0.22
0.27	18.19	0.01	74.05	0.73	6.36	0.64
0.57	18.07	-	74.27	0.69	6.42	0.52
1.25	17.99	0.01	74.06	0.62	5.82	1.46
1.55	18.13	0.01	74.60	0.65	6.39	0.20
2.26	18.05	0.01	74.40	0.69	6.34	0.42
2.56	18.12	0.01	74.29	0.71	6.48	0.36

RUN # 14

Catalyst: Ni/ γ -Al₂O₃

wt. = 10.016 g

Reduction Conditions:

T = 450 °C

Space Velocity = 3000 hr⁻¹H₂ flow = 490 ml/min.

Time = 8 hr

Reducing gas = H₂

rpm = 859

Reaction Conditions:

T = 350 °C

Space Velocity = 3654 hr⁻¹

Feed in = 598 ml/min.

Pressure = 30 psig

H₂/CO = 3.9

Product out = 526 ml/min

Feed Composition (Vol.%)

Time (hr)	H ₂	O ₂	N ₂	CO
0.00	26.84	0.03	66.41	6.70
0.15	27.17	0.02	66.13	6.65
4.35	26.47	0.03	66.74	6.75

Product Composition (Vol.%)

Time (hr)	H ₂	O ₂	N ₂	CO	CH ₄	CO ₂
0.00	14.83	-	78.72	0.70	5.39	0.34
0.28	16.80	0.01	75.55	0.78	6.29	0.43
0.59	16.59	-	75.54	0.73	6.75	0.38
1.30	16.36	0.01	75.94	0.77	6.50	0.40
1.59	16.74	0.01	75.41	0.73	6.57	0.51
2.29	16.62	0.01	75.48	0.74	6.65	0.48
3.17	18.33	-	73.89	0.75	6.48	0.52
4.04	19.09	0.01	73.19	0.76	6.59	0.32

RUN # 15

Catalyst: Ni/ γ -Al₂O₃

wt. = 10.013 g

Reduction Conditions:

T = 500 °C

Time = 8 hr

Space Velocity = 3000 hr⁻¹Reducing gas = H₂H₂ flow = 491 ml/min.

rpm = 859

Reaction Conditions:

T = 350 °C

Pressure = 30 psig

Space Velocity = 3636 hr⁻¹H₂/CO = 3.9

Feed in = 595 ml/min.

Product out = 531 ml/min

Feed Composition (Vol.%)

Time (hr)	H ₂	O ₂	N ₂	CO
0.00	26.60	0.02	66.64	6.73
4.30	27.10	0.01	66.19	6.67
4.45	26.44	-	66.86	6.69

Product Composition (Vol.%)

Time (hr)	H ₂	O ₂	N ₂	CO	CH ₄	CO ₂
0.00	16.91	0.01	79.39	0.68	2.68	0.30
0.47	18.29	-	74.44	0.78	6.09	0.39
1.15	17.98	0.01	74.21	0.81	6.38	0.58
1.48	17.80	0.01	74.49	0.75	6.43	0.50
2.20	17.71	0.01	73.65	0.76	6.40	1.44
2.53	18.32	-	74.33	0.73	6.27	0.34
3.32	17.78	-	74.33	0.73	6.64	0.50
4.01	18.18	0.02	74.30	0.75	6.34	0.39

RUN # 16

Catalyst: Ni/ γ -Al₂O₃

wt. = 10.015 g

Reduction Conditions:

T = 300 °C

Time = 4 hr

Space Velocity = 3000 hr⁻¹Reducing gas = H₂H₂ flow = 532 ml/min.

rpm = 859

Reaction Conditions:

T = 350 °C

Pressure = 30 psig

Space Velocity = 3697 hr⁻¹H₂/CO = 3.9

Feed in = 605 ml/min.

Product out = 525 ml/min

Feed Composition (Vol.%)

Time (hr)	H ₂	O ₂	N ₂	CO
0.00	26.74	0.06	66.69	6.50
0.15	26.71	0.05	66.27	6.95
4.45	26.59	0.01	66.67	6.71

Product Composition (Vol.%)

Time (hr)	H ₂	O ₂	N ₂	CO	CH ₄	CO ₂
0.00	14.18	0.05	81.10	0.87	3.32	0.45
0.27	18.23	-	73.89	0.72	6.51	0.63
1.27	17.84	-	74.53	0.70	6.31	0.60
1.56	17.82	0.01	74.52	0.73	6.31	0.58
2.22	17.73	0.01	74.52	0.78	6.33	0.62
2.59	17.99	0.01	74.55	0.79	6.10	0.54
3.25	18.05	0.02	73.36	0.76	7.22	0.56
3.51	18.45	-	73.72	0.81	6.45	0.54
4.22	17.57	0.01	74.68	0.81	6.30	0.60

RUN # 17

Catalyst: Ni/ γ -Al₂O₃

wt. = 10.016 g

Reduction Conditions:

T = 300 °C

Time = 12 hr

Space Velocity = 3000 hr⁻¹Reducing gas = H₂H₂ flow = 532 ml/min.

rpm = 859

Reaction Conditions:

T = 350 °C

Pressure = 30 psig

Space Velocity = 3623 hr⁻¹H₂/CO = 3.9

Feed in = 593 ml/min.

Product out = 510 ml/min

Feed Composition (Vol.%)

Time (hr)	H ₂	O ₂	N ₂	CO
0.00	26.37	0.20	66.40	7.01
0.15	25.37	0.13	67.41	7.06
4.00	26.05	0.04	67.15	6.75

Product Composition (Vol.%)

Time (hr)	H ₂	O ₂	N ₂	CO	CH ₄	CO ₂
0.00	12.91	0.05	82.66	0.53	3.42	0.41
0.34	16.23	0.03	76.07	0.70	6.37	0.58
1.01	17.30	0.01	74.98	0.70	6.46	0.52
1.37	16.04	0.01	72.41	0.68	6.28	4.55
2.10	16.85	-	76.11	0.63	6.03	0.35
2.40	16.96	0.01	75.36	0.67	6.42	0.56
3.17	16.73	0.01	75.38	0.69	6.60	0.56

RUN # 18

Catalyst: Ni/ γ -Al₂O₃

wt. = 10.013 g

Reduction Conditions:

T = 300 °C

Time = 16 hr

Space Velocity = 3000 hr⁻¹Reducing gas = H₂H₂ flow = 480 ml/min.

rpm = 859

Reaction Conditions:

T = 350 °C

Pressure = 30 psig

Space Velocity = 3734 hr⁻¹H₂/CO = 4.0

Feed in = 611 ml/min.

Product out = 526 ml/min

Feed Composition (Vol.%)

Time (hr)	H ₂	O ₂	N ₂	CO
0.00	25.85	0.25	66.64	7.23
0.15	26.03	0.14	66.70	7.10
0.32	25.87	0.15	66.88	7.09
3.30	27.28	0.05	66.04	6.61
3.45	26.99	0.04	66.30	6.66

Product Composition (Vol.%)

Time (hr)	H ₂	O ₂	N ₂	CO	CH ₄	CO ₂
0.00	12.10	0.09	84.56	1.07	1.81	0.34
0.47	18.19	0.02	73.89	0.72	6.60	0.56
1.16	18.40	-	73.76	0.71	6.61	0.50
1.50	18.20	0.02	74.01	0.74	6.38	0.62
2.26	18.06	-	74.19	0.74	6.40	0.59
2.56	18.41	0.01	74.15	0.74	6.40	0.26

RUN # 19

Catalyst: Ni/ γ -Al₂O₃

wt. = 10.013 g

Reduction Conditions:

T = 300 °C

Time = 2 hr

Space Velocity = 3000 hr⁻¹Reducing gas = H₂H₂ flow = 473 ml/min.

rpm = 859

Reaction Conditions:

T = 350 °C

Pressure = 30 psig

Space Velocity = 3636 hr⁻¹H₂/CO = 3.7

Feed in = 595 ml/min.

Product out = 520 ml/min

Feed Composition (Vol.%)

Time (hr)	H ₂	O ₂	N ₂	CO
0.00	26.28	0.06	66.93	6.71
2.40	25.05	0.03	68.07	6.84
2.55	25.05	0.04	68.05	6.84

Product Composition (Vol.%)

Time (hr)	H ₂	O ₂	N ₂	CO	CH ₄	CO ₂
0.00	16.13	0.03	77.66	0.96	4.37	0.83
0.28	16.64	0.02	75.22	1.10	5.99	0.99
1.07	16.81	0.01	75.36	1.00	5.83	0.95
1.38	16.46	0.01	75.67	1.02	5.81	1.01
2.09	16.32	0.01	75.84	0.98	5.86	0.95

RUN # 20

Catalyst: Ni/ γ -Al₂O₃

wt. = 10.015 g

Reduction Conditions:

T = 300 °C

Time = 8 hr

Space Velocity = 3000 hr⁻¹Reducing gas = H₂H₂ flow = 535 ml/min.

rpm = 859

Reaction Conditions:

T = 350 °C

Pressure = 30 psig

Space Velocity = 3660 hr⁻¹H₂/CO = 3.8

Feed in = 599 ml/min.

Product out = 521 ml/min

Feed Composition (Vol.%)

Time (hr)	H ₂	O ₂	N ₂	CO
0.00	25.87	0.06	67.53	6.52
0.15	28.52	0.03	64.94	6.48
8.30	26.01	0.03	67.18	6.77
14.40	26.02	0.01	67.17	6.77

Product Composition (Vol.%)

Time (hr)	H ₂	O ₂	N ₂	CO	CH ₄	CO ₂
0.00	15.61	0.03	78.37	0.68	4.74	0.56
0.30	16.39	0.03	75.99	0.59	6.34	0.63
1.13	17.82	0.02	75.18	0.68	6.29	-
1.53	18.95	0.01	75.50	0.57	5.64	0.29
2.36	18.66	0.01	74.11	0.71	6.01	0.48
3.19	18.68	0.01	73.93	0.82	6.05	0.49
4.01	18.45	0.01	73.78	0.78	6.42	0.53
4.42	17.27	-	75.27	0.85	6.01	0.59
5.22	17.28	-	75.07	0.84	6.29	0.50
6.03	16.77	0.01	75.22	0.85	6.31	0.81
6.44	16.54	0.01	75.68	0.83	6.30	0.62
7.26	16.18	0.02	76.01	0.85	6.34	0.59
8.08	16.75	0.01	75.44	0.87	6.33	0.58
10.0	16.74	0.01	75.43	0.87	6.32	0.58
12.0	16.73	0.01	75.44	0.86	6.33	0.57
14.0	16.74	0.01	75.43	0.87	6.32	0.58

RUN # 21

Catalyst: Ni/ γ -Al₂O₃

wt. = 10.015 g

Reduction Conditions:

T = 300 °C

Time = 8 hr

Space Velocity = 3000 hr⁻¹Reducing gas = H₂H₂ flow = 535 ml/min.

rpm = 859

Reaction Conditions:

T = 350 °C

Pressure = 30 psig

Space Velocity = 3660 hr⁻¹H₂/CO = 3.8

Feed in = 599 ml/min.

Product out = 521 ml/min

Feed Composition (Vol.%)

Time (hr)	H ₂	O ₂	N ₂	CO
0.00	26.01	0.03	67.18	6.77
5.15	25.88	0.04	67.29	6.78

Product Composition (Vol.%)

Time (hr)	H ₂	O ₂	N ₂	CO	CH ₄	CO ₂
0.00	16.77	0.01	75.72	0.98	5.89	0.61
0.43	16.22	0.02	75.89	0.88	6.35	0.62
1.28	16.15	-	75.90	0.86	6.30	0.74
2.13	16.31	0.01	75.91	0.85	6.32	0.59
2.59	16.05	0.03	76.14	0.86	6.32	0.58
3.44	16.22	0.01	75.69	0.88	6.37	0.80
4.30	16.14	0.02	75.66	0.88	6.29	0.58

RUN # 22

Catalyst: Ni/ γ -Al₂O₃

wt. = 10.015 g

Reduction Conditions:

T = 300 °C

Space Velocity = 3000 hr⁻¹H₂ flow = 535 ml/min.

Time = 8 hr

Reducing gas = H₂

rpm = 859

Reaction Conditions:

T = 350 °C

Space Velocity = 5084 hr⁻¹

Feed in = 832 ml/min.

Pressure = 30 psig

H₂/CO = 3.9

Product out = 746 ml/min

Feed Composition (Vol.%)

Time (hr)	H ₂	O ₂	N ₂	CO
0.00	25.06	0.17	67.65	7.10
0.15	26.24	0.03	66.94	6.77
2.10	26.62	0.02	66.63	6.72

Product Composition (Vol.%)

Time (hr)	H ₂	O ₂	N ₂	CO	CH ₄	CO ₂
0.00	14.85	0.16	79.66	1.47	3.32	0.51
0.43	18.87	-	73.60	1.19	5.84	0.49
1.28	19.32	-	73.18	1.18	5.76	0.55

RUN # 23

Catalyst: Ni/ γ -Al₂O₃

wt. = 10.015 g

Reduction Conditions:

T = 300 °C

Time = 8 hr

Space Velocity = 3000 hr⁻¹Reducing gas = H₂H₂ flow = 535 ml/min.

rpm = 859

Reaction Conditions:

T = 350 °C

Pressure = 30 psig

Space Velocity = 5927 hr⁻¹H₂/CO = 3.8

Feed in = 970 ml/min.

Product out = 848 ml/min

Feed Composition (Vol.%)

Time (hr)	H ₂	O ₂	N ₂	CO
0.00	25.13	0.20	65.58	7.20
0.15	25.48	0.13	67.29	7.08
4.20	25.66	0.03	67.57	6.73

Product Composition (Vol.%)

Time (hr)	H ₂	O ₂	N ₂	CO	CH ₄	CO ₂
0.00	16.95	0.03	75.74	1.26	5.40	0.57
0.31	18.38	0.01	74.03	1.29	5.66	0.58
1.03	18.44	-	73.77	1.23	5.96	0.51
2.08	18.78	0.01	73.84	1.27	5.29	0.59
2.35	18.76	-	73.59	1.32	5.86	0.45
3.04	17.96	0.02	74.15	1.25	5.86	0.60
3.46	17.93	0.02	74.24	1.28	5.90	0.60

RUN # 24

Catalyst: Ni/ γ -Al₂O₃

wt. = 10.015 g

Reduction Conditions:

T = 300 °C

Time = 8 hr

Space Velocity = 3000 hr⁻¹Reducing gas = H₂H₂ flow = 535 ml/min.

rpm = 859

Reaction Conditions:

T = 350 °C

Pressure = 30 psig

Space Velocity = 6746 hr⁻¹H₂/CO = 3.9

Feed in = 1104 ml/min.

Product out = 1000 ml/min

Feed Composition (Vol.%)

Time (hr)	H ₂	O ₂	N ₂	CO
0.00	24.97	0.20	65.50	6.94
0.16	24.74	0.19	67.88	7.17
2.15	26.26	0.03	66.96	6.72

Product Composition (Vol.%)

Time (hr)	H ₂	O ₂	N ₂	CO	CH ₄	CO ₂
0.00	18.01	-	75.87	1.86	3.64	0.61
0.30	18.78	-	73.50	1.52	5.52	0.66
1.01	18.57	-	73.71	1.45	5.50	0.76
1.44	19.06	0.01	73.49	1.37	5.50	0.55

RUN # 25

Catalyst: Ni/ γ -Al₂O₃

wt. = 10.015 g

Reduction Conditions:

T = 300 °C

Time = 8 hr

Space Velocity = 3000 hr⁻¹Reducing gas = H₂H₂ flow = 535 ml/min.

rpm = 859

Reaction Conditions:

T = 350 °C

Pressure = 30 psig

Space Velocity = 8451 hr⁻¹H₂/CO = 4.6

Feed in = 1383 ml/min.

Product out = 1214 ml/min

Feed Composition (Vol.%)

Time (hr)	H ₂	O ₂	N ₂	CO
0.00	27.37	0.12	65.75	6.74
3.45	30.00	0.03	63.55	6.41
4.00	29.86	0.04	63.68	6.41

Product Composition (Vol.%)

Time (hr)	H ₂	O ₂	N ₂	CO	CH ₄	CO ₂
0.00	19.62	0.04	72.04	1.88	4.29	0.25
0.40	21.02	-	71.32	1.58	5.27	0.81
1.25	20.27	0.01	72.02	1.51	5.56	0.61
2.02	21.08	0.01	70.47	1.55	4.97	1.43
2.38	21.99	0.01	71.30	1.52	4.93	0.23
3.19	22.00	0.01	70.84	1.57	4.93	0.62

RUN # 26

Catalyst: Ni/ γ -Al₂O₃

wt. = 10.015 g

Reduction Conditions:

T = 300 °C

Time = 8 hr

Space Velocity = 3000 hr⁻¹Reducing gas = H₂H₂ flow = 535 ml/min.

rpm = 859

Reaction Conditions:

T = 350 °C

Pressure = 30 psig

Space Velocity = 2416 hr⁻¹H₂/CO = 3.9

Feed in = 395 ml/min.

Product out = 319 ml/min

Feed Composition (Vol.%)

Time (hr)	H ₂	O ₂	N ₂	CO
0.00	26.26	0.03	66.94	6.74
5.15	25.02	0.02	68.13	6.81
5.30	24.76	0.03	68.31	6.88

Product Composition (Vol.%)

Time (hr)	H ₂	O ₂	N ₂	CO	CH ₄	CO ₂
0.00	13.04	0.01	78.87	0.56	8.87	0.62
0.28	12.58	0.01	79.07	0.56	7.04	0.71
1.10	13.11	-	78.44	0.59	7.18	0.66
1.53	14.31	-	77.33	0.64	7.18	0.51
2.36	14.43	-	76.99	0.62	7.10	0.85
3.19	15.05	-	76.68	0.59	7.07	0.60
4.02	15.12	-	76.61	0.63	7.03	0.59
4.46	14.49	-	77.42	0.59	6.91	0.57

RUN # 27

Catalyst: Ni/ γ -Al₂O₃

wt. = 10.015 g

Reduction Conditions:

T = 300 °C

Time = 8 hr

Space Velocity = 3000 hr⁻¹Reducing gas = H₂H₂ flow = 535 ml/min.

rpm = 859

Reaction Conditions:

T = 350 °C

Pressure = 30 psig

Space Velocity = 1764 hr⁻¹H₂/CO = 4.1

Feed in = 288 ml/min.

Product out = 252 ml/min

Feed Composition (Vol.%)

Time (hr)	H ₂	O ₂	N ₂	CO
0.00	27.26	0.03	66.06	6.63
3.45	25.20	0.01	66.86	6.63

Product Composition (Vol.%)

Time (hr)	H ₂	O ₂	N ₂	CO	CH ₄	CO ₂
0.00	15.45	0.01	77.16	0.57	6.23	0.55
0.43	17.66	0.02	74.69	0.47	6.85	0.30
1.18	19.73	-	72.46	0.47	6.96	0.35
1.51	18.51	-	73.62	0.45	7.12	0.27
2.29	16.75	0.01	75.35	0.49	7.01	0.38
3.13	18.84	0.01	73.56	0.46	6.83	0.29

RUN # 28

Catalyst: Ni/ γ -Al₂O₃

wt. = 10.015 g

Reduction Conditions:

T = 300 °C

Time = 8 hr

Space Velocity = 3000 hr⁻¹Reducing gas = H₂H₂ flow = 535 ml/min.

rpm = 859

Reaction Conditions:

T = 350 °C

Pressure = 35 psig

Space Velocity = 3794 hr⁻¹H₂/CO = 3.9

Feed in = 621 ml/min.

Product out = 521 ml/min

Feed Composition (Vol.%)

Time (hr)	H ₂	O ₂	N ₂	CO
0.00	25.44	0.09	66.05	7.04
1.45	25.54	0.13	66.03	6.98
2.00	26.08	0.04	67.07	6.77

Product Composition (Vol.%)

Time (hr)	H ₂	O ₂	N ₂	CO	CH ₄	CO ₂
0.00	14.29	0.01	80.36	0.98	3.60	0.74
0.45	13.62	-	78.29	0.77	6.57	0.73
1.20	13.88	-	78.03	0.72	6.71	0.64

RUN # 29

Catalyst: Ni/ γ -Al₂O₃

wt. = 10.015 g

Reduction Conditions:

T = 300 °C

Time = 8 hr

Space Velocity = 3000 hr⁻¹Reducing gas = H₂H₂ flow = 535 ml/min.

rpm = 859

Reaction Conditions:

T = 350 °C

Pressure = 59 psig

Space Velocity = 3752 hr⁻¹H₂/CO = 4.0

Feed in = 614 ml/min.

Product out = 526 ml/min

Feed Composition (Vol.%)

Time (hr)	H ₂	O ₂	N ₂	CO
0.00	26.78	0.04	66.50	6.68
8.15	26.97	0.02	66.33	6.67

Product Composition (Vol.%)

Time (hr)	H ₂	O ₂	N ₂	CO	CH ₄	CO ₂
0.00	17.33	0.04	74.89	0.55	7.17	-
0.29	17.27	-	75.00	0.44	6.56	0.38
1.05	17.05	-	75.56	0.41	6.81	0.12
1.41	16.81	0.03	75.17	0.42	7.19	0.33
2.20	17.38	-	75.07	0.44	6.76	0.32
3.02	16.75	0.03	75.36	0.44	7.12	0.29
3.46	17.74	-	74.14	0.47	7.34	0.29
4.31	17.92	0.01	74.25	0.46	7.01	0.32
5.16	18.87	-	73.19	0.48	7.19	0.24
6.01	18.41	-	73.79	0.45	6.92	0.42
6.46	19.19	-	72.90	0.47	7.13	0.28

RUN # 30

Catalyst: Ni/ γ -Al₂O₃

wt. = 10.015 g

Reduction Conditions:

T = 300 °C

Time = 8 hr

Space Velocity = 3000 hr⁻¹Reducing gas = H₂H₂ flow = 535 ml/min.

rpm = 859

Reaction Conditions:

T = 350 °C

Pressure = 72 psig

Space Velocity = 3465 hr⁻¹H₂/CO = 4.1

Feed in = 614 ml/min.

Product out = 526 ml/min

Feed Composition (Vol.%)

Time (hr)	H ₂	O ₂	N ₂	CO
0.00	27.55	0.03	65.78	6.62
3.00	27.55	0.01	65.80	6.63

Product Composition (Vol.%)

Time (hr)	H ₂	O ₂	N ₂	CO	CH ₄	CO ₂
0.00	23.16	-	69.94	0.84	5.92	0.14
0.44	22.57	0.01	70.21	0.38	6.65	0.16
1.30	24.39	-	68.25	0.37	6.78	0.19
2.02	23.35	-	69.51	0.36	6.60	0.16
2.33	22.65	0.01	70.20	0.39	6.68	0.05

RUN # 31

Catalyst: Ni/ γ -Al₂O₃

wt. = 10.015 g

Reduction Conditions:

T = 300 °C

Time = 8 hr

Space Velocity = 3000 hr⁻¹Reducing gas = H₂H₂ flow = 535 ml/min.

rpm = 859

Reaction Conditions:

T = 350 °C

Pressure = 30 psig

Space Velocity = 3703 hr⁻¹H₂/CO = 3.1

Feed in = 606 ml/min.

Product out = 526 ml/min

Feed Composition (Vol.%)

Time (hr)	H ₂	O ₂	N ₂	CO
0.00	22.27	0.02	70.60	7.09
2.32	22.25	0.01	70.50	7.12

Product Composition (Vol.%)

Time (hr)	H ₂	O ₂	N ₂	CO	CH ₄	CO ₂
0.00	12.16	0.01	79.54	1.05	6.23	0.99
0.38	13.09	-	78.67	1.04	6.21	0.97
2.07	12.56	-	29.25	1.04	6.21	0.93

RUN # 32

Catalyst: Ni/ γ -Al₂O₃

wt. = 10.015 g

Reduction Conditions:

T = 300 °C

Time = 8 hr

Space Velocity = 3000 hr⁻¹Reducing gas = H₂H₂ flow = 535 ml/min.

rpm = 859

Reaction Conditions:

T = 350 °C

Pressure = 30 psig

Space Velocity = 3923 hr⁻¹H₂/CO = 2.2

Feed in = 642 ml/min.

Product out = 535 ml/min

Feed Composition (Vol.%)

Time (hr)	H ₂	O ₂	N ₂	CO
0.00	17.11	0.03	75.26	7.58
4.32	17.28	0.01	75.08	7.54

Product Composition (Vol.%)

Time (hr)	H ₂	O ₂	N ₂	CO	CH ₄	CO ₂
0.00	66.83	0.09	29.01	0.76	1.94	0.44
3.03	7.38	0.01	83.89	1.24	5.48	1.99
3.34	7.36	0.07	83.66	1.66	5.36	1.96
4.03	7.09	0.03	83.73	1.73	5.39	2.00

RUN # 33

Catalyst: Ni/ γ -Al₂O₃

wt. = 10.015 g

Reduction Conditions:

T = 300 °C

Time = 8 hr

Space Velocity = 3000 hr⁻¹Reducing gas = H₂H₂ flow = 535 ml/min.

rpm = 859

Reaction Conditions:

T = 350 °C

Pressure = 30 psig

Space Velocity = 3739 hr⁻¹H₂/CO = 1.3

Feed in = 612 ml/min.

Product out = 547 ml/min

Feed Composition (Vol.%)

Time (hr)	H ₂	O ₂	N ₂	CO
0.00	10.83	0.07	80.75	8.33
4.17	11.23	0.07	80.37	8.32

Product Composition (Vol.%)

Time (hr)	H ₂	O ₂	N ₂	CO	CH ₄	CO ₂
0.00	32.87	0.08	59.88	1.43	2.93	1.94
0.39	5.05	-	85.56	1.63	4.56	3.17
1.19	3.90	0.04	86.68	1.98	4.23	3.14
1.59	3.84	0.06	86.30	1.95	3.94	3.14
2.38	4.10	0.01	87.23	1.60	4.47	2.56
3.18	4.42	0.06	86.16	1.91	4.46	2.95
3.46	3.18	0.03	86.63	1.62	4.38	3.13

RUN # 34

Catalyst: Ni/ γ -Al₂O₃

wt. = 10.015 g

Reduction Conditions:

T = 300 °C

Time = 8 hr

Space Velocity = 3000 hr⁻¹Reducing gas = H₂H₂ flow = 535 ml/min.

rpm = 859

Reaction Conditions:

T = 350 °C

Pressure = 30 psig

Space Velocity = 3654 hr⁻¹H₂/CO = 4.0

Feed in = 598 ml/min.

Product out = 526 ml/min

Feed Composition (Vol.%)

Time (hr)	H ₂	O ₂	N ₂	CO
0.00	27.08	-	66.29	6.70
1.50	26.12	-	66.93	6.74

Product Composition (Vol.%)

Time (hr)	H ₂	O ₂	N ₂	CO	CH ₄	CO ₂
0.00	17.13	0.01	74.78	0.79	6.68	0.56
0.25	17.12	-	74.85	0.76	6.77	0.48
0.51	17.14	-	74.89	0.76	6.61	0.58
1.18	16.30	0.01	75.82	0.76	6.65	0.44

RUN # 35

Catalyst: Ni/ γ -Al₂O₃

wt. = 10.015 g

Reduction Conditions:

T = 300 °C

Time = 8 hr

Space Velocity = 3000 hr⁻¹Reducing gas = H₂H₂ flow = 535 ml/min.

rpm = 859

Reaction Conditions:

T = 350 °C

Pressure = 30 psig

Space Velocity = 3599 hr⁻¹H₂/CO = 5.0

Feed in = 589 ml/min.

Product out = 522 ml/min

Feed Composition (Vol.%)

Time (hr)	H ₂	O ₂	N ₂	CO
0.00	31.55	-	62.20	6.24
2.10	32.00	0.01	61.77	6.21

Product Composition (Vol.%)

Time (hr)	H ₂	O ₂	N ₂	CO	CH ₄	CO ₂
0.00	23.66	0.07	70.30	1.11	4.52	0.32
0.33	24.93	0.01	67.92	0.73	6.01	0.37
1.13	24.74	0.01	68.24	0.70	6.05	0.23
1.40	24.73	0.01	68.22	0.69	6.07	0.24

RUN # 36

Catalyst: Ni/ γ -Al₂O₃

wt. = 10.015 g

Reduction Conditions:

T = 300 °C

Time = 8 hr

Space Velocity = 3000 hr⁻¹Reducing gas = H₂H₂ flow = 535 ml/min.

rpm = 859

Reaction Conditions:

T = 350 °C

Pressure = 30 psig

Space Velocity = 3697 hr⁻¹H₂/CO = 5.5

Feed in = 605 ml/min.

Product out = 532 ml/min

Feed Composition (Vol.%)

Time (hr)	H ₂	O ₂	N ₂	CO
0.00	34.79	-	57.94	6.17
2.00	34.53	0.12	57.90	6.22

Product Composition (Vol.%)

Time (hr)	H ₂	O ₂	N ₂	CO	CH ₄	CO ₂
0.00	29.21	0.02	66.72	0.71	3.08	0.22
0.30	29.72	-	63.48	0.72	5.85	0.21
1.00	29.63	0.02	63.94	0.69	5.58	0.11
1.28	28.64	-	64.53	0.71	5.88	0.22

RUN # 37

Catalyst: Ni/ γ -Al₂O₃

wt. = 10.015 g

Reduction Conditions:

T = 300 °C

Time = 8 hr

Space Velocity = 3000 hr⁻¹Reducing gas = H₂H₂ flow = 535 ml/min.

rpm = 859

Reaction Conditions:

T = 350 °C

Pressure = 30 psig

Space Velocity = 3800 hr⁻¹H₂/CO = 6.5

Feed in = 622 ml/min.

Product out = 587 ml/min

Feed Composition (Vol.%)

Time (hr)	H ₂	O ₂	N ₂	CO
0.00	36.90	0.02	57.26	5.76
3.00	37.30	-	56.90	5.73

Product Composition (Vol.%)

Time (hr)	H ₂	O ₂	N ₂	CO	CH ₄	CO ₂
0.00	30.61	-	62.26	0.99	6.11	-
0.50	32.59	0.01	60.89	0.70	5.29	0.09
1.40	33.08	-	60.66	0.71	5.23	0.28
2.33	33.39	-	60.30	0.70	5.49	0.10